6-2015

TSLP-induced Mechanisms and Potential Therapies for CRLF2 B-cell Acute Lymphoblastic Leukemia

Olivia L. Francis

LOMA LINDA UNIVERSITY
School of Medicine
in conjunction with the
Faculty of Graduate Studies

TSLP-induced Mechanisms and Potential Therapies for CRLF2 B-cell Acute Lymphoblastic Leukemia

by

Olivia L Francis

A Dissertation submitted in partial satisfaction of
the requirements for the degree
Doctor of Philosophy in Anatomy

June 2015

Each person whose signature appears below certifies that this dissertation in his/her opinion is adequate, in scope and quality, as a dissertation for the degree Doctor of Philosophy.

_____, Chairperson
Kimberly Payne, Associate Professor of Pathology & Human Anatomy

_____
Sinisa Dovat, Associate Professor of Pediatrics, Pennsylvania State University, Hershey

_____
Mary Kearns-Jonker, Associate Professor of Pathology & Human Anatomy

_____
Kerby Oberg, Professor of Pathology & Human Anatomy

_____
Ubaldo Soto-Wegner, Assistant Research Professor of Microbiology

_____
David J. Weldon, Associate Professor of Pharmaceutical Science, School of Pharmacy

ACKNOWLEDGEMENTS

All glory and honor be given to God for the magnificent work he has done. He has filled me with wisdom and has revealed the secret nuances of science from the inception to the completion of this project.

I express sincere gratitude to Dr. Payne who willingly gave me the opportunity to explore and fulfill my dream of contributing to the diagnosis and treatment of children with Leukemia. Her support, passion, creativity and dedication to making a positive difference in the world and her overall contributions to the university in relation to pediatric cancer speaks volumes of her dedication to this cause.

I extend special thanks to my committee members for scientific guidance and constructive criticisms that allowed this project to make indelible contributions to the scientific community. To my lab colleagues, with whom I have laughed, vented, enjoyed great conversations and great meals, I say thank you. I could not complete this journey without all of you.

Finally, to my family and friends words cannot express the value of your support and prayers for me over the years. God called each of you specifically to fulfill that purpose and he will bless all of you abundantly in return for the kindness you have shown me. I am forever indebted to all of you and so I say thank you.

CONTENTS

TABLES

Tables Page

FIGURES

Figures Page

ABBREVIATIONS

CRLF2	Cytokine Receptor Like Factor 2
B-ALL	B-cell Acute Lymphoblastic Leukemia
TSLP	Thymic Stromal Lymphopoietin
JAK	Janus Kinase
STAT5	Signal Transducer and Activator of Transcription 5
PI3K	Phosphoinositide-3-Kinase
AKT	Protein Kinase B
mTOR	Mammalian Target Of Rapamycin
hTSLP	Human TSLP
MIM1	Mcl-1 Inhibitor Molecule 1
Mcl-1	Myeloid Cell Leukemia 1
BM	Bone Marrow
HSC	Hematopoietic Stem Cell
MPP	Multi-Potent Progenitor
LMPP	Lymphoid primed Multi-Potent Progenitor
CLP	Common Lymphoid Progenitor
RAG1/2	Recombination Activating Gene (1 or 2)
SLC	Surrogate Light Chain
IGH	Immunoglobulin Heavy chain
VDJ	Variable, Diversity and Joining gene segments
BCR	B-cell Receptor
IgM	Immunoglobulin M

IgA	Immunoglobulin A
IgD	Immunoglobulin D
IgE	Immunoglobulin E
IgG	Immunoglobulin G
Igκ	Immunoglobulin light chain Kappa
Igλ	Immunoglobulin light chain Lambda
BMSC	Bone Marrow Stromal Cells
CXCL	Chemokine (C-X-C motif) ligand
IL-7	Interleukin 7
Flt3	Fms-Like Tyrosine kinase 3
IL-7Rα	Interleukin 7 Receptor alpha chain
TSLPR	Thymic Stromal Lymphopoietin receptor
SH2	Src Homology 2
Bcl2	B-cell Lymphoma 2
PU.1	PU-box (binds purine rich sequence)
EBF	Early B-cell Factor
E2A	Transcription factor 3
Pax5	Paired Box 5
BCR-ABL	Breakpoint Cluster Region joined to *ABL1* gene
Ph+ BALL	Philadelphia positive Bcell Acute Lymphoblastic Leukemia
P2RY8	Purinergic receptor p2y g protein coupled 8
IKZF1	Ikaros
TKI	Tyrosine Kinase Inhibitor

BaF3	Murine Pro-B cell line

ABSTRACT OF THE DISSERTATION

TSLP-induced Mechanisms and Potential Therapies for
CRLF2 B-cell Acute Lymphoblastic Leukemia

by

Olivia L Francis

Doctor of Philosophy, Graduate Program in Anatomy
Loma Linda University, June 2015
Dr. Kimberly J Payne, Chairperson

Childhood CRLF2 B-cell Acute Lymphoblastic Leukemia (CRLF2 B-ALL) is a high-risk form of leukemia that is associated with poor patient survival outcomes. CRLF2 B-ALL is five times more prevalent in Hispanic children than others and is associated with a higher rate of relapse, thus contributing significantly to childhood cancer health disparities**.** This disease occurs due to alterations of the *CRLF2* gene, leading to over-expression of the CRLF2 protein- a component of the receptor signaling complex for the cytokine Thymic Stromal LymphoPoietin (TSLP) on the surface of B-ALL cells. TSLP has been shown to induce proliferation of human and mouse B-cell precursors via activation of the JAK-STAT5 and more recently the PI3K/AKT/mTOR pathways**.** However, the mechanisms by which TSLP-CRLF2 interactions contribute to high-risk leukemia have not been elucidated. Therefore the objective of our studies was to elucidate the TSLP-induced mechanisms that contribute to high-risk CRLF2 B-ALL and to evaluate promising drug candidates to target high-risk B-ALL. Based on literature findings and preliminary data, we hypothesized that *TSLP contributes to CRLF2 B-ALL by increasing proliferation and/or survival of leukemia cells via regulation of genes downstream of CRLF2 pathway activation*. This hypothesis was tested using experiments

developed under the following specific aims:- Aim 1: Optimize the novel hTSLP+/- xenograft model for use in defining the role of TSLP in CRLF2 B-ALL; Aim 2: Identify TSLP-induced cellular and molecular mechanisms that contribute to CRLF2 B-ALL; Aim 3: Assess candidate drugs' efficacy against high-risk B-ALL. Results from the studies conducted to address the specific aims show that 1) the hTSLP+/hTSLP- mouse model produces detectable levels of hTSLP, which activates CRLF2 and expands normal B-cells and activates the mTOR cell survival pathway in CRLF2 B-ALL cells *in vivo;* 2) cellular assays of apoptosis along with gene expression data demonstrate that TSLP regulates the expression of genes that promote cell death and survival of CRLF2 B-ALL cells *in vivo* and *in vitro*; 3) drug efficacy studies performed on high-risk leukemia cells using several drug candidates demonstrate that the Mcl-1 inhibitor MIM1 and the Novomedix drug series induced cell death in CRLF2 B-ALL and Nalm6 cells respectively. Taken together, the data provide evidence that TSLP regulates cell survival mechanisms in CRLF2 B-ALL cells and provides a rationale for the use of combination therapies that include drugs which target cell survival molecules and/or cellular functions regulated by TSLP.

CHAPTER ONE

INTRODUCTION

Normal B-cell Development

Stages of Early B-cell Differentiation

Human B-cells are derived from hematopoietic stem cells (HSCs) in the bone marrow (BM), where they undergo lineage specific changes to develop into mature B-cells [1]. HSCs produce multi-potent progenitors (MPPs) which give rise to lymphoid-primed MPPs (LMPPs) followed by common lymphoid progenitors (CLPs). CLPs then differentiate through the following consecutive B-cell stages to produce functional B-cells: Pro-B, Pre-B, Immature-B and Mature B (Figure 1.1)[2]. The pro-B to pre-B transition requires successful rearrangement and expression of genes that encode the immunoglobulin heavy chain (IGHμ), specifically the gene segments from the germ line-variable, diversity and joining regions during VDJ recombination [3-4]. This process is facilitated by recombination activating genes 1 and 2 (RAG1 and RAG2) [3]. Approximately 1/3 of the pro-B cells successfully express the IgHμ chain and a surrogate light chain (SLC) in their cytoplasm along with a pre-BCR on their surface, becoming pre-B cells. This transition is often referred to as the first checkpoint [1, 5]. These pre-B cells then undergo polyclonal expansion (proliferation of cells that have successfully rearranged IGH) and prepare to rearrange their light chain.

The pre-B to immature-B transition is characterized by rearrangement of genes that encode the immunoglobulin light chain (Igκ then Igλ), and the suppression of SLC as well as pre-BCR [1, 4]. This transition is the second checkpoint. Successful rearrangements of both heavy and light chains contribute to the generation of a diverse

antibody repertoire [3]. B-cells that fail to successfully rearrange and express functional IgH and IgL chains are removed by programmed cell death also known as apoptosis[6]. The mature B-cells produced by this process express surface immunoglobulin M (IgM) and subsequently undergo class switch recombination to produce a variety of antibody isotypes (IgA, IgD, IgE, IgG) with high antigen specificity and affinity. The B-cells then migrate to secondary lymphoid organs where they are able to mount a robust humoral response against pathogens as part of the adaptive immune system machinery [7].

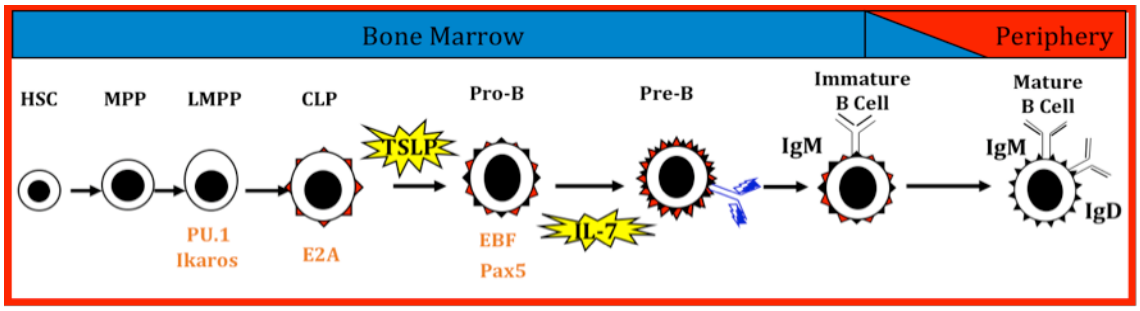

Fig.1.1 Stages of Early B-cell Differentiation

Cytokine Function in Normal B-cells

In order for the complex process of B-cell differentiation to occur, developing B-cells depend on extrinsic factors that are present in the BM microenvironment including non-hematopoietic cells such as stromal cells and the factors that they secrete [8]. In the bone marrow, B-cells associate with bone marrow stromal cells (BMSCs) which have been described as progenitors of skeletal, muscle and neural tissues [9]. In addition to their functions listed above, these BMSCs support the development of hematopoietic (blood) cells including B-cells by secreting cytokines (growth factors) that are required

for the B-cells to develop [1, 10]. Cytokines are peptides or glycoproteins that promote cell growth, differentiation and/or survival [1].

CXCL12, Flt3, and interleukin 7 (IL-7) are among cytokines that are produced by BMSCs and are required for the development of B-cells [1]. Specifically, IL-7 is required for the survival, expansion and differentiation of mouse B-cell precursors [11-13]. Our lab has demonstrated that IL-7 induces the expansion of human Pro-B cells, which is crucial for providing large cell numbers to progress through the stages of B-cell differentiation [14]. The cytokine Thymic Stromal Lymphopoietin (TSLP), which is produced by epithelial cells of the lung and skin as well as BMSCs has also been shown to contribute to B-development [15-16]. In addition to activating dendritic cells, regulating inflammation and contributing to asthma and allergic responses; TSLP also induces proliferation in human pro-B cells and promotes B-cell survival by protecting cells from apoptosis, [17-20][Milford unpub. data].

TSLP and IL-7 Signaling in Normal B-cells

Cytokines interact with their receptors, which are often found on the surface or within a cell, to activate signal transduction pathways and in turn promote cell survival, proliferation and differentiation [10]. TSLP performs its function in B-cells by binding to its receptor, which comprises of two subunits: IL-7Rα and TSLPR (also known as CRLF2). Upon binding to its receptor, TSLP traditionally activates the JAK-STAT pathway [10, 21]. TSLP binds its receptor subunits, which dimerize leading to the recruitment and activation of Janus kinases (JAK1 and JAK2) via cross-phosphorylation followed by phosphorylation of tyrosine residues found in the cytoplasmic domain of the

receptors [22]. Signal transducers and activators of transcription-STAT (primarily STAT5) proteins- bind to the tyrosine-phosphorylated receptors via their SH2 domains and become phosphorylated by the JAKs [22]. STATs then dissociate from the receptors, form dimers, translocate to the nucleus and bind to the promoter of target genes in order to regulate gene transcription. Studies have shown that STAT5 regulates B-cell survival and differentiation; a process that is mediated by the Bcl2 family members [23]. More recently, it has been shown that in addition to the JAK-STAT pathway, TSLP also binds its receptor and signals through other downstream pathways such as the PI3K/AKT and mTOR pathways [24-25][appdx]. It is important to note that IL-7 shares the IL-7Rα, which has implications for studies discussed later in this dissertation (Figure.1.2). To perform its functions, IL-7 binds to its receptor which comprises of two subunits: IL-7Rα and IL-2Rγ and also activates the JAK-STAT pathway [21]. IL-7 binds its receptor and follows the signal transduction cascade described above for TSLP, with the exception that IL-7 signals through JAK1 and JAK3 [22].

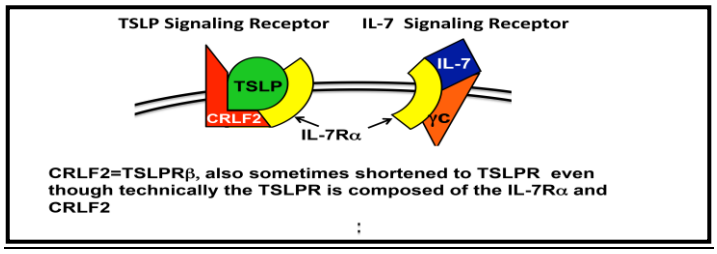

Fig.1.2 TSLP and IL-7 Receptors

The Role of Transcription Factors in Normal B-cells

Several transcription factors primarily Ikaros, PU.1, EBF, E2A and Pax5 all work in concert to regulate the early stages of B-cell development (Figure 1.1)[26]. These

transcription factors function to activate or repress genes that are responsible for ensuring B-cell lineage commitment during each stage of differentiation [26]. PU.1 regulates lymphoid versus myeloid differentiation [2]. E2A maintains the stem cell pool, is required to promote the lymphoid lineage at the LMPP and CLP stages and it turns on and maintains the expression of EBF and Pax5 [27]. EBF regulates the genes that are required for producing B-cells such as Pax5. Pax5 is absolutely required for maintaining B-cell identity; in the absence of Pax5, cells de-differentiate to a progenitor stage where they can commit to other lineages such as the T-lineage [28-29]. Ikaros promotes B-cell development by regulating chromatin availability required for VDJ recombination, regulating B-cell related genes and contributing to commitment to the B-lineage [2]. As a result, B-cell differentiation is a tightly regulated process that is controlled by interactions between transcription factors, the cytokines they regulate and the cellular processes that occur during differentiation.

High-risk B-cell Acute Lymphoblastic Leukemia

Despite this tightly regulated process, aberrations can occur at various developmental stages leading to B-cell related diseases such as lymphoma, autoimmune diseases and leukemia [30-31]. Recent studies show that the dysregulation of genes involved in B-cell differentiation, survival, proliferation and cell cycle contribute to human leukemogenesis [32-35]. B-cell differentiation is blocked at the B-cell precursor (BCP) stage where cells are rapidly proliferating due to genetic alterations in transcription factors e.g. IKaros and Pax5, leading to the development of B-cell Acute Lymphoblastic Leukemia (B-ALL) [36]. The loss of mechanisms that would normally

induce apoptosis in B-cells that fail to differentiate, causes these aberrantly proliferating cells to survive [37]. B-ALL is characterized by rapid accumulation of malignant B-cells in the BM compared to other cell types.

Studies have identified several subtypes of B-ALL in which patients are resistant to chemotherapy and suffer high rates of relapse, often resulting in death. These patients are referred to as "high-risk" patients. High-risk patients are identified based on several clinical features at diagnosis such as white blood cell count, age, ethnicity, cytogenic abnormalities, response to treatment and minimal residual disease. After assessment, risk classification schemes are used to place patients into low-risk, medium-risk or high-risk categories [38]. Cytogenic abnormalities such as genetic mutations, genetic deletions and chromosomal translocations are identified using genome wide association studies that screen high-risk B-ALL patient samples [33, 39].

These studies proved useful in that they reported high-risk B-ALL patients as having translocations such as BCR-ABL (also known as Philadelphia chromosome-positive (Ph+)) or mutations and/or deletions in the *IKZF1* and *CRLF2* genes [40-41] . More recently, a high-risk subset of B-ALL was identified. This subset is referred to as BCR-ABL-like or Ph-like ALL. Patients in this subset have a similar genetic profile to Ph+ B-ALL, but lack the BCR-ABL fusion protein [41]. This subset is characterized by an increased occurrence of *IKZF1* gene defects and 50% of these patients have *CRLF2* gene alterations [41]. The *CRLF2* gene alterations include a translocation between the IGH promoter and the *CRLF2* gene producing a fusion transcript or an intra-chromosomal deletion that forms a P2RY8-CRLF2 fusion transcript [41-42]. The CRLF2 genetic defects lead to the over-expression of the CRLF2 protein (the receptor component

for TSLP) on the surface of B-ALL cells and this subset of B-ALL is referred to as CRLF2 B-ALL.

Significance of Study

Identifying Molecular Targets in CRLF2 Signaling Pathway

ALL is the most common childhood malignancy and B-ALL accounts for 80% of these cases [37]. With current therapies, ~25% of pediatric B-ALL patients still relapse and ~15% of these children are most likely to fail therapy and die [38]. The high-risk Ph-like B-ALL accounts for 10-15% of childhood B-ALL. Though Ph-like B-ALL has a heterogeneous genetic profile (unlike Ph+ B-ALL), ~50% of this subset of B-ALL have genetic defects in the *CRFL2* gene [41]. The translocation leading to the BCR-ABL+ B-ALL subtype was the first of the genetic alterations to be identified and tyrosine kinase inhibitors (TKIs) that specifically target the aberrant kinase activity produced by the BCR-ABL translocation have been developed into drugs and are currently used to treat patients [43-44]. This provides a paradigm for targeting pathways that are activated as a result of genetic defects that are associated with high-risk leukemia. Despite the progress made in relation to the survival outcomes of patients with the BCR-ABL translocation, the survival outcomes of patients with *CRLF2* gene defects continue to experience poor survival outcomes. Further, the mechanism of disease and downstream molecular mediators that contribute to CRLF2 B-ALL remains to be elucidated. The studies described in the subsequent chapters of this dissertation are significant because they identified molecular targets in the CRLF2 signaling pathway that regulate CRLF2 B-ALL cell survival and can serve as druggable targets.

Reducing Childhood Cancer Health Disparities

For ten years we have known that Hispanic children are more likely to develop ALL (1.2 times more likely) and when they do, they are more likely to die (39% higher death rate) when compared to other children [45]. Genome-wide association studies of samples from high-risk B-ALL patients revealed that CRLF2 B-ALL is five times more prevalent in Hispanic children and they experience a higher rate of relapse and an overall poorer prognosis [46]. This is further accentuated in geographical locations where there is a dense population of Hispanics such as California. Thus, over-expression of CRLF2 is one of most significant biological components of childhood cancer health disparities identified to date and is likely a major contributor to the increased incidence and higher mortality rate for ALL in Hispanic children. Most of the health disparity studies conducted so far focus on 1) examining the relationship between ethnicity and mortality; 2) the relationship between ethnicity and treatment outcomes and 3) the prevalence of genetic defects and ancestry-related genetic alterations such as single nucleotide polymorphisms [46-48]. The studies described in this dissertation are significant because we identified TSLP-induced biological pathways and molecules that regulate the survival of CRLF2 B-ALL, which is most prevalent among Hispanics. Additionally, the animal model we developed provides a tool that can be used to study the mechanisms of CRLF2 B-ALL in Hispanic patient samples. The results from these studies offer the potential to identify biological factors that contribute to the health disparity observed in Hispanic children and can be targeted with appropriate therapies to improve survival outcomes, thereby alleviating the disparity.

Identifying Therapies to Target CRLF2 Signaling Pathway

Improved remission rates in recent years are primarily due to the administration of higher doses of standard chemotherapy [49]. Despite the success of current therapeutic strategies with some high-risk B-ALL such as Ph+ B-ALL, CRLF2 B-ALL patients still experience a 65% relapse rate [34]. Therefore current treatment regimens have been ineffective in reducing the relapse-rate of CRLF2 B-ALL. In addition**,** higher doses of chemotherapy have resulted in increased toxicity and side effects for patients [50-52]. Imatinib, when used in combination with standard therapy, increased survival of children with Ph+ B-ALL from ~35% to 80% [44, 53]. The results achieved with Imatinib's ability to target the kinase in Ph+ B-ALL was ground breaking and provided a model that can be followed in order to identify therapies to treat CRLF2 B-ALL. The studies outlined in this dissertation are significant in that they identified therapeutic candidates that exhibited efficacy on CRLF2 B-ALL and other high-risk B-ALL by targeting molecular mediators of the CRLF2 signaling pathway and cellular processes. These drug candidates show promise and have the potential to be used in combination with standard therapy to increase efficacy of treatment for CRLF2 B-ALL.

Scientific Approach

Rationale

Studies in high-risk B-ALL including CRLF2 B-ALL, which were conducted by Children Oncology Groups (COGs), have been directed towards genetic screening to identify high-risk patients using risk stratification schemes [33, 38]. Additional studies were conducted to assess CRLF2 B-ALL patient response to current treatment options

and to determine therapeutic outcome, but very little is known about the cellular and molecular mechanisms that contribute to the progression of the disease [34, 54]. Recent molecular studies have shown that in some cases CRLF2 is associated with activating mutations in JAKs that act downstream of TSLP-CRLF2 interactions. These activating mutations have been shown to promote constitutive dimerization, constitutive JAK-STAT activation and cytokine independent growth in the murine BAF3 cellular model system [42, 55]. These data have led others to the conclusion that over-expression of CRLF2 and activating JAK mutations are the major contributors to this disease suggesting that CRLF2 B-ALL cells do not require TSLP-induced signals for survival and proliferation due to constitutive activation of the JAK-STAT pathway. However, all JAK mutations are not activating and 30% of CRLF2 B-ALL patients have no mutations in JAKs.

Our lab and others have shown that TSLP induces proliferation of normal human B-cell precursors via activation of JAK-STAT or mTOR pathways [20, 24][TM unpub data]. In addition, our lab has demonstrated that TSLP is produced by bone marrow stromal cells and thus is present in the BM microenvironment where leukemia develops [TM unpub data]. Our lab also showed that TSLP increases STAT5 phosphorylation in CRLF2 B-ALL. These data provided a rationale for evaluating the role of the TSLP-induced CRLF2 signaling in the development and/or maintenance of CRLF2 B-ALL. Not long after, Tasian, et al showed that stimulating primary CRLF2 B-ALL cells resulted in what they termed as "aberrant" activation of JAT-STAT and PI3K/mTOR signaling [25]. Further their studies confirmed that TSLP can indeed stimulate CRLF2 B-ALL cells with or without JAK mutations thereby strengthening our rationale for conducting TSLP-induced studies. Additionally, *in vivo* studies to evaluate the efficacy of treatments for

CRLF2 B-ALL are conducted in context of the presence or absence of JAK-mutations and without TSLP-induced CRLF2 signals [56]. Thus, the contributions of TSLP (the ligand that stimulates CRLF2 signaling) to the development, maintenance and/or progression of CRLF2 B-ALL and the cellular and molecular mediators involved remain to be fully elucidated. Therefore the objective of my dissertation studies was to elucidate the TSLP-induced cellular and molecular mechanisms that contribute to CRLF2 B-ALL and to identify promising drug candidates to target this disease.

Based on findings from the literature and data obtained from our lab, we hypothesized that TSLP contributes to CRLF2 B-ALL by increasing proliferation and/or survival of leukemia cells via regulation of genes downstream of TSLP-CRLF2 pathway activation. The hypothesis was tested conducting experiments according to three specific aims and their respective sub-aims. **Aim 1: Optimize the novel hTSLP+/- xenograft model for use in defining the role of TSLP in CRLF2 B-ALL.** *Aim 1.1 Engineer immune deficient mice to express human TSLP; Aim 1.2 determine whether CRLF2 pathways are activated in vivo in hTSLP+ mice*. **In Aim 2: Identify TSLP-induced cellular and molecular mechanisms that contribute to CRLF2 B-ALL.** *Aim 2.1 compare apoptosis status of CRLF2 B-ALL cells from hTSLP+ and hTSLP- mice; Aim 2.2 identify pro-survival genes that are regulated by TSLP*. **Aim 3: Assess candidate drugs' efficacy against high-risk B-ALL.** *Aim 3.1 evaluate candidate cancer drugs for in vitro efficacy in high-risk B-ALL; Aim 3.2 use the human-mouse xenograft model to evaluate the in vivo efficacy of candidate drugs in high-risk B-ALL.*

Innovation

A Novel *In-vivo* Model to Identify TSLP-induced Molecular Mediators in CRLF2 B-ALL

Preliminary data from our lab shows that pediatric BM stromal cells express the TSLP growth factor and thus provide an *in vivo* source of TSLP to stimulate CRLF2 B-ALL cells [TM unpub data]. Therefore it is important that *in vivo* studies to evaluate therapies for CRLF2 B-ALL be performed in an *in vivo* model that includes TSLP, which can stimulate activation of the CRLF2 signaling pathway in these cells. Human-mouse xenograft models produced by injecting human leukemia cells into immune deficient mice are the *in vivo* models of choice for identifying effective chemotherapies to treat leukemia [57-58]. These models are possible because many growth factors and cytokines produced in the mouse act on human cells. However, mouse TSLP does not stimulate human CRLF2 [59]. Therefore standard xenograft models are inadequate for evaluating the role of TSLP-induced signaling and downstream molecular mediators in CRLF2 B-ALL. Our lab has modified the human-mouse xenograft model currently used by other researchers to produce a novel human TSLP+/– xenograft model system composed of mice that express human TSLP (hTSLP+) or mice without human TSLP (hTSLP–) [60]. Studies shown in this dissertation include xenograft mice that were transplanted with primary CRLF2 B-ALL cells taken from patient samples collected at the Loma Linda University Medical Center (LLUMC) through collaboration with the Pediatric Oncology Group (POG). These studies are innovative in that they are the first studies in which human leukemia cells harvested from hTSLP+/hTSLP- xenograft mice were used to

identify TSLP-induced *in vivo* cellular processes and molecular mediators in CRLF2 B-ALL.

New Therapeutics to Target the CRLF2-Signaling Pathway

CRLF2 B-ALL patients experience a high rate of relapse with current therapies. We have ongoing collaborations with internal and external research groups that have synthesized novel compounds to test for the treatment of high-risk B-ALL, including CRLF2 B-ALL. Candidate drugs included the following: 1) Novomedix (NM) lead series drugs: a series of small molecule drugs that have been shown to target cell cycle and protein translation functions in cells; 2) Mcl-1 inhibitor: a small molecule inhibitor that shows selective inhibition of the anti-apoptotic functions of the Bcl2 family member, Mcl-1 [62]. These studies are innovative in that they explore novel therapeutic candidates (in the case of the NM drugs) as well they utilize a novel approach of using known drug candidates (such as the Mcl-1 inhibitor) to identify potential therapeutic candidates to treat high-risk leukemia such CRLF2 B-ALL and Nalm6.

Tools and Models

CRLF2 B-ALL Cell Lines

Human CRLF2 B-ALL cell lines were used to study the role of TSLP stimulation in CRLF2 B-ALL cells *in vitro* and *in vivo* as well as in drug efficacy studies. Cell lines are easy to culture, thus they are excellent tools for performing cellular and molecular *in vitro* studies.

Primary CRLF2 B-ALL Cells

Even though cell lines are excellent tools, these cells may undergo changes over time, which may make them different from the original cells taken directly from a patient. Primary cells are difficult to culture and to manipulate, but they are the closest representation of the patient condition, thus it is important to study these cells. Therefore primary cells were also used to validate results. Primary cells were collected from collaborations with Hematology Oncologists in the LLUMC under approved IRB protocols.

HTSLP+/HTSLP- Xenograft Samples

Studies that assessed the effects of TSLP on CRLF2 B-ALL at the cellular and molecular levels were conducted using CRLF2 B-ALL cell lines or primary cells that were expanded in hTSLP+ and hTSLP- mice. These samples allowed us to compare proliferation, apoptosis, gene expression and protein expression of human CRLF2 B-ALL cells taken from an *in vivo* microenvironment containing human TSLP compared to those taken from mice without TSLP.

References

1. Monroe, J.G. and K. Dorshkind, *Fate decisions regulating bone marrow and peripheral B lymphocyte development*. Adv Immunol, 2007. **95**: p. 1-50.

2. Ramirez, J., K. Lukin, and J. Hagman, *From hematopoietic progenitors to B cells: mechanisms of lineage restriction and commitment*. Current Opinion in Immunology, 2010. **22**(2): p. 177-184.

3. Jung, D., et al., *Mechanism and control of V(D)J recombination at the immunoglobulin heavy chain locus*. Annu Rev Immunol, 2006. **24**: p. 541-70.

4. Hamel, K.M., et al., *Balancing Proliferation with Igkappa Recombination during B-lymphopoiesis*. Front Immunol, 2014. **5**: p. 139.

5. Alt, F.W., T.K. Blackwell, and G.D. Yancopoulos, *Development of the primary antibody repertoire*. Science, 1987. **238**(4830): p. 1079-87.

6. Vettermann, C. and M.S. Schlissel, *Allelic exclusion of immunoglobulin genes: models and mechanisms*. Immunol Rev, 2010. **237**(1): p. 22-42.

7. Kracker, S. and A. Durandy, *Insights into the B cell specific process of immunoglobulin class switch recombination*. Immunology Letters, 2011. **138**(2): p. 97-103.

8. Nagasawa, T., *Microenvironmental niches in the bone marrow required for B-cell development*. Nat Rev Immunol, 2006. **6**(2): p. 107-16.

9. Bianco, P., et al., *Bone marrow stromal stem cells: nature, biology, and potential applications*. Stem Cells, 2001. **19**(3): p. 180-92.

10. Krebs, D.L. and D.J. Hilton, *SOCS proteins: negative regulators of cytokine signaling*. Stem Cells, 2001. **19**(5): p. 378-87.

11. Carvalho, T.L., et al., *Arrested B lymphopoiesis and persistence of activated B cells in adult interleukin 7(-/)- mice*. J Exp Med, 2001. **194**(8): p. 1141-50.

12. Dias, S., et al., *Interleukin-7 is necessary to maintain the B cell potential in common lymphoid progenitors*. J Exp Med, 2005. **201**(6): p. 971-9.

13. Miller, J.P., et al., *The earliest step in B lineage differentiation from common lymphoid progenitors is critically dependent upon interleukin 7*. J Exp Med, 2002. **196**(5): p. 705-11.

14. Parrish, Y.K., et al., *IL-7 Dependence in human B lymphopoiesis increases during progression of ontogeny from cord blood to bone marrow*. J Immunol, 2009. **182**(7): p. 4255-66.

15. Yadava, K., et al., *Thymic stromal lymphopoietin plays divergent roles in murine models of atopic and non-atopic airway inflammation*. Allergy, 2014.

16. He, R., et al., *TSLP acts on infiltrating effector T cells to drive allergic skin inflammation*. Proc Natl Acad Sci U S A, 2008. **105**(33): p. 11875-80.

17. Ito, T., et al., *TSLP-activated dendritic cells induce an inflammatory T helper type 2 cell response through OX40 ligand*. Journal of Experimental Medicine, 2005. **202**(9): p. 1213-1223.

18. Ying, S., et al., *Thymic stromal lymphopoietin expression is increased in asthmatic airways and correlates with expression of Th2-attracting chemokines and disease severity*. J Immunol, 2005. **174**(12): p. 8183-90.

19. Zhou, B.H., et al., *Thymic stromal lymphopoietin as a key initiator of allergic airway inflammation in mice*. Nature Immunology, 2005. **6**(10): p. 1047-1053.

20. Scheeren, F.A., et al., *Thymic stromal lymphopoietin induces early human B-cell proliferation and differentiation*. Eur J Immunol, 2010.

21. Kang, J. and M. Coles, *IL-7: The global builder of the innate lymphoid network and beyond, one niche at a time*. Seminars in Immunology, 2012. **24**(3): p. 190-197.

22. Rochman, Y., et al., *Thymic stromal lymphopoietin-mediated STAT5 phosphorylation via kinases JAK1 and JAK2 reveals a key difference from IL-7-induced signaling*. Proc Natl Acad Sci U S A, 2010. **107**(45): p. 19455-60.

23. Malin, S., et al., *Role of STAT5 in controlling cell survival and immunoglobulin gene recombination during pro-B cell development*. Nature Immunology, 2010. **11**(2): p. 171-9.

24. Brown, V.I., et al., *Thymic stromal-derived lymphopoietin induces proliferation of pre-B leukemia and antagonizes mTOR inhibitors, suggesting a role for interleukin-7Ralpha signaling*. Cancer Res, 2007. **67**(20): p. 9963-70.

25. Tasian, S.K., et al., *Aberrant STAT5 and PI3K/mTOR pathway signaling occurs in human CRLF2-rearranged B-precursor acute lymphoblastic leukemia*. Blood, 2012.

26. Hagman, J. and K. Lukin, *Transcription factors drive B cell development*. Curr Opin Immunol, 2006. **18**(2): p. 127-34.

27. Dias, S., et al., *E2A proteins promote development of lymphoid-primed multipotent progenitors*. Immunity, 2008. **29**(2): p. 217-27.

28. Nutt, S.L., et al., *Pax5 determines the identity of B cells from the beginning to the end of B-lymphopoiesis*. Int Rev Immunol, 2001. **20**(1): p. 65-82.

29. Cobaleda, C., W. Jochum, and M. Busslinger, *Conversion of mature B cells into T cells by dedifferentiation to uncommitted progenitors*. Nature, 2007. **449**(7161): p. 473-7.

30. Payne, K.J. and G.M. Crooks, *Human hematopoietic lineage commitment*. Immunological Reviews, 2002. **187**: p. 48-64.

31. Downing, J.R. and C.G. Mullighan, *Tumor-specific genetic lesions and their influence on therapy in pediatric acute lymphoblastic leukemia*. Hematology Am Soc Hematol Educ Program, 2006: p. 118-22, 508.

32. Dovat, S., et al., *Ikaros, CK2 kinase, and the road to leukemia*. Mol Cell Biochem, 2011. **356**(1-2): p. 201-7.

33. Mullighan, C.G., et al., *Genome-wide analysis of genetic alterations in acute lymphoblastic leukaemia*. Nature, 2007. **446**(7137): p. 758-64.

34. Chen, I.M., et al., *Outcome modeling with CRLF2, IKZF1, JAK and minimal residual disease in pediatric acute lymphoblastic leukemia: a Children's Oncology Group Study*. Blood, 2012.

35. Swanson, P.J., et al., *Fatal acute lymphoblastic leukemia in mice transgenic for B cell-restricted bcl-xL and c-myc*. Journal of Immunology, 2004. **172**(11): p. 6684-91.

36. Mullighan, C.G., *The molecular genetic makeup of acute lymphoblastic leukemia*. Hematology Am Soc Hematol Educ Program, 2012. **2012**: p. 389-96.

37. Pui, C.H., L.L. Robison, and A.T. Look, *Acute lymphoblastic leukaemia*. Lancet, 2008. **371**(9617): p. 1030-43.

38. Harvey, R.C., et al., *Identification of novel cluster groups in pediatric high-risk B-precursor acute lymphoblastic leukemia with gene expression profiling: correlation with genome-wide DNA copy number alterations, clinical characteristics, and outcome*. Blood, 2010.

39. Collins-Underwood, J.R. and C.G. Mullighan, *Genomic profiling of high-risk acute lymphoblastic leukemia*. Leukemia, 2010.

40. Hunger, S.P., *Tyrosine Kinase Inhibitor Use in Pediatric Philadelphia Chromosome-Positive Acute Lymphoblastic Anemia*. Hematology-American Society Hematology Education Program, 2011: p. 361-365.

41. Roberts, K.G., et al., *Outcomes of Children With BCR-ABL1-Like Acute Lymphoblastic Leukemia Treated With Risk-Directed Therapy Based on the Levels of Minimal Residual Disease*. Journal of Clinical Oncology, 2014.

42. Yoda, A., et al., *Functional screening identifies CRLF2 in precursor B-cell acute lymphoblastic leukemia*. Proc Natl Acad Sci U S A, 2010. **107**(1): p. 252-7.

43. Druker, B.J., et al., *Activity of a specific inhibitor of the BCR-ABL tyrosine kinase in the blast crisis of chronic myeloid leukemia and acute lymphoblastic leukemia with the philadelphia chromosome*. New England Journal of Medicine, 2001. **344**(14): p. 1038-1042.

44. Fielding, A.K., *Current treatment of Philadelphia chromosome-positive acute lymphoblastic leukemia*. Hematology Am Soc Hematol Educ Program, 2011. **2011**: p. 231-7.

45. Ensor, H.M., et al., *Demographic, clinical, and outcome features of children with acute lymphoblastic leukemia and CRLF2 deregulation: results from the MRC ALL97 clinical trial*. Blood, 2011. **117**(7): p. 2129-36.

46. Harvey, R.C., et al., *Rearrangement of CRLF2 is associated with mutation of JAK kinases, alteration of IKZF1, Hispanic/Latino ethnicity, and a poor outcome in pediatric B-progenitor acute lymphoblastic leukemia*. Blood, 2010.

47. Patel, M.M., Y; Mitchell, BS; Rhoads, KF, *Understanding disparities in leukemia: a national study*. Cancer Causes and Control, 2012.

48. Pui, C.H.M., C.G.; Evans, W.E.; Relling, M.V., *Pediatric acute lymphoblastic leukemia: where are we going and how do we get there?* Blood, 2012. **120**(6): p. 1165-1174.

49. Nguyen, K., et al., *Factors influencing survival after relapse from acute lymphoblastic leukemia: a Children's Oncology Group study*. Leukemia, 2008. **22**(12): p. 2142-50.

50. Nguyen, K., et al., *Factors influencing survival after relapse from acute lymphoblastic leukemia: a Children's Oncology Group study*. Leukemia, 2008. **22**(12): p. 2142-2150.

51. Pui, C.H., *Central nervous system disease in acute lymphoblastic leukemia: prophylaxis and treatment*. Hematology Am Soc Hematol Educ Program, 2006: p. 142-6.

52. Kamdem, L.K., et al., *Genetic predictors of glucocorticoid-induced hypertension in children with acute lymphoblastic leukemia*. Pharmacogenet Genomics, 2008. **18**(6): p. 507-14.

53. Hunger, S.P., et al., *Improving outcomes for high-risk ALL: translating new discoveries into clinical care*. Pediatr Blood Cancer, 2011. **56**(6): p. 984-93.

54. Cario, G., et al., *Presence of the P2RY8-CRLF2 rearrangement is associated with a poor prognosis in non-high-risk precursor B-cell acute lymphoblastic leukemia in children treated according to the ALL-BFM 2000 protocol*. Blood, 2010.

55. Mullighan, C.G., et al., *Rearrangement of CRLF2 in B-progenitor- and Down syndrome-associated acute lymphoblastic leukemia*. Nat Genet, 2009. **41**(11): p. 1243-6.

56. Maude, S.L.T., S.K.; Vincent, T.; Hall, J.W.; Sheen, C. et al, *Targeting JAK1/2 and mTOR in murine xenograft models of Ph-like acute lymphoblastic leukemia (ALL)*Blood, 2012.

57. Liem, N.L., et al., *Characterization of childhood acute lymphoblastic leukemia xenograft models for the preclinical evaluation of new therapies*. Blood, 2004. **103**(10): p. 3905-14.

58. Lock, R.B., N.L. Liem, and R.A. Papa, *Preclinical testing of antileukemic drugs using an in vivo model of systemic disease*. Methods Mol Med, 2005. **111**: p. 323-34.

59. Reche, P.A., et al., *Human thymic stromal lymphopoietin preferentially stimulates myeloid cells*. J Immunol, 2001. **167**(1): p. 336-43.

60. Agliano, A., et al., *Human acute leukemia cells injected in NOD/LtSz-scid/IL-2Rgamma null mice generate a faster and more efficient disease compared to other NOD/scid-related strains*. Int J Cancer, 2008. **123**(9): p. 2222-7.

61. de Paiva, L.S., et al., *Selective blockade of lymphopoiesis induced by kalanchosine dimalate: inhibition of IL-7-dependent proliferation*. J Leukoc Biol, 2008. **83**(4): p. 1038-48.

62. Cohen, N.A., et al., *A competitive stapled peptide screen identifies a selective small molecule that overcomes MCL-1-dependent leukemia cell survival*. Chem Biol, 2012. **19**(9): p. 1175-86.

CHAPTER TWO

A NOVEL XENOGRAFT MODEL TO STUDY THE ROLE OF TSLP-CRLF2 SIGNALS IN NORMAL AND MALIGNANT HUMAN B-LYMPHOPOIESIS

Abstract

The cytokine, TSLP, stimulates *in vitro* proliferation of human fetal B cell progenitors, however, its *in vivo* role during normal human B lymphopoiesis is unknown. Genetic alterations that cause overexpression of the TSLP receptor component, CRLF2, lead to B cell acute lymphoblastic leukemia (CRLF2 B-ALL), implicating the TSLP-CRLF2 pathway in leukemogenesis. Engineered cellular models suggest that mouse TSLP is unlikely to activate human CRLF2-mediated signals, limiting the utility of classic human-mouse xenografts for studies of the TSLP-CRLF2 pathway in normal and malignant B lymphopoiesis. First, we show that mouse TSLP does not induce activation of the CRLF2 downstream pathways (JAK/STAT5 and PI3K/AKT/mTOR) that are activated by human TSLP (hTSLP) in CRLF2 B-ALL cells. Next, we engineered xenograft mice to produce hTSLP (+T mice) by transplantation with stromal cells transduced to express hTSLP. Controls (–T mice) were produced by transplantation with stroma transduced with a control vector. Normal serum levels of hTSLP were achieved in +T mice, while hTSLP was undetectable in –T mice. hTSLP produced by +T stroma induced JAK/STAT5 and PI3K/AKT/mTOR pathway activation and showed functional *in vivo* effects on normal human B cell progenitors and primary CRLF2 B-ALL cells. Gene expression profiling of primary CRLF2 B-ALL cells showed an induction of mTOR regulated gene expression and increased TSLP-regulated gene responsiveness

when cells were expanded in +T as compared to –T mice. The novel +T/–T xenograft model developed here provides a tool for understanding the role of the TSLP-CRLF2 pathway in normal and malignant hematopoiesis.

Abbreviations

B-ALL	B-cell Acute Lymphoblastic Leukemia
TSLP	Thymic Stromal Lymphopoietin
CRLF2	Cytokine Receptor-Like Factor 2
JAK	Janus Kinase
STAT5	Signal Transducer and Activator of Transcription 5
mTOR	Mammalian Target Of Rapamycin
PDX	Patient Derived Xenograft
PI3K	Phosphoinositide-3-Kinase
AKT	Protein Kinase B
IL-7Rα	Interleukin 7 Receptor alpha chain
mTSLP	Mouse TSLP
hTSLP	Human TSLP
S6	Ribosomal protein S6
NSG	NOD/SCID Gamma (NOD.Cg-Prkdc^{scid}Il2rg^{tm1Wjl}/SzJ)
BM	Bone Marrow
HS27	Human Stroma 27 (bone marrow stromal cell line)

Introduction

TSLP plays key roles at several points in normal hematopoietic cell development and function, including early stages of B cell development (1-4). TSLP is an IL-7-like cytokine that can replace IL-7 in stimulating the expansion of murine B cell precursors (5, 6). The role of TSLP in the production of human B cells is less clear, although it has been shown to support the proliferation of human fetal B cell progenitors (7, 8). Genetic alterations that cause overexpression of a TSLP receptor component, CRLF2, have been linked to B cell acute lymphoblastic leukemia (B-ALL), thus implicating the TSLP pathway in leukemogenesis (9-12).

B-ALL is the most common childhood malignancy (13-15) and despite advances in treatment strategies**,** ~25% of pediatric B-ALL patients relapse (16). Genomic profiling studies have identified several high-risk B-ALL subtypes that are resistant to chemotherapy (17-20). CRLF2 B-ALL is a high-risk subtype characterized by alterations of the *CRLF2* gene leading to over-expression of the CRLF2 protein on the surface of B-ALL cells (9-12). CRLF2 and the IL-7 receptor alpha chain (IL-7Rα) together form a cytokine receptor signaling complex that is activated by TSLP (Figure 2.1) (6, 21). Binding of TSLP induces CRLF2 to dimerize with the IL-7R component leading to activation of the JAK-STAT5 pathway (22, 23) as well as the PI3K/AKT/mTOR pathway (24, 25). The finding that JAK kinases are mutated in CRLF2 B-ALL (26) suggested that CRLF2 and mutated JAK cooperate to induce constitutive STAT5 activation in CRLF2 B-ALL (27, 28). However, approximately half of CRLF2 B-ALL lack JAK mutations. Thus, the role of TSLP in CRLF2 B-ALL remains unclear.

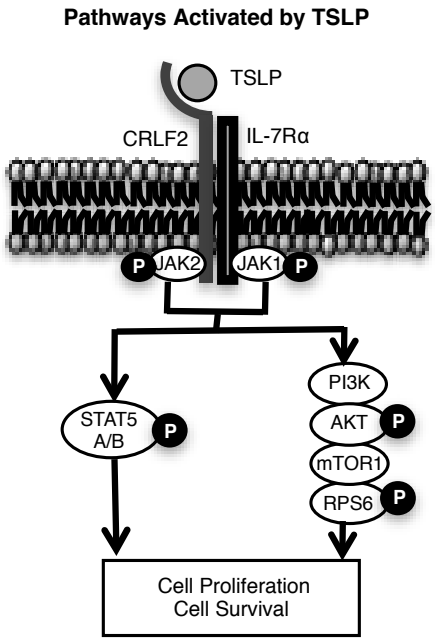

Fig. 2.1: Pathways activated downstream of TSLP receptor signaling in human cells.

Patient-derived xenograft (PDX) models produced by injecting human cells into immune deficient mice provide *in vivo* preclinical models for understanding disease mechanisms and identifying effective therapies. However, the available data (6) suggests that TSLP produced in the mouse (mTSLP) is unlikely to stimulate CRLF2-mediated signaling in human cells. Given the role of TSLP in activating the CRLF2 pathway and the downstream proliferation of human B cell progenitors, it will be important that studies to identify disease mechanisms and potential therapies for CRLF2 B-ALL be performed in preclinical models that provide human TSLP (hTSLP).

Here we describe the development of a novel xenograft model system comprised of mice that provide hTSLP (+T mice) and mice that do not (–T mice). +T xenograft mice show functional *in vivo* hTSLP effects, expanding the production of normal B lineage cells from hematopoietic stem cells and inducing changes in mTOR-regulated

gene expression in primary CRLF2 B-ALL cells. The +T/–T xenograft model system provides an important new model for understanding the role of TSLP in normal and malignant B lymphopoiesis.

Materials and Methods

Human Samples and Cell Lines

Human CRLF2 B-ALL cell lines MUTZ5 and MHH-CALL4 were purchased from DSMZ (Braunschweig, Germany). The human stromal cell line HS27 was purchased from ATCC (Manassas, VA). Primary human CRLF2 B-ALL cells and umbilical cord blood (CB) were obtained in accordance with protocols approved by the Loma Linda University Institutional Review Board (IRB) and with the Helsinki Declaration of 1975, as revised in 2008. CD34+ cells were isolated from CB as described in companion paper. Culture media are described in the online supplementary methods.

Mice

Studies were performed using NOD.Cg-Prkdc^{scid} Il2rg^{tm1Wjl}/SzJ (NSG) mice (Jackson Laboratory). Mice were housed under pathogen-free conditions in the Loma Linda University Animal Care Facility and studies were conducted in accordance with Loma Linda University Institutional Animal Care and Use Committee (IACUC) approved protocols.

Flow Cytometry

Cells were prepared for flow cytometry to detect surface antigens using protocols

described in companion paper. Details of phospho-flow cytometry and specific antibody clones and conjugates are described in online supplementary methods. Flow cytometry analysis was performed using a MACSQuant analyzer (MiltenyiBiotec, Inc, Auburn, CA) and Flowjo flow cytometry data analysis software (TreeStar, Ashland, OR)

Stromal Cell Transduction

Human HS27 stromal cells were transduced to express hTSLP (+T stroma) or with control vector (–T stroma) at a multiplicity of infection of 0.5-5/cell overnight. After transduction, cells were washed, expanded in culture, and frozen in aliquots. For the generation of +T and –T mice, stromal cells were thawed, cultured, and injected into mice within 15 passages after thawing. Details of lentiviral vector production and ELISAs to determine hTSLP levels are available in online supplementary methods.

Xenograft Transplantation

HS27 stroma that were transduced to be +T or –T were injected intraperitoneally into NSG mice at doses of 5 or $10x10^6$ cells at time points described in the results section. Mice were sub-lethally irradiated with 225 cGy, then transplanted by tail vein injection with freshly thawed human umbilical cord blood CD34+ cells ($1x10^5$) or primary CRLF2 B-ALL ($5x10^5$) cells.

Microarray Analysis of Gene Expression in CRLF2 B-ALL Cells

Microarray analysis of gene expression in patient-derived CRLF2 B-ALL cells following TSLP stimulation *in vivo* and *ex vivo* were performed by Miltenyi Biotec's

Genomic Services (Miltenyi Biotec GmbH, Bergisch Gladbach) using Agilent Whole Human Genome Oligo Microarrays (Design ID 039494, 8x60K v2). Gene Set Enrichment Analysis (GSEA) was performed by Novogenix Laboratories, LLC (Los Angeles, CA). Details of microarray assays, data processing, differential gene expression analysis, GSEA, Ingenuity Pathway Analysis (IPA) and quantitative RT-PCR analysis are described in the online supplementary methods. The data discussed in this publication have been deposited in NCBI's Gene Expression Omnibus (29) and are accessible through GEO Series accession number GSE65274 (http://www.ncbi.nlm.nih.gov/geo/query/acc.cgi?acc= GSE65274).

Results

Mouse TSLP does not Activate the Human TSLP Receptor Complex

Activation of the human TSLP receptor complex can be induced by hTSLP, but not by mTSLP, in murine Ba/F3 cells transduced to express human CRLF2 and IL-7Rα (6). These data suggest that mTSLP is unlikely to activate human CRLF2-mediated signals in human-mouse xenograft models. However, the ability of mTSLP to activate CRLF2- signaling in human cells, particularly those expressing high levels of CRLF2 observed in CRLF2 B-ALL, has not been reported. To determine if mTSLP can induce CRLF2-mediated signals we tested its ability to activate downstream pathways in human CRLF2 B-ALL cells. First, we verified that the CRLF2 B-ALL cell lines and primary CRLF2 B-ALL cells used in our studies express both of the TSLP receptor components. Expression of IL-7Rα, as well as high levels of CRLF2, was observed in both CRLF2 B-

ALL cell lines and in the primary CRLF2 B-ALL cells used in studies described here (Figure 2.2).

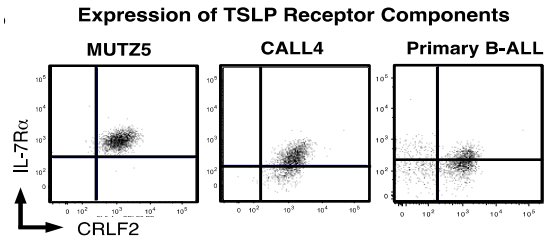

Figure 2.2: CRLF2 B-ALL cell lines (MUTZ5, MHH-CALL4) and primary CRLF2 B-ALL cells used to produce patient-derived xenografts (PDX) used in the studies described here were stained for flow cytometry to detect the TSLP receptor components (IL-7Rα and CRLF2). Plotted are cells within living cell light scatter. Quadrants shown were set based on isotype controls.

Next we used phospho-flow cytometry to determine whether mTSLP can activate the JAK-STAT5 and PI3K/AKT/mTOR pathways activated by hTSLP in CRLF2 B-ALL cells (30). Although hTSLP induced clear increases in phosphorylated STAT5 (pSTAT5) in CRLF2 B-ALL cell lines and primary CRLF2 B-ALL cells, mTSLP showed no effect (Figure 2.3).

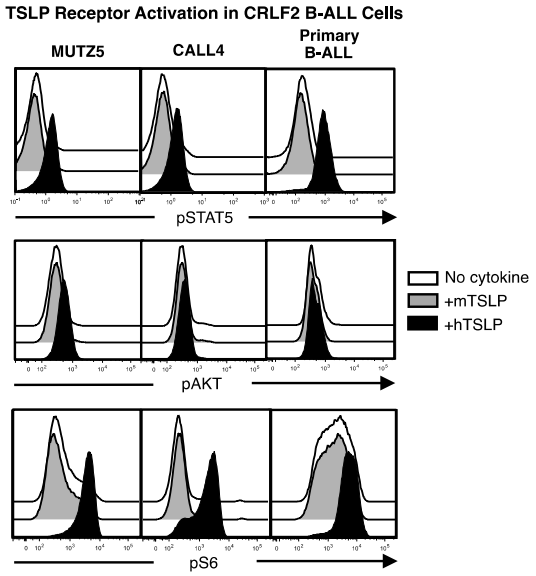

Figure 2.3: CRLF2 B-ALL cell lines and CRLF2 B-ALL cells from a PDX generated from the primary cells in panel C were stimulated with human TSLP (hTSLP) and mouse TSLP (mTSLP) at 15ng/ml, or no cytokine and evaluated for phosphorylated STAT5 (pSTAT5) AKT (pAKT), and S6 (pS6) by intracellular phospho-flow cytometry.

Stimulation of CRLF2 B-ALL cells with mTSLP also failed to increase phosphorylated AKT (pAKT), while hTSLP produced modest increases (Figure 2.3). The ribosomal protein S6 is phosphorylated downstream of mTOR activation (31) and a robust induction of phosphorylated S6 (pS6) was observed in CRLF2 B-ALL cells stimulated with hTSLP (Figure 2.3). In contrast, no increases in pS6 were observed when cells were stimulated with mTSLP (Figure 2.3). Taken together, these data show that mTSLP fails to induce the STAT5, AKT, or S6 phosphorylation that are characteristic of CRLF2-mediated signals induced by hTSLP in human CRLF2 B-ALL cells. Thus, TSLP produced in the mouse cannot induce human CRLF2-mediated signals in existing human-mouse xenograft models.

Engineering Xenograft Mice to Express Normal Serum Levels of Human TSLP

We developed a strategy for engineering xenograft mice that can provide hTSLP to activate CRLF2-mediated signals (Figure 2.4). Expression of human cytokines in xenograft mice has been achieved by transplanting mice with human stromal cells (32). Our strategy was to build on this approach and engineer immune deficient NSG mice that express stable, sustained serum levels of hTSLP similar to normal reported levels in children (range 13-32 pg/ml (33)). This would be achieved by intraperitoneal injection of stromal cells transduced to express high levels of hTSLP. Human HS27 stromal cells were transduced with lentiviral vector containing hTSLP (+T stroma) or with control vector (–T stroma).

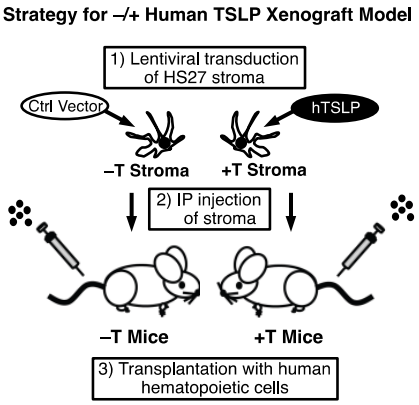

Figure 2.4: Strategy for developing the +/–hTSLP xenograft model: 1) HS27 stromal cells transduced with a lentiviral vector to express hTSLP (+T) or with empty vector control (–T). 2) Transduced stroma intraperitoneally injected to produce +T and –T NSG mice. 3) Human cells injected to produce xenograft mice with hTSLP (+T xenograft mice) and without hTSLP (–T xenograft mice)

Supernatant collected from stroma after multiple passages following the initial transduction with hTSLP was evaluated by ELISA and showed TSLP levels of ~500

pg/ml (Figure 2.5, transduction 1). The ability of +T stroma to generate measureable serum levels of TSLP *in vivo* was evaluated. NSG mice receiving weekly intraperitoneal injections of $5X10^6$ +T stroma showed serum hTSLP levels that were low but detectable (4-10 pg/ml; data not shown) as measured by ELISA. To achieve higher levels of sustained hTSLP expression NSG mice were injected with 3 doses of $1X10^7$ +T or –T stroma over a 1 week period (loading dose) followed by weekly injections of $1X10^7$ stromal cells. Serum was collected at weekly time points and hTSLP levels were evaluated by ELISA. The initial 3 doses of stroma gave serum TSLP levels that were ~80 pg/ml which quickly dropped to 15-20 pg/ml with weekly injections of +T stroma (Figure 2.6, transduction 1). hTSLP was not detectable in the sera of mice transplanted with –T stroma (Figure 2.6, transduction 1). These data show that +T stroma can generate normal serum levels of hTSLP and that serum levels of hTSLP correspond to the number of stromal cells injected during the previous one to two week period. Thus, the loading dose that allowed us to achieve normal serum levels resulted in an initial spike in hTSLP rather than stable sustained levels of serum hTSLP that we had hoped to achieve. These data suggested that stable, sustained TSLP production might be more likely with weekly injections of stroma that could deliver slightly higher doses of TSLP.

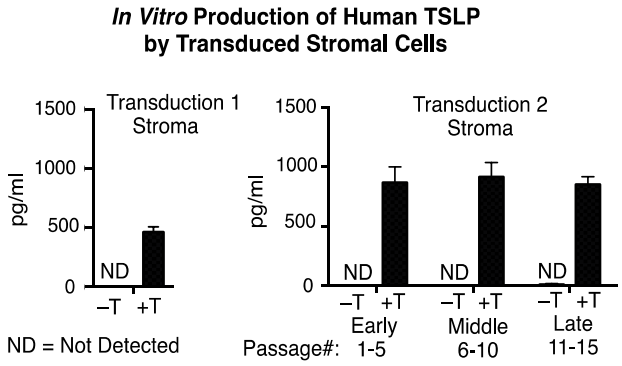

Figure 2.5: Culture supernatant from HS27 +T and HS27 –T stromal cells was assessed by ELISA to determine levels of hTSLP protein produced by HS27 cells from transduction 1 (+T only). Supernatant from transduction 2 was collected at early (passage 1-5), mid (passages 6-10) and late (passages 11-15) post thaw passages and hTSLP levels were evaluated by ELISA.

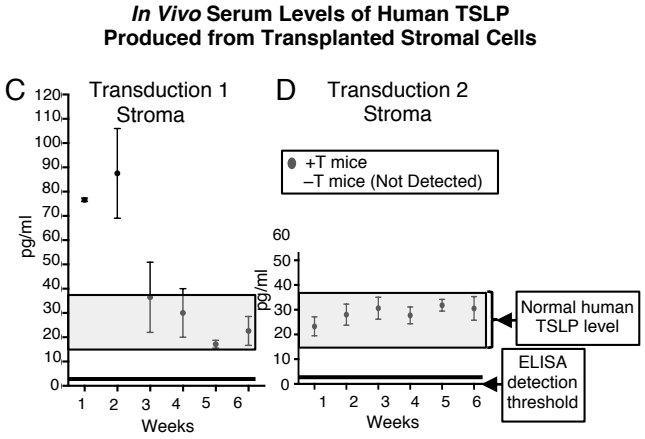

Figure 2.6: Serum levels of hTSLP in blood collected at indicated time points from +T or –T mice injected with stroma as determined by ELISA were as follows: C) loading dose (3 doses of 1X107 in first week) followed by weekly doses of 1X107 stromal cells (transduction 1 cells), graphed are the means ± SEM of n = 2-7 mice at each time point. D) injection of 5X106 stromal cells (transduction 2) at weekly intervals; graphed are the means ± SEM n ≥ 24 mice at each time point.

A second stromal cell transduction was performed. Supernatant was collected at each passage for evaluation of hTSLP protein expression by ELISA. Stable production of hTSLP averaging ~900 pg/ml was observed at early, mid and late passages in +T stroma

across multiple thaws of frozen aliquots from the second transduction (Figure 2.5, transduction 2). hTSLP was undetectable in supernatant from similarly passaged –T stroma (Figure 2.5, transduction 2). NSG mice transplanted at weekly time points with $5X10^6$ stroma from transduction 2 showed serum hTSLP levels of approximately 20 pg/ml that were stable up to 11 weeks (Figure 2.6, transduction 2 and data not shown). To verify that the hTSLP produced in our model induces CRLF2-mediated signals, we assessed CRLF2 B-ALL cell lines for activation of the JAK/STAT5 and PI3K/AKT/mTOR pathways by phospho-flow cytometry. Supernatant from +T stroma induced robust pSTAT5 and pS6 and minimal pAKT (Figure 2.7). In contrast, CRLF2 B-ALL cells stimulated with supernatant from –T stroma showed background levels of pSTAT5, pAKT, and pS6, similar to levels observed in cells incubated with medium alone (Figure 2.7). These data show that +T stroma, but not –T stroma used in our model produce hTSLP that can activate signaling in human CRLF2 B-ALL cells.

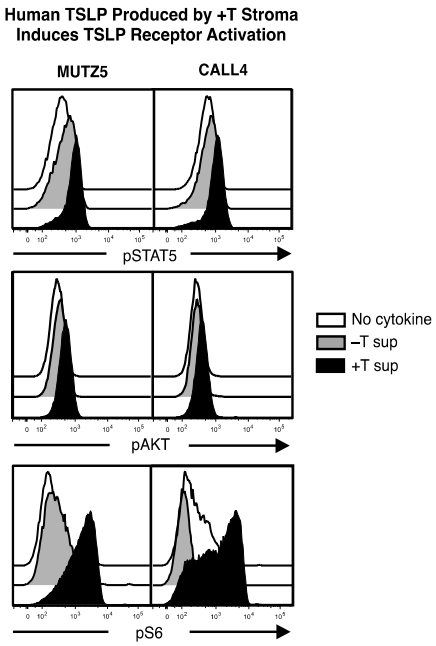

Figure 2.7: CRLF2 B-ALL cell lines were stimulated with stromal cell supernatant and levels of pSTAT5, pAKT and pS6 were measured by intracellular phospho-flow cytometry.

HTSLP Produced in Xenograft Mice Shows Functional Effects on Normal Human B-lineage Cells

Next we evaluated the ability of hTSLP in +T mice to induce functional effects in human B lineage cells in vivo. Normal B cell precursors respond to direct stimulation by TSLP ((4) and companion paper, Figure 1), despite their low levels of CRLF2 expression ((4) and Figure S1-Appdx A), and thus provide a sensitive *in vivo* functional test of the hTSLP produced in our xenograft model. To test our xenograft model we compared normal B cell production in +T and –T NSG mice transplanted with umbilical CB CD34+ cells followed by weekly injections of +T and –T stroma (Figure 2.8A). Five weeks post-transplant mice were euthanized and bone marrow (BM) was harvested for flow cytometry to evaluate the production of B lineage and other hematopoietic cells. Mouse

and human cells were identified based on expression of mouse CD45 (mCD45) and human CD45 (hCD45) respectively (Figure 2.8B). Levels of human cell engraftment were high (>90%) in +T and –T animals, consistent with what we have previously observed in NSG mice transplanted with CB CD34+ cells (Su, unpublished data).

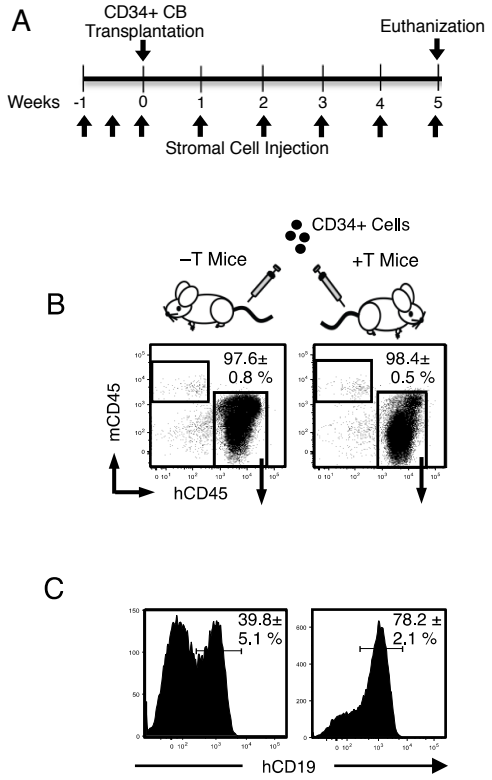

Figure 2.8 A-C: hTSLP produced in +T xenograft mice shows functional effects on normal human B lineage cells. A) –T and +T NSG mice were transplanted with 1 X 10^5 CD34+ human cord blood (CB) cells and injected with weekly doses of $1X10^7$ stromal cells. B) Five weeks post-transplant, mice were euthanized, BM harvested and cells were stained for flow cytometry to detect mouse CD45 (mCD45), human CD45 (hCD45), and hCD19. Total living cells were gated mCD45 vs. hCD45 is plotted with gates to identify mouse and human leukocytes respectively, in the BM. C) hCD45+ cells were gated and hCD19 expression is shown by histogram. Percents are mean + SEM.

TSLP has been shown to increase the *in vitro* production of human B cells ((4) and companion paper). To determine if hTSLP levels achieved in vivo in +T mice could

exert functional effects on normal human B lineage cells we compared the production of hCD19+ B lineage cells in the BM of +T and –T mice. Flow cytometry analysis of hCD19 expression on gated human (mCD45–hCD45+) cells showed that the percentage of B lineage cells was almost double in +T as compared to –T xenograft mice (Figure 2.8C). A comparison of cell numbers in the BM showed that the number of B cells in +T mice was 3-4 fold that observed in the –T animals. This increase was not due to a global increase in hematopoiesis, but rather a selective increase in B cell production, since the number of hCD19– cells in the BM was slightly less in +T as compared to –T xenograft mice (Figure 2.8D). These data show that hTSLP produced in vivo in +T animals has a functional effect on normal human B lineage cells that express low levels of CRLF2.

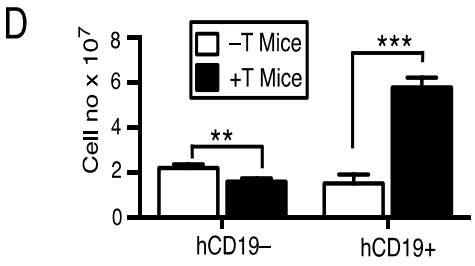

Figure 2.8D: Graphed are the average numbers of non-B lineage (hCD19–) and B lineage (hCD19+) cells isolated from the BM (2 tibia plus 2 femurs) of –T and +T mice as determined by hemocytometer count and flow cytometry (n=3 –T mice and n=5 +T mice). Statistical significance was calculated using a 2-tailed, unpaired t-test (** $p \leq 0.01$; *** $P \leq 0.001$).

HTSLP in Xenograft Mice Induces MTOR-regulated Genes in Primary CRLF2 B-ALL

Our next question was whether hTSLP in the +T animals induces gene expression profiles associated with pathway activation downstream of CRLF2-mediated signaling in primary CRLF2 B-ALL cells. NSG mice for these studies were injected with +T stroma

from transduction 1 and without a loading dose of stroma (Figure 2.9A). Serum levels of hTSLP produced in these mice were detectable but below normal levels (4-10 pg/ml) and therefore provide a sensitive test of hTSLP activity in +T mice.

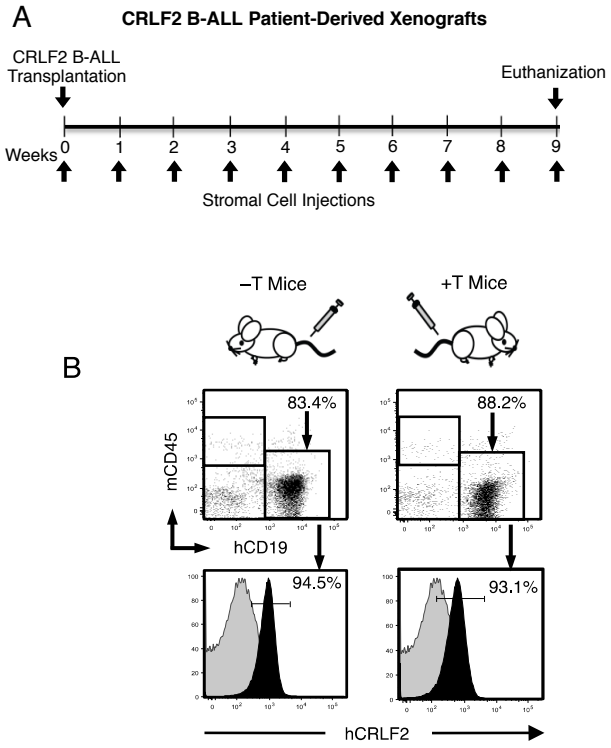

Figure 2.9 A-B: A) –T and +T NSG mice were transplanted with primary CRLF2 B-ALL cells and injected weekly with 5X106 stromal cells. B) 9 weeks post-transplant, mice were euthanized, BM was harvested and cells were stained with mCD45 and hCD19 to identify human B-ALL cells. CRLF2 staining on gated hCD19+ cells is shown in bottom panels.

First, we evaluated the ability of NSG mice transplanted with HS27 stroma to support engraftment of primary B-ALL cells. +T and –T NSG mice were transplanted with primary cells (Figure 2.9B) aspirated from the BM of a Hispanic pediatric patient with CRLF2 B-ALL. Animals were euthanized at 9 weeks when peripheral blood chimerism reached 80%. BM was harvested and stained for mCD45 and human-specific

markers (CRLF2 and CD19) to identify CRLF2 B-ALL cells (Figure 2.9B). Flow cytometry analysis showed BM chimerism of human CRLF2 B-ALL cells was >90% in BM from both +T and –T mice (Figure 2.9B). These data show that NSG mice injected with –T and with +T stroma support engraftment of primary B-ALL cells.

Next we compared gene expression in primary CRLF2 B-ALL cells from +T and –T mice using whole human genome oligo microarrays. Human CRLF2 B-ALL cells were isolated from the BM of +T and –T mice by magnetic separation and whole genome microarray was performed in triplicate using the Agilent platform. Differential gene expression analysis identified 280 gene reporters that were upregulated and 281 gene reporters that were downregulated at least 2 fold (Figure 2.9C). Microarray was validated by quantitative RT-PCR (qRT-PCR) analysis of selected differentially expressed genes (Table 5). Changes in gene expression by microarray and qRT-PCR were strongly correlated as indicated by linear regression (Figure 2.9D).

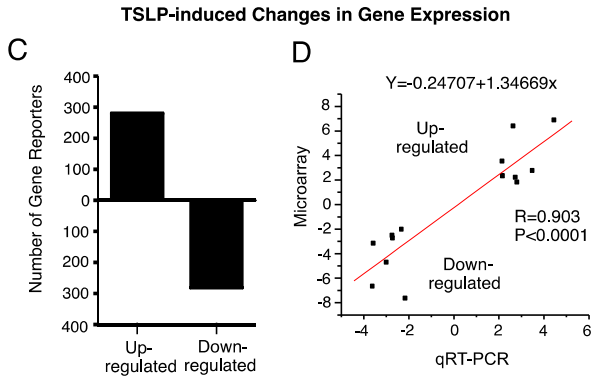

Figure 2.9 C-D: C) Human hCD19+ B-ALL cells were isolated by magnetic separation and analyzed using whole genome microarray to identify genes that are differentially regulated in +T as compared to –T mice. Graphed are the number of Agilent gene reporters up or down-regulated (≥2 fold, p≤ .05) in CRLF2 B-ALL cells from +T as compared to –T mice. D) qRT-PCR validation of whole genome microarray. Regression analysis of fold changes measured by microarray versus fold changes measured by qRT-PCR.

GSEA (34, 35) was used to determine whether pathways induced by TSLP were activated in CRLF2 B-ALL cells from +T as compared to –T xenograft mice. GSEA of whole genome microarray data showed a strong enrichment (FDR q-value = 0.022) for genes regulated downstream of mTOR activation in CRLF2 B-ALL cells from +T animals as compared to –T animals (Figure 2.9E and Table 6).

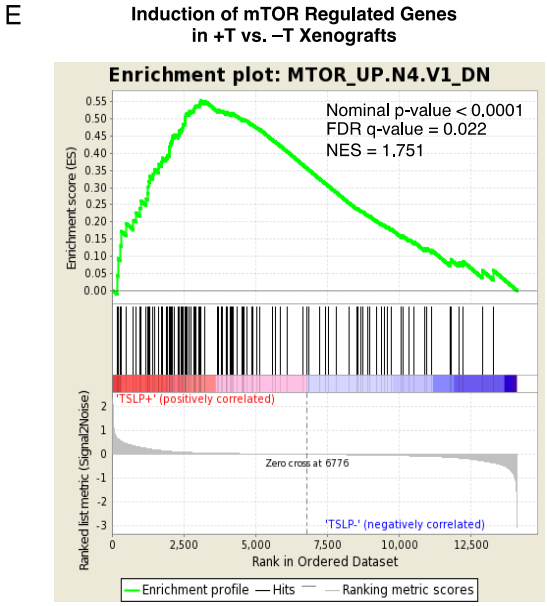

Figure 2.9E: Gene Set Enrichment Analysis (GSEA) of whole genome microarray data showed that CRLF2 B-ALL cells harvested from +T mice evidenced an increase in expression of genes regulated downstream of mTOR signaling as compared to cells from –T mice. The top half of the GSEA enrichment plot shows the enrichment score for each gene and the bottom half shows the values of the ranking metric moving down the list of the ranked genes.

IPA of microarray data was used to identify the most significantly regulated canonical pathways in CRLF2 B-ALL cells from +T as compared to –T xenograft mice (Figure 2.9F). IPA showed that the mTOR pathway, as well as associated pathways (EIF2 Signaling; Regulation of eIF4 and p70S6K Signaling) are among pathways significantly regulated in CRLF2 B-ALL cells from +T as compared to –T mice.

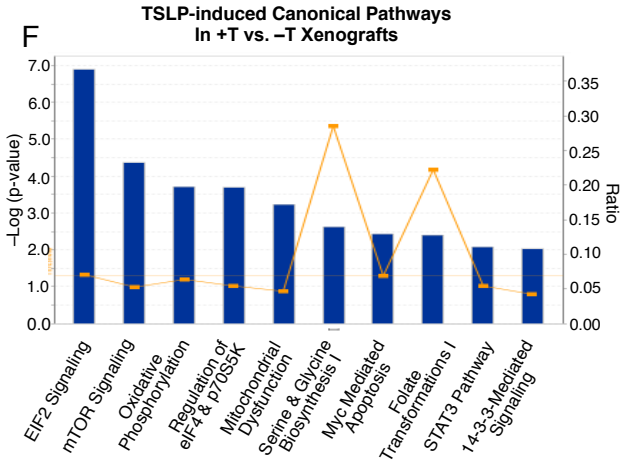

Figure 2.9F: Ingenuity Pathway Analysis (IPA) was performed based on gene reporters that were significantly up or down-regulated (1.7 fold, $p \leq 0.05$). Graphed are the canonical pathways significantly enriched in samples taken from +T as compared to –T mice.

Taken together, GSEA and IPA analysis of gene expression data obtained from CRLF2 B-ALL cells show that mTOR signaling is up-regulated in +T as compared to –T xenograft mice. These data provide evidence that the hTSLP in +T mice, even when present at low levels, acts on CRLF2 B-ALL cells to increase mTOR pathway activation downstream of CRLF2. These data validate the use of +T/–T xenograft mice as a model system for studies to understand the role of TSLP in normal B cell production and in the development and progression of CRLF2 B-ALL.

TSLP Responsiveness is Reduced in Primary CRLF2 B-ALL Cells Expanded in Xenografts Without HTSLP

TSLP is normally expressed by human BM stroma cells (see companion paper), thus, TSLP-mediated CRLF2 signaling is likely to be present during the initiation and

progression of CRLF2 B-ALL. PDX samples used for studies of CRLF2 B-ALL are expanded in xenograft mice that lack the hTSLP required to activate CRLF2-mediated signals. Thus, it is important to determine whether the production of CRLF2 B-ALL PDX samples in xenograft mice that lack hTSLP can affect the subsequent response of these cells to TSLP. To address this question, we compared the *ex vivo* TSLP responses of CRLF2 B-ALL PDX samples generated in –T mice (–T PDX) to those generated in +T mice (+T PDX) by evaluating downstream changes in gene expression (Figure 2.10A).

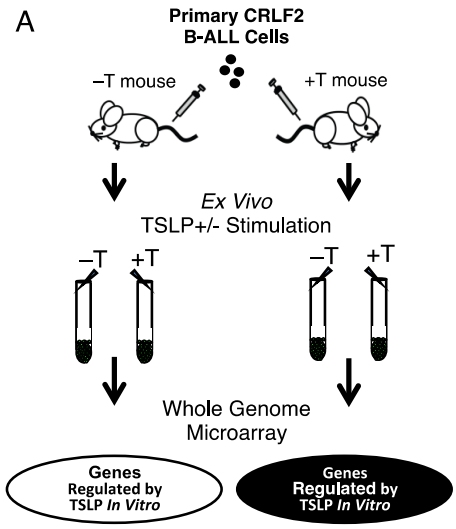

Figure 2.10A: TSLP responsiveness is reduced in primary CRLF2 B-ALL cells expanded in xenografts without hTSLP. A) BM from the –T and +T patient-dervied xenografts (PDX) generated from primary CRLF2 B-ALL cells as described in Figure 4 were stimulated with or without TSLP ex vivo for 3 days. Cells were harvested and hCD19+ cells were isolated by magnetic separation and assessed using whole genome microarray.

BM harvested from the –T and +T PDX generated from primary CRLF2 B-ALL cells (Figure 2.9) was cultured *ex vivo* with and without TSLP (Figure 2.10A). After 3 days of culture, cells were harvested and CRLF2 B-ALL cells were isolated by magnetic separation for whole genome microarray using the Agilent platform. Differential gene

expression analysis showed that 1632 gene reporters were up-regulated and 1754 gene reporters were down-regulated (fold change ≥ 2.0; p≤0.05) when +T PDX were stimulated ex vivo with TSLP (Figure 7B). In contrast, the number of gene reporters differentially regulated by TSLP was reduced by almost half (844 up-regulated and 914 down-regulated) in –T PDX (Figure 2.10B). These data suggest that primary CRLF2 B-ALL cells expanded in the absence of hTSLP have a reduced TSLP response with respect to TSLP-regulated gene expression.

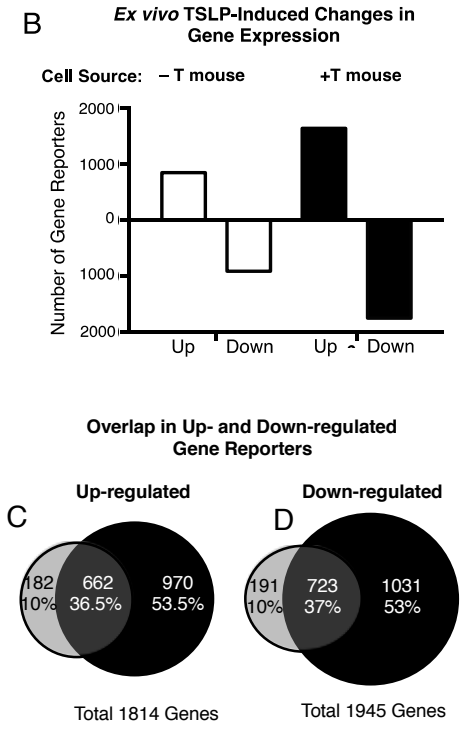

Figure 2.10B-D: B) Graphed are the number of Agilent gene reporters that are up- or down-regulated (≥2 fold, p≤ 0.05) in –T PDX (white) and +T PDX (black) following *ex vivo* stimulation by TSLP. C-D) Overlap (grey) between up- and down-regulated gene reporters in –T PDX (white) or +T PDX (black) following ex vivo stimulation by TSLP

Our next question was whether the TSLP-regulated genes in –T PDX are the same

as those in +T PDX. We examined the total gene reporters differentially regulated in CRLF2 B-ALL cells, regardless of whether cells were expanded in +T or –T animals (1814 total up-regulated and 1945 total down-regulated gene reporters) (Figure 2.10C-D). Of the total gene reporters regulated by TSLP, approximately half were up- or down-regulated in +T PDX, but not in –T PDX. Conversely, 10% of gene reporters were up or down-related in –T PDX but not +T PDX. A little more than a third of gene reporters were regulated by TSLP in both –T and +T PDX. While the gene sets up and down-regulated *by ex vivo* TSLP stimulation were only partially overlapping, it is important to note that no genes were oppositely regulated in +T and –T PDX samples.

Taken together these data suggest that primary CRLF2 B-ALL cells expanded in xenograft mice without hTSLP show a reduced capacity to respond to TSLP as indicated by a reduction in TSLP-induced changes in gene expression.

Discussion

Human-mouse xenografts provide a critical complement to other models in understanding normal and malignant human B lymphopoiesis in context of the broad background of human genetic variation. A limitation of these models is the lack of cross-species activity observed for some cytokines. Here we show that mTSLP does not induce the increases in STAT5 and PI3K/AKT/mTOR phosphorylation induced by hTSLP in CRLF2 B-ALL cells (Figure 2.3). CRLF2 B-ALL cells express abundant IL-7Rα and CRLF2 as compared to normal B cell precursors (Figure 2.2 and Figure S1-Appdx A) and thus provide a sensitive test for mTSLP activity. These data establish that the classic

mouse xenograft models do not provide cross-species activation of the human TSLP receptor.

We developed a strategy to overcome the lack of mTSLP cross-species activity while providing a +/– hTSLP (+T/–T) xenograft model system for studying the *in vivo* role of TSLP in normal and malignant hematopoiesis. NSG mice were engineered to express normal serum levels of hTSLP by intraperitoneal injection with stroma that had been transduced to express hTSLP (+T mice) or transduced with a control vector (–T mice). hTSLP produced in HS27 +T stroma induced STAT5 and PI3K/AKT/mTOR pathway activation and exerted *in vivo* functional effects on primary CRLF2 B-ALL cells (Figure 2.7) as well as normal B cell precursors (see Figure 2.8 and for a detailed analysis see companion paper). Further, we found that primary CRLF2 B-ALL expanded in –T mice showed a loss of TSLP responsiveness, as measured by TSLP-induced gene regulation, when compared to cells from the same patient expanded in +T mice (Figure 2.10). The studies described here establish and validate a novel hTSLP+/– xenograft model system while providing the first data on the *in vivo* impact of TSLP in normal human B cell development and on primary CRLF2+ B-ALL cells.

Normal serum levels of hTSLP were achieved in our model, however, a novel aspect of our model is the ability to modulate serum levels of hTSLP based on the timing and number of injected stromal cells. The ability to vary hTSLP levels or to initiate stromal cell injection (and TSLP production) at time points after transplantation offers advantages for experimental design. A potential limitation of our model is that the hTSLP is not produced directly from stroma in the BM. Although human BM stroma do produce TSLP (see companion paper), the cells believed to produce the most hTSLP–a range of

immune cells, smooth muscle cells, gut and skin epithelial cells (36)–reside outside the BM. Thus, the major source of TSLP that acts on normal and malignant B cells in vivo in patients may be produced outside the marrow as it is in our model. The ability to modulate serum levels of TSLP is also biologically relevant because TSLP production is increased by environmental factors such as pollutants and allergens and is up-regulated in some autoimmune diseases and solid tumors (37) making this model relevant to studies in these fields.

CRLF2 B-ALL is five times more prevalent in Hispanic and Native American children than in others and is associated with poor outcome (26). CRLF2 B-ALL also comprises more than 50% of B-ALL in children with Down syndrome (10, 17, 38). Studies of the relationship between inherited genetic variation and susceptibility to ALL provide some clues to the relationship of ALL to ethnicity (39). However, little is known about cellular mechanisms that contribute to the initiation, progression and maintenance of CRLF2 B-ALL or the biological factors that contribute to the health disparities associated with this disease. Patient-derived xenograft (PDX) models are particularly critical for health disparities diseases where inherited genetic variation or alterations such as Down syndrome are likely to play a role in disease progression (40, 41). The primary CRLF2 B-ALL sample used to develop the model described here was obtained from a Hispanic pediatric patient. This PDX together with additional ones currently being generated with the +T/–T xenograft model will allow us to study disease mechanisms 1) in context of a genetic background associated with CRLF2 B-ALL health disparities and 2) in context of TSLP-CRLF2 mediated signals present in vivo in the patient.

The model developed here provides an important new tool for understanding the mechanisms of TSLP activity in normal and malignant B lymphopoiesis. It also provides a preclinical model for identifying therapies to effectively treat CRLF2 B-ALL in an environment that can induce the TSLP-mediated signals present in vivo in patients and in context of the genetic background that leads to health disparities in this disease.

References

1. Ito T, Wang YH, Duramad O, Hori T, Delespesse GJ, Watanabe N, et al. TSLP-activated dendritic cells induce an inflammatory T helper type 2 cell response through OX40 ligand. Journal of Experimental Medicine. 2005 Nov 7;202(9):1213-23.

2. Ying S, O'Connor B, Ratoff J, Meng Q, Mallett K, Cousins D, et al. Thymic stromal lymphopoietin expression is increased in asthmatic airways and correlates with expression of Th2-attracting chemokines and disease severity. J Immunol. 2005 Jun 15;174(12):8183-90.

3. Zhou BH, Comeau MR, De Smedt T, Liggitt HD, Dahl ME, Lewis DB, et al. Thymic stromal lymphopoietin as a key initiator of allergic airway inflammation in mice. Nature Immunology. 2005 Oct;6(10):1047-53.

4. Scheeren FA, van Lent AU, Nagasawa M, Weijer K, Spits H, Legrand N, et al. Thymic stromal lymphopoietin induces early human B-cell proliferation and differentiation. Eur J Immunol. 2010 Feb 1.

5. Ray RJ, Furlonger C, Williams DE, Paige CJ. Characterization of thymic stromal-derived lymphopoietin (TSLP) in murine B cell development in vitro. Eur J Immunol. 1996 Jan;26(1):10-6.

6. Reche PA, Soumelis V, Gorman DM, Clifford T, Liu M, Travis M, et al. Human thymic stromal lymphopoietin preferentially stimulates myeloid cells. J Immunol. 2001 Jul 1;167(1):336-43.

7. Johnson SE, Shah N, Panoskaltsis-Mortari A, LeBien TW. Murine and human IL-7 activate STAT5 and induce proliferation of normal human pro-B cells. J Immunol. 2005 Dec 1;175(11):7325-31.

8. Parrish YK, Baez I, Milford TA, Benitez A, Galloway N, Rogerio JW, et al. IL-7 Dependence in human B lymphopoiesis increases during progression of ontogeny from cord blood to bone marrow. J Immunol. 2009 Apr 1;182(7):4255-66.

9. Yoda A, Yoda Y, Chiaretti S, Bar-Natan M, Mani K, Rodig SJ, et al. Functional screening identifies CRLF2 in precursor B-cell acute lymphoblastic leukemia. Proc Natl Acad Sci U S A. 2010 Jan 5;107(1):252-7.

10. Russell LJ, Capasso M, Vater I, Akasaka T, Bernard OA, Calasanz MJ, et al. Deregulated expression of cytokine receptor gene, CRLF2, is involved in lymphoid transformation in B-cell precursor acute lymphoblastic leukemia. Blood. 2009 Sep 24;114(13):2688-98.

11. Chapiro E, Russell L, Lainey E, Kaltenbach S, Ragu C, Della-Valle V, et al. Activating mutation in the TSLPR gene in B-cell precursor lymphoblastic leukemia. Leukemia. 2010 Mar;24(3):642-5.

12. Cario G, Zimmermann M, Romey R, Gesk S, Vater I, Harbott J, et al. Presence of the P2RY8-CRLF2 rearrangement is associated with a poor prognosis in non-high-risk precursor B-cell acute lymphoblastic leukemia in children treated according to the ALL-BFM 2000 protocol. Blood. 2010 Jul 1;115(26):5393-7.

13. Portell CA, Wenzell CM, Advani AS. Clinical and pharmacologic aspects of blinatumomab in the treatment of B-cell acute lymphoblastic leukemia. Clin Pharmacol. 2013;5(Suppl 1):5-11.

14. Bhatia S, Sather HN, Heerema NA, Trigg ME, Gaynon PS, Robison LL. Racial and ethnic differences in survival of children with acute lymphoblastic leukemia. Blood. 2002 Sep 15;100(6):1957-64.

15. Armstrong SA LA. Molecular genetics of acute lymphoblastic leukemia. Journal of Clinical Oncology. 2005;23(26):6306-15.

16. Nguyen K, Devidas M, Cheng SC, La M, Raetz EA, Carroll WL, et al. Factors influencing survival after relapse from acute lymphoblastic leukemia: a Children's Oncology Group study. Leukemia. 2008 Dec;22(12):2142-50.

17. Mullighan CG, Collins-Underwood JR, Phillips LA, Loudin MG, Liu W, Zhang J, et al. Rearrangement of CRLF2 in B-progenitor- and Down syndrome-associated acute lymphoblastic leukemia. Nat Genet. 2009 Nov;41(11):1243-6.

18. Mullighan CG, Goorha S, Radtke I, Miller CB, Coustan-Smith E, Dalton JD, et al. Genome-wide analysis of genetic alterations in acute lymphoblastic leukaemia. Nature. 2007 Apr 12;446(7137):758-64.

19. Mullighan CG. Genomic profiling of B-progenitor acute lymphoblastic leukemia. Best Pract Res Clin Haematol. 2011 Dec;24(4):489-503.

20. Chen IM, Harvey RC, Mullighan CG, Gastier-Foster J, Wharton W, Kang H, et al. Outcome modeling with CRLF2, IKZF1, JAK, and minimal residual disease in pediatric acute lymphoblastic leukemia: a Children's Oncology Group study. Blood. 2012 Apr 12;119(15):3512-22.

21. Park LS, Martin U, Garka K, Gliniak B, Di Santo JP, Muller W, et al. Cloning of the murine thymic stromal lymphopoietin (TSLP) receptor: Formation of a functional heteromeric complex requires interleukin 7 receptor. J Exp Med. 2000 Sep 4;192(5):659-70.

22. Wohlmann A, Sebastian K, Borowski A, Krause S, Friedrich K. Signal transduction by the atopy-associated human thymic stromal lymphopoietin

(TSLP) receptor depends on Janus kinase function. Biol Chem. 2010 Feb-Mar;391(2-3):181-6.

23. Rochman Y, Kashyap M, Robinson GW, Sakamoto K, Gomez-Rodriguez J, Wagner KU, et al. Thymic stromal lymphopoietin-mediated STAT5 phosphorylation via kinases JAK1 and JAK2 reveals a key difference from IL-7-induced signaling. Proc Natl Acad Sci U S A. 2010 Nov 9;107(45):19455-60.

24. Zhong J, Kim MS, Chaerkady R, Wu X, Huang TC, Getnet D, et al. TSLP signaling network revealed by SILAC-based phosphoproteomics. Mol Cell Proteomics. 2012 Feb 16.

25. Zhong J, Sharma J, Raju R, Palapetta SM, Prasad TS, Huang TC, et al. TSLP signaling pathway map: a platform for analysis of TSLP-mediated signaling. Database (Oxford). 2014;2014:bau007.

26. Harvey RC, Mullighan CG, Chen IM, Wharton W, Mikhail FM, Carroll AJ, et al. Rearrangement of CRLF2 is associated with mutation of JAK kinases, alteration of IKZF1, Hispanic/Latino ethnicity, and a poor outcome in pediatric B-progenitor acute lymphoblastic leukemia. Blood. 2010 Jul 1;115(26):5312-21.

27. Roll JD, Reuther GW. CRLF2 and JAK2 in B-progenitor acute lymphoblastic leukemia: a novel association in oncogenesis. Cancer Res. 2010 Oct 1;70(19):7347-52.

28. Malin S, McManus S, Cobaleda C, Novatchkova M, Delogu A, Bouillet P, et al. Role of STAT5 in controlling cell survival and immunoglobulin gene recombination during pro-B cell development. Nature Immunology. 2010 Feb;11(2):171-9.

29. Edgar R, Domrachev M, Lash AE. Gene Expression Omnibus: NCBI gene expression and hybridization array data repository. Nucleic Acids Res. 2002 Jan 1;30(1):207-10.

30. Tasian SK, Doral MY, Borowitz MJ, Wood BL, Chen IM, Harvey RC, et al. Aberrant STAT5 and PI3K/mTOR pathway signaling occurs in human CRLF2-rearranged B-precursor acute lymphoblastic leukemia. Blood. 2012 Jul 26;120(4):833-42.

31. Dann SG, Selvaraj A, Thomas G. mTOR Complex1-S6K1 signaling: at the crossroads of obesity, diabetes and cancer. Trends in molecular medicine. 2007 Jun;13(6):252-9.

32. Dao MA, Pepper KA, Nolta JA. Long-term cytokine production from engineered primary human stromal cells influences human hematopoiesis in an in vivo xenograft model. Stem Cells. 1997;15(6):443-54.

33. Lee EB, Kim KW, Hong JY, Jee HM, Sohn MH, Kim KE. Increased serum thymic stromal lymphopoietin in children with atopic dermatitis. Pediatric allergy and immunology : official publication of the European Society of Pediatric Allergy and Immunology. 2010 Mar;21(2 Pt 2):e457-60.

34. Mootha VK, Lindgren CM, Eriksson KF, Subramanian A, Sihag S, Lehar J, et al. PGC-1alpha-responsive genes involved in oxidative phosphorylation are coordinately downregulated in human diabetes. Nat Genet. 2003 Jul;34(3):267-73.

35. Subramanian A, Tamayo P, Mootha VK, Mukherjee S, Ebert BL, Gillette MA, et al. Gene set enrichment analysis: a knowledge-based approach for interpreting genome-wide expression profiles. Proc Natl Acad Sci U S A. 2005 Oct 25;102(43):15545-50.

36. Takai T. TSLP expression: cellular sources, triggers, and regulatory mechanisms. Allergol Int. 2012 Mar;61(1):3-17.

37. Ziegler SF, Roan F, Bell BD, Stoklasek TA, Kitajima M, Han H. The biology of thymic stromal lymphopoietin (TSLP). Adv Pharmacol. 2013;66:129-55.

38. Hertzberg L, Vendramini E, Ganmore I, Cazzaniga G, Schmitz M, Chalker J, et al. Down syndrome acute lymphoblastic leukemia, a highly heterogeneous disease in which aberrant expression of CRLF2 is associated with mutated JAK2: a report from the International BFM Study Group. Blood. 2010 Feb 4;115(5):1006-17.

39. Xu H, Yang W, Perez-Andreu V, Devidas M, Fan Y, Cheng C, et al. Novel susceptibility variants at 10p12.31-12.2 for childhood acute lymphoblastic leukemia in ethnically diverse populations. J Natl Cancer Inst. 2013 May 15;105(10):733-42.

40. Liem NL, Papa RA, Milross CG, Schmid MA, Tajbakhsh M, Choi S, et al. Characterization of childhood acute lymphoblastic leukemia xenograft models for the preclinical evaluation of new therapies. Blood. 2004 May 15;103(10):3905-14.

41. Lock RB, Liem NL, Papa RA. Preclinical testing of antileukemic drugs using an in vivo model of systemic disease. Methods Mol Med. 2005;111:323-34.

CHAPTER THREE

TSLP EXERTS EFFECTS THAT ARE DISTINCT FROM IL-7 DURING NORMAL B-CELL DEVELOPMENT

Abstract

The role of TSLP in human B cell development is largely unknown and its function in context of IL-7 has not been studied. We found that TSLP can replace IL-7 in providing a signal essential for in vitro production and proliferation of human CD19+Pax-5+ B cell progenitors. To study the role of TSLP in human B cell development, in the context of IL-7 stimulation, we developed a novel xenograft model. Mouse IL-7 is active on human cells; however, this is not the case for TSLP. We took advantage of this to develop a xenograft model system comprised of mice that provide human TSLP (+T mice) and control mice that do not (–T mice). Using this model we found that TSLP increases proliferation and up-regulates Mcl-1 in CD19–CD34+IL7Rα+ progenitors resulting in a 3-4-fold expansion of the CD34+ pro-B cell compartment in +T as compared to –T mice. This expansion is maintained during subsequent stages of B cell development, partially due to increased protection from apoptosis that occurs independently of Bcl-2 family pro-survival proteins. TSLP stimulated in vitro proliferation of pro-B cells, however, in vivo proliferation of B lineage precursors was similar in +T and –T mice suggesting redundancy with IL-7. B cell subsets in normal pediatric BM samples show progenitor ratios and Mcl-1 expression that mirrors that in +T xenograft mice. These data provide evidence that TSLP function in human B

lymphopoiesis includes both unique activities as well as activities redundant to those of IL-7.

Abbreviations

TSLP	Thymic Stromal Lymphopoietin
CRLF2	Cytokine Receptor-Like Factor 2
IL-7Pα	Interleukin 7 Receptor alpha chain
JAK	Janus Kinase
mTOR	Mammalian Target Of Rapamycin
PI3K	Phosphoinositide-3-Kinase
AKT	Protein Kinase B
PAX5	Paired Box 5
CD19	Cluster of Differentiation 19 (B-cell marker)
CD34	Cluster of Differentiation 34 (stem cell marker)
NSG	NOD/SCID Gamma (NOD.Cg-Prkdc^{scid}Il2rg^{tm1Wjl}/SzJ)
BM	Bone Marrow
CB	Cord Blood (umbilical cord blood)
HSC	Hematopoietic Stem Cell
Mcl-1	Myeloid Cell Leukemia 1
Bcl-xl	Bcl-2 Like protein X
Bcl-2	B-cell Lymphoma 2
Flt-3	Fms-Like Tyrosine kinase 3
Ig	Immunoglobulin
7-AAD	7-Amino-Actinomycin D
BrdU	5-Bromo-2'-deoxyuridine

Introduction

The roles of TSLP and IL-7 in mouse B lymphopoiesis include overlapping and unique functions (1-5). In vitro studies of human B cell development show that TSLP acts on fetal B cell precursors to induce proliferation (6), while IL-7 provides a signal critical for the production and proliferation of non-fetal B lineage cells (7-9). The role of TSLP in human B cell development beyond the fetal period has not been studied. Furthermore, its role in context of IL-7 during normal in vivo B cell development is unknown. Aberrant signaling in both the TSLP (10) and IL-7 (11) pathways is linked to B cell acute lymphoblastic leukemia, underscoring the importance of understanding the role of these cytokines in human B lymphopoiesis.

TSLP and IL-7 signal through distinct complexes comprised of the IL-7Rα and homologous secondary chains (12). The secondary chain for the IL-7 receptor complex is the common gamma chain (γc) (13), while the secondary chain of the TSLP receptor complex is CRLF2 (TSLPRβ) (14, 15). Both cytokines induce STAT5 activation, however, TSLP acts through JAK2, while IL-7 effects are mediated through JAK3 (17). Additionally, in human B lineage cells, TSLP induces the PI3K/AKT/mTOR pathway activation (18), although available evidence suggests that this pathway is not activated by IL-7 (19). Thus, TSLP and IL-7 exhibit both shared and distinct receptor components as well as downstream signaling pathways.

IL-7R-mediated signals are likely to play different roles in mouse and human B cell development. In mice, IL-7 activates the PI3K/AKT pathway in B lineage cells, but this is not the case in humans (19). Furthermore, homologies in TSLP and in CRLF2, between the two species are very low (~40% protein level identity) (20, 21). This

contrasts with other cytokines and receptor components, including IL-7 and the IL-7Rα which show ~70% homology between mouse and human. As a consequence, mouse TSLP does not show cross-species activity on human cells (14) and companion manuscript) while IL-7 does. This simultaneously highlights the importance of studying B cell development in human systems, while identifying a challenge of doing so: mouse TSLP does not activate the human TSLP receptor complex. Consequently, IL-7Rα signaling in human B lineage cells generated in classic human-mouse xenografts, is activated exclusively by mouse IL-7.

Here we use a novel human-mouse xenograft system that produces human TSLP, together with human-only *in vitro* cultures and primary patient samples, to identify the role of TSLP in human B cell development *in vivo*, in context of IL-7.

Materials and Methods

Human Samples

Umbilical cord blood (CB) and bone marrow (BM) were obtained in accordance with protocols approved by the Loma Linda University Institutional Review Board (IRB) and with the Helsinki Declaration of 1975, as revised in 2008. CD34+ cells were isolated by magnetic separation with CD34+ microbeads (Miltenyi Biotec, Auburn, CA) from mononuclear cells. Detection of human TSLP production in BM stromal cells is described in online supplementary methods.

Selective-Cytokine Co-cultures

Human-only co-cultures were as described (9). Briefly, CB CD34+ hematopoietic

stem cells (HSC) cells were seeded on primary human BM stromal cells. Cultures were maintained in medium supplemented with 5% human AB serum (Omega Scientific, Tarzana, CA) lot tested to support human B cell production. All cultures, including control, were supplemented with IL-3 and Flt-3 Ligand. For selective cytokine stimulation, TSLP and/or IL-7 (R&D Systems Inc., Minneapolis, MN) were added. If TSLP and/or IL-7 were not added, cultures were further supplemented with an anti-human neutralizing antibody to counter activity of endogenously produced TSLP and/or IL-7. Cultures without specific neutralizing antibody (anti-IL-7 and/or anti-TSLP) were supplemented with an isotype-matched control for the neutralizing antibody. Cultures were maintained for three weeks, and then harvested. For BrdU incorporation, co-cultures were labeled with 10 uM BrdU (Sigma-Aldrich, St. Louis, MO) for the final 24 hours of culture.

Flow Cytometry

Cells were prepared for flow cytometry to detect surface antigens according to manufacturer's protocols. Details of intracellular staining and specific antibody clones and conjugates are described in online supplemental methods. Flow cytometry analysis was performed using a MACSQuant analyzer (Miltenyi Biotec, Inc. Auburn, CA) and Flowjo data analysis software (TreeStar, Ashland, OR).

Statistical Analysis

Statistical analysis was performed using Students t test or one-way analysis of variation (ANOVA) and data expressed as mean ± SEM. Statistical significance was

defined as $p<0.05$.

Animal Studies

Studies were performed using NOD.Cg-Prkdcscid Il2rgtm1Wjl/SzJ (NSG) mice (Jackson Laboratory) under protocols approved by the Loma Linda University Institutional Animal Care and Use Committee (IACUC). Mice were engineered by intraperitoneal injection with stroma transduced to express human TSLP (+T mice) or stroma transduced with control vector (–T mice) as described in the companion paper. +T and –T mice were transplanted with 1"105 CD34+ cells by tail vein injection, after sub-lethal irradiation at 225 cGy. Mice were euthanized 5-7 weeks after transplantation and tissues harvested and frozen for flow cytometry analysis.

Results

TSLP can Replace IL-7 in Supporting the In vitro Production and Proliferation of Human CD19+Pax-5+ B cell Progenitors

To compare the effects of TSLP and IL-7 in early stages of human B cell production, we developed a human-only culture model that provides selective cytokine stimulation. Human CD34+ HSCs were cultured with primary human BM stromal cells in media supplemented with human serum. Selective cytokine stimulation was achieved by supplementing with combinations of exogenous IL-7 and/or TSLP and with neutralizing antibodies to counter activity of endogenously produced IL-7 and TSLP in cultures where cytokine is not added (Figure 3.1A). CB CD34+ HSCs were plated in human-only selective cytokine cultures to compare the production of B cell progenitors

under the influence of TSLP or IL-7 alone and in combination. Culture progeny were harvested and stained for flow cytometry to identify CD19+PAX-5+ B lineage cells. Control cultures that lacked TSLP or IL-7 showed little B cell production (Figure 3.1B). In contrast, TSLP, IL-7, and TSLP+IL-7 cultures showed robust production of CD19+PAX-5+ B lineage cells (Figure 3.1B). There was no significant difference in the numbers of B lineage cells produced in cultures with TSLP as compared to cultures with IL-7 (Figure 3.1C). Furthermore, there was no additive effect when cultures were supplemented with both cytokines.

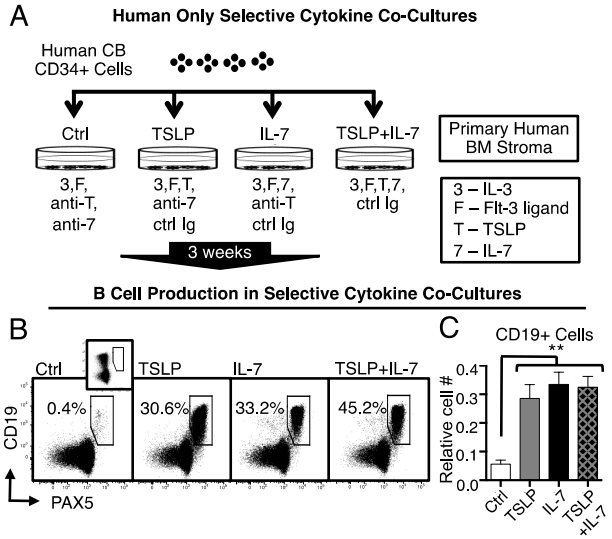

Figure 3.1 A-C: (A) Human-only cultures were produced by plating primary human CB CD34+ cells on primary BM stromal cells. Selective cytokine stimulation was achieved by supplementing cultures with exogenous IL-7 and/or TSLP or neutralizing antibodies to TSLP (anti-T) or IL-7 (anti-7) as indicated. Cultures without a particular neutralizing antibody were supplemented, as a control with non-specific isotype-matched antibodies (ctrl Ig). All culture conditions included IL-3 and Flt-3 ligand, two cytokines that support early lymphoid progenitors (35, 36). Cultures were maintained for three weeks, then harvested and stained for flow cytometry. (B) Dot plots showing CD19 vs. Pax5 staining in each culture condition are shown (representative of n=3 independent experiments). PAX-5 fluorescence minus one (FMO) control is displayed in inset. (C) Graphed are the relative numbers of CD19+ cells generated in vitro under indicated conditions at three weeks (n=14).

To determine if TSLP-induced proliferation contributes to the increased production of human B cell precursors from CB HSCs, we compared BrdU incorporation in cells generated under selective cytokine conditions (Figure 3.1D). Proliferation of B cell precursors was significantly increased in TSLP cultures as compared to control cultures without TSLP or IL-7 (Figure 3.1E). The percentage of BrdU+ cells in TSLP cultures was similar to that observed for cultures with IL-7 or TSLP+IL-7. Collectively, these data provide evidence that TSLP can replace IL-7 in providing signals that are critical for the in vitro production and proliferation of CD19+PAX-5+ B cell precursors. Further, the absence of additive effects observed in cultures with TSLP+IL-7 suggests that TSLP and IL-7 do not act on different populations of cells but rather a common set of B cell progenitors that can respond to either TSLP or IL-7.

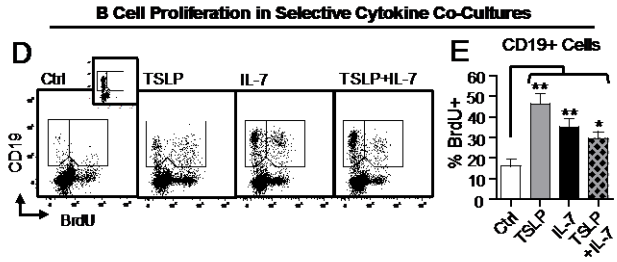

Figure 3.1D-E: (D) Representative dot plots of CD19 vs BrdU staining in indicated conditions. BrdU FMO control is displayed in the inset of the Ctrl dot plot. (E) Graphed is the percent BrdU+ cells (mean± SEM) in the total CD19+ population generated under indicated conditions at three weeks (n=8). Statistical analysis was performed using a one-way ANOVA, with Dunnett multiple comparisons post test, *$p<0.05$, **$p<0.001$.

In vivo Human B cell Production in Xenografts With and Without Human TSLP

The above data suggest that TSLP and IL-7 might provide redundant proliferative signals but do not address the potential for differential effects at specific stages during *in vivo* B cell development. We developed a novel xenograft model that allows us to study

in vivo stage-specific development of human B lineage cells in the presence and absence of TSLP. Unlike mouse IL-7, which can induce activation of the human IL-7R complex (8, 22, 23), mouse TSLP does not (see (21) and companion manuscript). We took advantage of this to develop a xenograft model system comprised of mice that provide human TSLP (+T mice) and control mice that do not (–T mice) (Figure 3.2A). The human TSLP in +T xenograft mice was active on normal human B lineage cells as indicated by the lineage-specific increases in CD19+ B lineage cells generated from CB CD34+ HSCs transplanted into +T as compared to –T mice (see chapter 2).

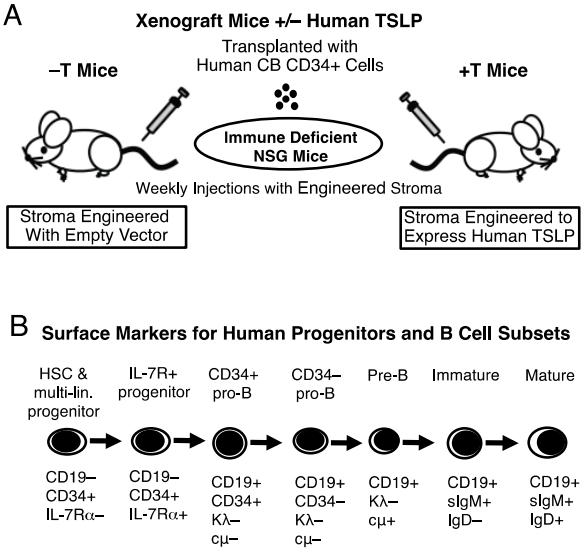

Figure 3.2A-B: Xenograft model of human B cell development. (A) Immune deficient NSG mice were engineered by weekly intraperitoneal injection of stromal cells that were transduced either with empty vector (–T mice) or to express human TSLP (+T mice) as described in companion paper. CB CD34+ cells were injected by tail vein into –T and +T mice. Five weeks later BM was harvested and stained for flow cytometry to detect anti-mouse CD45 (mCD45) and human-specific markers (B) to identify five developmentally sequential B cell subsets in the BM of –T and +T mice. IL-7R+ progenitors, a population of lymphoid-restricted multi-lineage progenitors (Su, unpublished data) were also identified. Gated subsets are shown for –T mice.

To distinguish *in vivo*, stage-specific effects of TSLP during human B cell development, we compared progenitor and B lineage subsets produced in mice that provide only IL-7 stimulation (–T mice) or both IL-7 and human TSLP stimulation (+T mice). Xenograft mice were engineered to be –T and +T and transplanted with CB CD34+ cells. Five weeks after transplantation, BM and spleens of mice were harvested and stained for flow cytometry to identify developmental subsets of human B lineage cells as well as IL-7R+ progenitors (Figure 3.2B). IL-7R+ progenitors are a population of CD19–CD34+ progenitors that represent the earliest hematopoietic progenitors capable of responding to TSLP and/or IL-7 based on their expression of IL-7Rα. We found that all five B cell subsets, as well as IL-7R+ progenitors, were present in the BM of xenograft mice irrespective of the presence of human TSLP (Figure 3.2C-D). Similarly, spleens from –T and +T animals showed both immature and mature B cell subsets (data not shown).

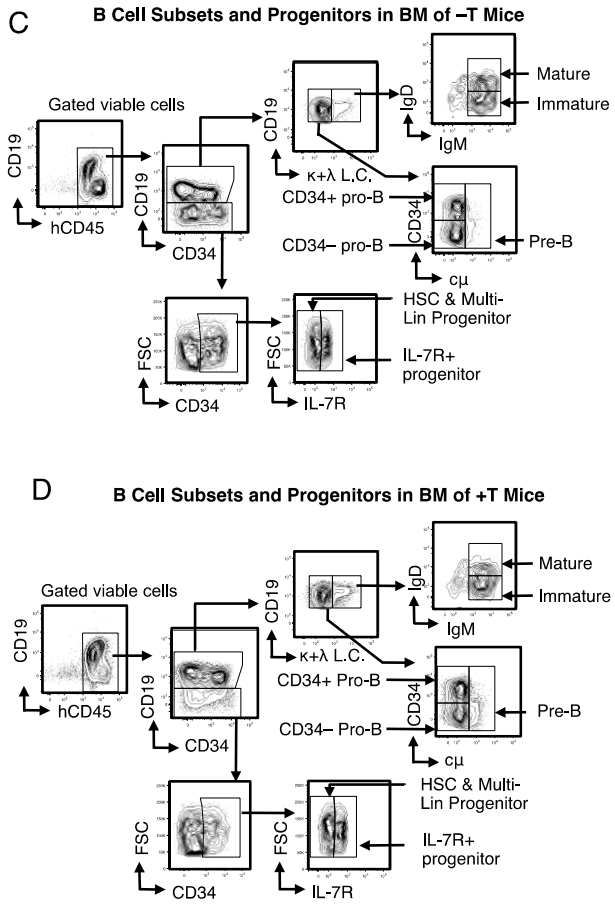

Figure 3.2C-D: Gated subsets are shown for –T mice (C) and +T mice (D). The same gating strategy was used to identify immature and mature B cells in the spleens of the –T and +T mice.

TSLP Alters the Distribution of Human CD34+ Progenitors in the BM of Xenograft Mice

In vitro studies of human fetal B cell development show that CD34+ progenitor populations are responsive to TSLP (6). To determine whether TSLP effects on CD34+ populations are distinct from those of IL-7, we compared the distribution of CD34+ stem cell and progenitor populations in the BM of –T and +T mice. Using gates shown in Figure 9C, D, we determined the distribution of total CD34+ cells from –T and +T

xenograft mice among three CD34+ subsets: HSCs/multi-lineage progenitors, IL-7R+ progenitors, and CD34+ pro-B cells. The progenitors produced with IL-7 stimulation alone (–T xenograft mice) were distributed almost evenly between the three CD34+ subsets (Figure 3.3, left panel). In contrast, CD34+ progenitors produced with TSLP and IL-7 showed a skewing toward CD34+ pro-B cells which made up more than 75% of the entire CD34+ BM pool in + T mice (Figure 3.3, right panel). These data suggest that rather than inducing a global expansion of B lineage cells by amplifying IL-7R signals in a redundant fashion, TSLP exerts specific effects on CD34+ cells that are at least partially distinct from those of IL-7 during the early stages of human B cell differentiation from CD34+ CB HSCs.

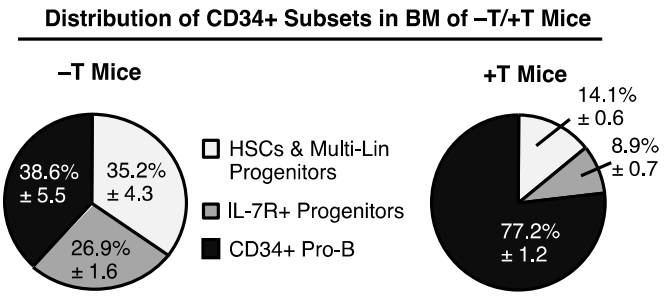

Figure 3.3: Distribution of total human CD34+ BM cells from –T and +T xenograft mice among three CD34+ subsets: HSCs/multi-lineage progenitors (CD19–CD34+IL-7R–), IL-7R+ progenitors (IL-7R+), and CD34+ pro-B cells (CD19+CD34+), in BM of –T mice and +T mice.

TSLP Expands the Earliest CD19+ B lineage Committed Cells at the Expense of CD19–CD34+ cells that Express the IL-7Rα

To gain insights into populations targeted uniquely by TSLP, we compared the absolute numbers of cells in developmental subsets produced in +T and –T mice. The

number of cells in the HSCs and multi-lineage progenitor compartment was similar in xenografts whether or not human TSLP was present. Surprisingly, in +T mice the number of IL-7Rα+ progenitors was reduced. This contrasts with subsequent stages of B cell development, from CD34+ pro-B to mature B cells, where cell numbers were significantly increased in +T as compared to –T mice (Figure 3.4, left panel). Similarly, splenic numbers of immature and mature human B cells were increased in +T as compared to –T mice (Figure 3.4, right panel).

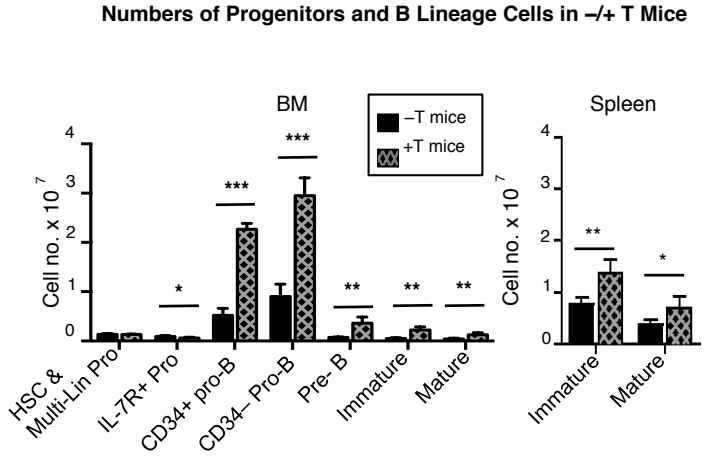

Figure 3.4: Absolute number of cells in each progenitor and B lineage subset in the BM (left panel) and spleen (right panel) of –T (n= 3) and +T (n=5) xenograft mice. Statistical analysis was performed using a one-tailed, t-test, *p<0.05, **p<0.01 and ***p<0.0001. Error bars represent mean ± SEM.

Taken together, these data show that TSLP alters the distribution of CD34+ progenitor populations, increasing the CD34+ pro-B compartment at the expense of IL-7R+ progenitors. These data suggest that TSLP exerts unique stage-specific effects during early stages of B cell development. Furthermore, TSLP-induced increases in cell numbers early in the B lineage extend through all stages of B cell development in the BM

and spleen. These effects do no occur with IL-7 stimulation alone, suggesting that TSLP plays a role that is distinct from IL-7 in expanding the B cell progenitor compartment during *in vivo* human B lymphopoiesis.

TSLP-induced Expansion of CD34+ Pro-B cells is Maintained, but not Augmented at Later Stages of In vivo B cell Development

Because cells in early developmental subsets give rise to cells that progress to more mature stages of B cell development, the effect of TSLP on the most immature progenitors will result in increased cell numbers at each subsequent stage of development, independent of effects at more mature stages of development. To pinpoint stage-specific effects of TSLP-induced expansion, we graphed the fold change in cell numbers at each stage of B lineage development in +T mice relative to –T mice (Figure 3.5, left panel).

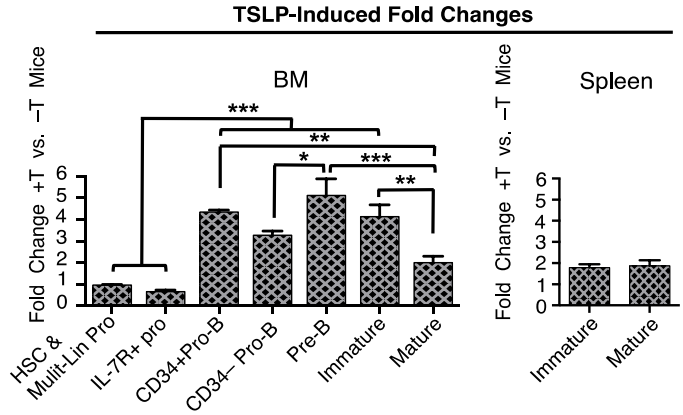

Figure 3.5: Graphed is the TSLP-induced fold change in the absolute number of progenitors and B lineage cells in the BM (left panel) and spleen (right panel) of +T as compared to –T xenograft mice. Subsets were gated as described in Figure 2. Statistical analysis was performed using a one-way ANOVA, *p<0.05, **p<0.01 and ***p<0.001. Error bars represent mean± SEM.

The pool of HSC/multi-lineage progenitors was unchanged, but the IL-7R+ progenitor compartment was reduced in +T as compared to –T mice. Despite its reduced size, the IL-7R+ progenitor population in +T xenograft mice gave rise to a CD34+ pro-B compartment that was more than 4-fold increased when compared to –T mice. As B cell development progressed, the ~4-fold increase was maintained until cells reached the mature B cell stage, where numbers in +T xenograft mice were only 2 fold that observed in –T mice. Similarly, the number of immature and mature splenic B cells (Figure 3.5, right panel), as well as the splenic weight (data not shown) in +T animals was ~2 fold that in –T xenograft mice. These data show that the overall increase in CD34+ pro-B cells that we observed in +T mice is largely maintained, but not further increased as B cell progenitors progress through each subsequent stage of development and migrate to the spleen.

TSLP Increases Proliferation of IL-7R+ Progenitors but not CD19+ B lineage Cells

To determine the cellular mechanism(s) responsible for increased *in vivo* B lineage production with TSLP stimulation, we first assessed proliferation based on Ki-67 expression in developmental subsets. The IL-7R+ progenitors generated in +T animals showed increased Ki-67 expression (Figure 3.6, top panel). However, no differences in proliferation were observed in any of the subsequent committed B cell subsets derived from BM of the –T and +T mice.

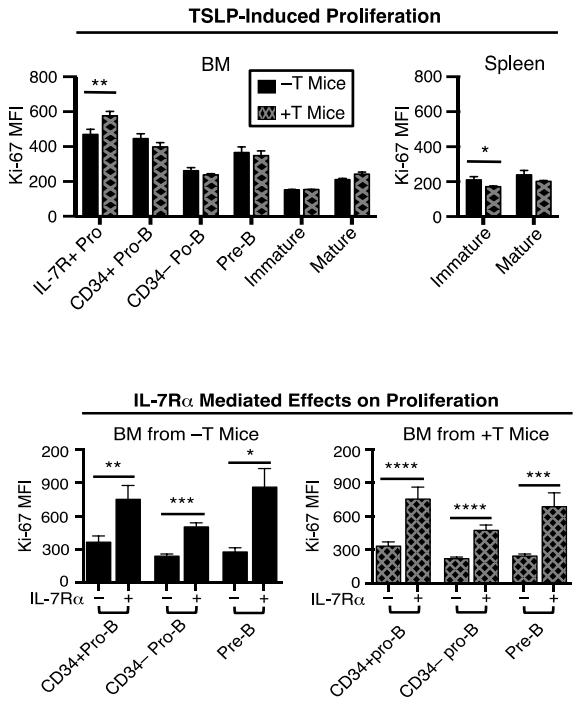

Figure 3.6: Top panel: Expression of Ki-67 proliferation antigen in developmentally sequential progenitor B cell subsets in BM (left panel) and spleen (right panel). Bottom panel: Progenitor and precursor IgM– subsets were further separated based on IL-7Rα, and Ki-67 expression as indicated by MFI is graphed for each subset in the –T and +T xenograft mice. Statistical analysis was performed using an unpaired one- tailed, t-test, *p<0.05, **p<0.01, ***p<0.001 and ****p<0.0001. Error bars represent mean ± SEM. Data shown are from –T mice (n = 3) and +T mice (n=5).

The IL-7Rα chain is required for both IL-7 and TSLP-mediated signals. However, typically only ~20-50% of human pro-B and pre-B cells express IL-7Rα (9) and it is undetectable by the immature stage of B cell development (Milford, unpublished data). To gain insights into the stage-specific roles of IL-7 and TSLP in the proliferation of B lineage committed progenitors, we compared Ki-67 expression in IL-7Rα+ and IL-7Rα– subsets from –T and +T xenograft mice (Figure 3.6, bottom panel). In both +T and –T mice, Ki-67 was significantly higher in the IL-7Rα+ cells than in IL-7Rα– cells in the pro-B and pre-B subsets.

Taken together with data in Figures 8 and 9, these results suggest that TSLP increases proliferation of IL-7R+ progenitors and promotes up-regulation of PAX-5 expression and differentiation to produce an expanded pool of differentiated CD34+CD19+ pro-B cells. They also provide evidence that IL-7 and TSLP act in a redundant manner to stimulate cycling of IL-7Rα+ pro-B and pre-B cells.

TSLP Protects Developing CD19+ B lineage Cells from Apoptosis

Our next question was whether increased survival of B lineage cells might contribute to the increased pool of B lineage cells that we observed in +T xenograft mice. To address this question we evaluated apoptosis in IL-7R+ progenitors and B cell subsets by flow cytometry. Graphed in Figure 3.7 are the percentage of cells in each subset that were non-apoptotic as indicated by the absence of staining for the apoptotic markers, Annexin V and 7-AAD. Notably, the percentage of non-apoptotic cells was significantly higher in human pro-B, pre-B and immature B cells from +T as compared to –T mice. Similar percentages of non-apoptotic cells were observed among IL-7R+ progenitors and mature B cells (Figure 3.7) regardless of whether TSLP was present. Thus, during the development of CD19+ B lineage cells, TSLP has a unique pro-survival function that is not provided by IL-7.

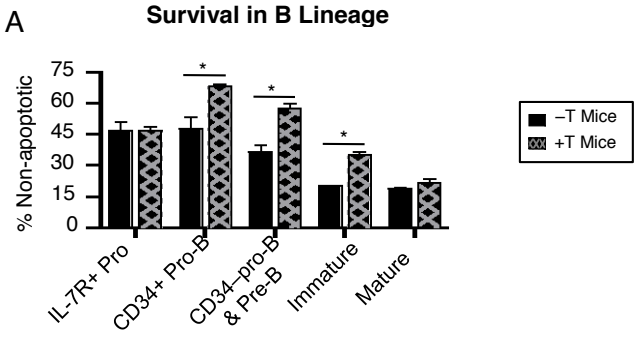

Figure 3.7: Graphed are the percentages of non-apoptotic cells (Annexin V– 7-AAD– cells) in each subset from –T and +T mice. B) CD34+ progenitors along with B cell progenitor and precursor subsets were gated into IL-7Rα– and IL-7Rα+ fractions.

TSLP-mediated Protection from Apoptosis is Independent of Bcl-2 Family Pro-survival Protein Expression

To gain insights into the role of TSLP and IL-7 in the survival of developing B lineage cells and the contribution of Bcl-2 family pro-survival proteins in this process, we compared the expression of Bcl-2, Bcl-xL and Mcl-1 in IL-7R– and IL-7R+ cells within early progenitor and B cell precursors subsets. Expression of pro-survival molecules was first evaluated in B lineage cells produced in –T mice under the influence of IL-7 alone. With only IL-7, Bcl-2, Bcl-xL, and Mcl-1 were significantly increased in IL-7R+ as compared to IL-7R– cells in almost all subsets examined, from the most primitive IL-7R+ progenitors through the pre-B cell stage (Figure 3.8 top panel). The exception was the marked absence of Mcl-1 up-regulation in IL-7R+ progenitors as compared to the HSC/multi-lineage progenitor population (CD19–CD34+IL-7R– cells).

Next, we evaluated the expression of Bcl-2 family proteins during human B cell development in +T mice that provide TSLP in context of IL-7. When we compared IL-7R– and IL-7R+ subsets from +T mice the pattern of Bcl-2, Bcl-xL, and Mcl-1

expression was almost identical to that observed in –T animals (Figure 3.8 top panel and Figure 3.8 bottom panel). However, in +T mice, we found that Mcl-1 expression was increased in the IL-7R+ progenitors as compared to their IL-7R– counterparts, which showed the same low level of Mcl-1 expression observed in all CD19–CD34+ cells in –T animals (bottom panel, far right). These data show that all three Bcl-2 family pro-survival proteins are up-regulated in human pro-B and pre-B cells that are IL-7R+ as compared to IL-7R– and that this up-regulation occurs whether or not TSLP is present. In contrast, TSLP exerts effects distinct from IL-7 to up-regulate Mcl-1 in human IL-7R+ progenitors.

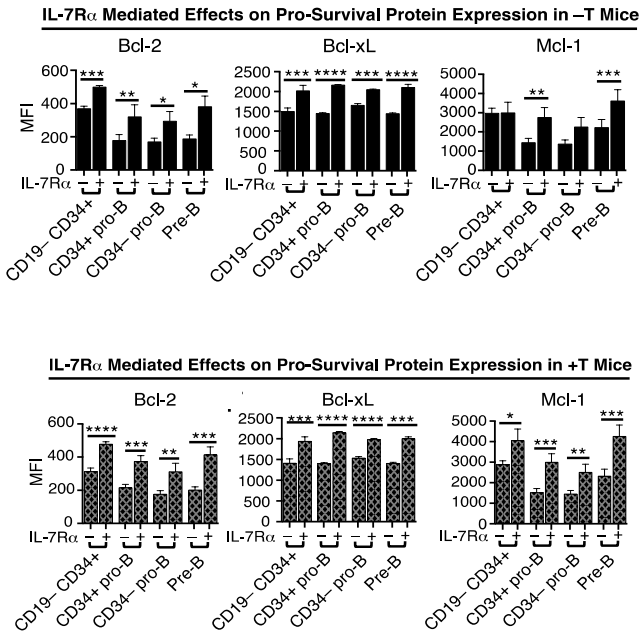

Figure 3.8: Top panel: Graphed are the median fluorescence intensities (MFI) of (B) Bcl-2, (C) Bcl-xL and (D) Mcl-1 in –T mice. Data are from n = 6 or 7 mice per group. Statistical analysis was performed using one-tailed, t-test, *p<0.05, **p<0.01 and ***p<0.001. Error bars represent mean ± SEM. Bottom panel: Graphed are the median fluorescence intensities (MFI) of (E) Bcl-2, (F) Bcl-xL and (G) Mcl-1 in +T mice. Data are from n = 6 or 7 mice per group. Statistical analysis was performed using one-tailed, t-test, *p<0.05, **p<0.01 and ***p<0.001. Error bars represent mean ± SEM.

Overall, our data show that TSLP targets IL-7R+ progenitors in a manner distinct from IL-7 to increase proliferation, up-regulate expression of the Mcl-1 pro-survival protein, and promote differentiation of an expanded CD34+ pro-B cell pool. This population is expanded and/or maintained in subsequent stages of development by TSLP via unidentified mechanism(s) that are independent of Bcl-2 family pro-survival protein expression.

TSLP is Expressed by Human BM Stromal Cells

Our next step was to investigate whether the TSLP effects we observed in +T xenograft mice are consistent with normal *in vivo* human B cell development. To determine if BM stroma provide an *in vivo* source of TSLP to support human B cell production, we isolated RNA from the stromal cells of normal BM donors and performed RT-PCR. We evaluated TSLP expression, and IL-7 for comparison. Figure 3.9A shows that BM stromal cells express transcripts for TSLP, as well as IL-7. To verify that TSLP transcripts result in protein production, supernatant taken from cultured BM stromal cells was evaluated by enzyme-linked immunosorbant assay (ELISA). TSLP, as well as IL-7 proteins were detected in culture supernatants (Figure 3.9B). These data demonstrate that human BM stromal cells produce TSLP, in addition to IL-7, and thus provide a source for both cytokines *in vivo* in the normal human BM microenvironment.

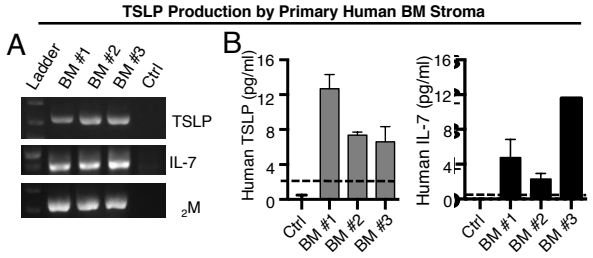

Figure 3.9: *In vivo* human B cell production mirrors xenograft mice with human TSLP. (A) RT-PCR was used to detect TSLP, IL-7 or beta-2 microglobulin (#2M, control) transcripts in primary human BM stromal cells from different human donors – pediatric (BM#1 and BM #2) and adult (BM #3) or water as a negative control. (B) Supernatant from confluent BM stromal cell cultures were assessed by ELISA for TSLP and IL-7 protein production. Dashed lines (---) represent ELISA threshold of detection.

In vivo B cell Production in Patients Shows Progenitor Ratios and Mcl-1 Expression that Mirrors Human B cell Production in Xenograft Mice with TSLP

In +T mice, the CD34+ pro-B compartment is expanded at the expense of IL-7R+ progenitors giving a dramatically different distribution of CD34+ subsets than in –T mice. To determine whether this altered distribution reflects normal human B cell development, we compared the ratio of CD19+CD34+ pro-B cells to IL-7R+ progenitors in BM from pediatric patients to that in xenograft mice. Xenograft or patient BM was stained for flow cytometry to detect human specific B lineage and progenitor markers. Total living CD34+ cells were gated into CD19+CD34+ pro-B and IL-7R+ progenitors (Figure 3.10, left panel). In pediatric BM, the ratio of CD19+CD34+ pro-B to IL-7R+ progenitors was 7.2 to 1 (Figure 3.10, right panel). This was similar to that observed in +T xenograft mice (9.1 to 1) but significantly higher than in –T mice (1.5 to 1) (Figure 3.10, right panel).

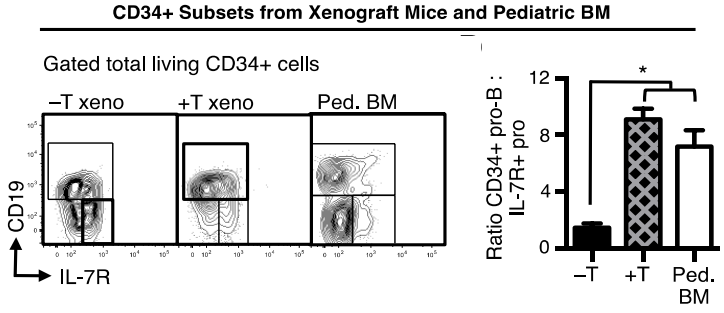

Figure 3.10: Left panel: Plotted are the gated living total CD34+ cells from the BM of –T xenograft, +T xenograft and normal pediatric patients. Right panel: Graphed is the ratio of CD34+ pro-B cells to IL-7R+ progenitors among BM-derived total CD34+ cells from –T xenograft mice (n=3), +T xenograft mice (n=5) and from normal pediatric patient samples (n=10). CD34+ progenitors and early B cell subsets from the BM of normal pediatric patients were gated into IL-7Rα– and IL-7Rα+ fractions.

We wanted to know whether the pattern of Bcl-2 family protein expression that implicates IL-7Rα-mediated signals in the survival of developing B cells in xenograft mice was also present *in vivo* in patient samples. Normal pediatric BM samples were analyzed for Bcl-2 family protein expression by flow cytometry. The pattern of up-regulated Bcl-2 and Mcl-1 in IL-7R+ subsets of pro-B and pre-B cells that we observed in pediatric patient samples was similar to that observed in –T and +T xenograft mice (Figure 3.11, left panel). Bcl-xL showed up-regulation in some, but not all IL-7R+ subsets (Figure 3.11, middle panel). Notably, in normal pediatric BM we found that Mcl-1 was up-regulated in IL-7R+ progenitors as compared to HSC/multi-lineage progenitor population (CD19–CD34+IL-7R– cells) (Figure 3.11, right panel) —a feature unique to B cell production in xenograft mice with TSLP. Taken together these data show that normal pediatric B cell development shares features unique to xenograft mice with human TSLP, namely a high ratio of CD34+ pro-B cells to IL-7R+ progenitors and up-regulated Mcl-1 in IL-7R+ progenitors.

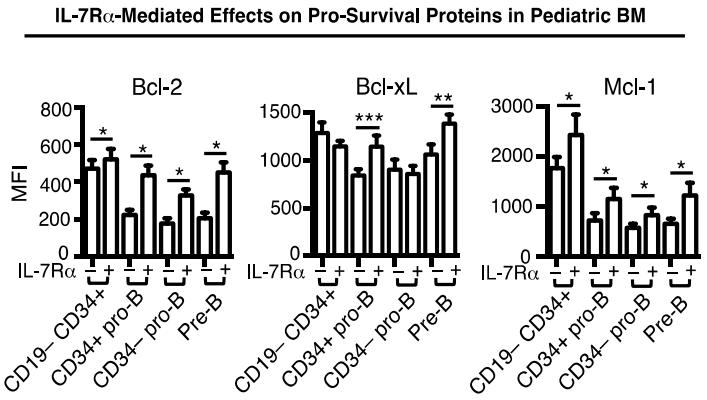

Figure 3.11: Left panel: Graphed are MFI of Bcl-2 (n=6); middle panel: Bcl-xL (n=10) and right panel: Mcl-1 (n=9) in the IL-7Rα–/+ fractions of normal pediatric BM. Statistical analysis was performed using two-tail, t-test, *p<0.05, **p<0.01 and ***p<0.001. Error bars represent mean ± SEM.

Discussion

Here we use a novel xenograft model system that allows us to study human B cell development in vivo with and without TSLP and in context of IL-7 stimulation. Using this model we show that TSLP uniquely targets CD19–CD34+ progenitors expressing the IL-7Rα, inducing increased proliferation and Mcl-1 expression that is not observed during in vivo human B cell development with IL-7 stimulation alone. Rather than expanding the IL-7R+ progenitor population, these activities result in a dramatically expanded CD34+CD19+ pro-B cell compartment suggesting that TSLP promotes the differentiation of newly produced cells into the B lineage. This is supported by in vitro experiments showing that TSLP promotes the production of CD19+Pax-5+ B lineage cells from CB CD34+ progenitors. In pediatric BM samples we observed a 7:1 ratio of CD34+ pro-B cells to IL-7R+ progenitors as well as up-regulated Mcl-1 in IL-7R+ progenitors. This mirrors what we observed in +T mice suggesting that the effects produced by TSLP occur during normal in vivo B cell development in children.

Genetic alterations leading to activation or overexpression of the TSLP receptor component, CRLF2, are linked to malignant transformation and high-risk B cell precursor acute lymphoblastic leukemia (26, 27). This suggests a role for TSLP receptor activation in the proliferation and/or survival of early human B lineage cells. Our data show that TSLP is similar to IL-7 in that it stimulates the in vitro proliferation of normal B cell precursors derived from CB CD34+ cells (Figure 8). Our data in normal B cell precursors are consistent with previous reports (28, 29) suggesting a role for TSLP-CRLF2 mediated signals in the proliferation of B-ALL cells. Our xenograft studies also suggest a role for TSLP, distinct from that of IL-7 and independent from Bcl-2 family

pro-survival molecules, in protecting developing CD19+ B lineage cells from death. It should be noted that the up-regulation of Bcl-2 family pro-survival proteins that we observed in IL-7R+ subsets of developing B lineage cells, with or without TSLP, could also be a function of TSLP that is redundant to IL-7 and therefore indistinguishable in our model.

Our studies suggest TSLP has roles that are both distinct and redundant to IL-7 in human B cell development. It is important to note that our studies were performed using postnatal sources that most closely reflect B cell development in the pediatric population. This is important because murine studies suggest that the role of IL-7 is less critical (30) and TSLP may play a larger role (2, 3) at early points in life, although the latter remains controversial (31). Thus, it will be important to evaluate the role of TSLP during adult B cell development using the model that we have developed here.

Understanding the potential contribution of TSLP to B cell production throughout life is important because a range of factors influence TSLP levels and potentially B cell production. TSLP expression is increased by environmental pollutants (32-34) and is elevated in inflammatory diseases including asthma, atopic dermatitis and arthritis (32-34). Our data show that increases in circulating TSLP increases the proliferation and reduces the numbers of IL-7R+ progenitors. This raises the question of whether high levels of circulating TSLP could exhaust the lymphoid progenitor population. If so, this has the potential for long-term impact on the production of adaptive immune cells in people with chronically elevated TSLP.

References

1. Ray RJ, Furlonger C, Williams DE, Paige CJ. Characterization of thymic stromal-derived lymphopoietin (TSLP) in murine B cell development *in vitro*. Eur J Immunol. 1996 Jan;26(1):10-6.

2. Vosshenrich CA, Cumano A, Muller W, Di Santo JP, Vieira P. Thymic stromal-derived lymphopoietin distinguishes fetal from adult B cell development. Nat Immunol. 2003 Aug;4(8):773-9.

3. Vosshenrich CA, Cumano A, Muller W, Di Santo JP, Vieira P. Pre-B cell receptor expression is necessary for thymic stromal lymphopoietin responsiveness in the bone marrow but not in the liver environment. Proc Natl Acad Sci U S A. 2004 Jul 27;101(30):11070-5.

4. Valenzona HO, Dhanoa S, Finkelman FD, Osmond DG. Exogenous interleukin 7 as a proliferative stimulant of early precursor B cells in mouse bone marrow: efficacy of IL-7 injection, IL-7 infusion and IL-7-anti-IL-7 antibody complexes. Cytokine. 1998 Jun;10(6):404-12.

5. von Freeden-Jeffry U, Vieira P, Lucian LA, McNeil T, Burdach SE, Murray R. Lymphopenia in interleukin (IL)-7 gene-deleted mice identifies IL-7 as a nonredundant cytokine. J Exp Med. 1995 Apr 1;181(4):1519-26.

6. Scheeren FA, van Lent AU, Nagasawa M, Weijer K, Spits H, Legrand N, et al. Thymic stromal lymphopoietin induces early human B-cell proliferation and differentiation. Eur J Immunol. 2010 Feb 1.

7. Saeland S, Duvert V, Pandrau D, Caux C, Durand I, Wrighton N, et al. Interleukin-7 induces the proliferation of normal human B-cell precursors. Blood. 1991 Nov 1;78(9):2229-38.

8. Johnson SE, Shah N, Panoskaltsis-Mortari A, LeBien TW. Murine and human IL-7 activate STAT5 and induce proliferation of normal human pro-B cells. J Immunol. 2005 Dec 1;175(11):7325-31.

9. Parrish YK, Baez I, Milford TA, Benitez A, Galloway N, Rogerio JW, et al. IL-7 Dependence in human B lymphopoiesis increases during progression of ontogeny from cord blood to bone marrow. J Immunol. 2009 Apr 1;182(7):4255-66.

10. Mullighan CG, Collins-Underwood JR, Phillips LAA, Loudin MG, Liu W, Zhang JH, et al. Rearrangement of CRLF2 in B-progenitor- and Down syndrome-associated acute lymphoblastic leukemia. Nature Genetics. 2009 Nov;41(11):1243-U111.

11. Shochat C, Tal N, Bandapalli OR, Palmi C, Ganmore I, Te Kronnie G, et al. Gain-of-function mutations in interleukin-7 receptor-{alpha} (IL7R) in childhood acute lymphoblastic leukemias. J Exp Med. 2011 May 9;208(5):901-8.

12. Zhang W, Wang J, Wang Q, Chen G, Zhang J, Chen T, et al. Identification of a novel type I cytokine receptor CRL2 preferentially expressed by human dendritic cells and activated monocytes. Biochem Biophys Res Commun. 2001 Mar 9;281(4):878-83.

13. Noguchi M, Nakamura Y, Russell SM, Ziegler SF, Tsang M, Cao X, et al. Interleukin-2 receptor gamma chain: a functional component of the interleukin-7 receptor. Science. 1993 Dec 17;262(5141):1877-80.

14. Park LS, Martin U, Garka K, Gliniak B, Di Santo JP, Muller W, et al. Cloning of the murine thymic stromal lymphopoietin (TSLP) receptor: Formation of a functional heteromeric complex requires interleukin 7 receptor. J Exp Med. 2000 Sep 4;192(5):659-70.

15. Pandey A, Ozaki K, Baumann H, Levin SD, Puel A, Farr AG, et al. Cloning of a receptor subunit required for signaling by thymic stromal lymphopoietin. Nat Immunol. 2000 Jul;1(1):59-64.

16. Palmer MJ, Mahajan VS, Trajman LC, Irvine DJ, Lauffenburger DA, Chen J. Interleukin-7 receptor signaling network: an integrated systems perspective. Cell Mol Immunol. 2008 Apr;5(2):79-89.

17. Rochman Y, Kashyap M, Robinson GW, Sakamoto K, Gomez-Rodriguez J, Wagner KU, et al. Thymic stromal lymphopoietin-mediated STAT5 phosphorylation via kinases JAK1 and JAK2 reveals a key difference from IL-7-induced signaling. Proc Natl Acad Sci U S A. 2010 Nov 9;107(45):19455-60.

18. Tasian SK, Doral MY, Borowitz MJ, Wood BL, Chen IM, Harvey RC, et al. Aberrant STAT5 and PI3K/mTOR pathway signaling occurs in human CRLF2-rearranged B-precursor acute lymphoblastic leukemia. Blood. 2012 Jul 26;120(4):833-42.

19. Johnson SE, Shah N, Bajer AA, LeBien TW. IL-7 activates the phosphatidylinositol 3-kinase/AKT pathway in normal human thymocytes but not normal human B cell precursors. J Immunol. 2008 Jun 15;180(12):8109-17.

20. Quentmeier H, Drexler HG, Fleckenstein D, Zaborski M, Armstrong A, Sims JE, et al. Cloning of human thymic stromal lymphopoietin (TSLP) and signaling mechanisms leading to proliferation. Leukemia. 2001 Aug;15(8):1286-92.

21. Reche PA, Soumelis V, Gorman DM, Clifford T, Liu M, Travis M, et al. Human thymic stromal lymphopoietin preferentially stimulates myeloid cells. J Immunol. 2001 Jul 1;167(1):336-43.

22. Barata JT, Silva A, Abecasis M, Carlesso N, Cumano A, Cardoso AA. Molecular and functional evidence for activity of murine IL-7 on human lymphocytes. Exp Hematol. 2006 Sep;34(9):1133-42.

23. Taguchi T, Takenouchi H, Shiozawa Y, Matsui J, Kitamura N, Miyagawa Y, et al. Interleukin-7 contributes to human pro-B-cell development in a mouse stromal cell-dependent culture system. Exp Hematol. 2007 Jul 24.

24. Chappaz S, Flueck L, Farr AG, Rolink AG, Finke D. Increased TSLP availability restores T- and B-cell compartments in adult IL-7 deficient mice. Blood. 2007 Dec 1;110(12):3862-70.

25. Carpino N, Thierfelder WE, Chang MS, Saris C, Turner SJ, Ziegler SF, et al. Absence of an essential role for thymic stromal lymphopoietin receptor in murine B-cell development. Mol Cell Biol. 2004 Mar;24(6):2584-92.

26. Russell LJ, Capasso M, Vater I, Akasaka T, Bernard OA, Calasanz MJ, et al. Deregulated expression of cytokine receptor gene, CRLF2, is involved in lymphoid transformation in B-cell precursor acute lymphoblastic leukemia. Blood. 2009 Sep 24;114(13):2688-98.

27. Chapiro E, Russell L, Lainey E, Kaltenbach S, Ragu C, Della-Valle V, et al. Activating mutation in the TSLPR gene in B-cell precursor lymphoblastic leukemia. Leukemia. 2010 Mar;24(3):642-5.

28. Brown VI, Hulitt J, Fish J, Sheen C, Bruno M, Xu Q, et al. Thymic stromal-derived lymphopoietin induces proliferation of pre-B leukemia and antagonizes mTOR inhibitors, suggesting a role for interleukin-7Ralpha signaling. Cancer Res. 2007 Oct 15;67(20):9963-70.

29. Tasian SK, Loh ML. Understanding the biology of CRLF2-overexpressing acute lymphoblastic leukemia. Crit Rev Oncog. 2011;16(1-2):13-24.

30. Carvalho TL, Mota-Santos T, Cumano A, Demengeot J, Vieira P. Arrested B lymphopoiesis and persistence of activated B cells in adult interleukin 7(-/)- mice. J Exp Med. 2001 Oct 15;194(8):1141-50.

31. Jensen CT, Kharazi S, Boiers C, Cheng M, Lubking A, Sitnicka E, et al. FLT3 ligand and not TSLP is the key regulator of IL-7-independent B-1 and B-2 B lymphopoiesis. Blood. 2008 Sep 15;112(6):2297-304.

32. Bleck B, Tse DB, Gordon T, Ahsan MR, Reibman J. Diesel exhaust particle-treated human bronchial epithelial cells upregulate Jagged-1 and OX40 ligand in myeloid dendritic cells via thymic stromal lymphopoietin. J Immunol. 2010 Dec 1;185(11):6636-45.

33. Bleck B, Tse DB, Curotto de Lafaille MA, Zhang F, Reibman J. Diesel exhaust particle-exposed human bronchial epithelial cells induce dendritic cell maturation and polarization via thymic stromal lymphopoietin. J Clin Immunol. 2008 Mar;28(2):147-56.

34. Ying S, O'Connor B, Ratoff J, Meng Q, Fang C, Cousins D, et al. Expression and cellular provenance of thymic stromal lymphopoietin and chemokines in patients with severe asthma and chronic obstructive pulmonary disease. J Immunol. 2008 Aug 15;181(4):2790-8.

35. Crooks GM, Hao QL, Petersen D, Barsky LW, Bockstoce D. IL-3 increases production of B lymphoid progenitors from human CD34+CD38- cells. J Immunol. 2000 Sep 1;165(5):2382-9.

36. Shah AJ, Smogorzewska EM, Hannum C, Crooks GM. Flt3 ligand induces proliferation of quiescent human bone marrow CD34+CD38- cells and maintains progenitor cells in vitro. Blood. 1996 May 1;87(9):3563-70.

CHAPTER FOUR

TSLP REGULATES CELL DEATH AND CELL SURVIVAL MECHANISMS AND INDUCES APOPTOSIS IN CRLF2 B-ALL CELLS

Abstract

Pediatric CRLF2 B-ALL is a high-risk form of leukemia that is associated with poor patient survival outcomes. CRLF2 B-ALL is five (5) times more prevalent in Hispanic children and is associated with a higher rate of relapse. Genetic defects in the *CRLF2* gene have led to the overexpression of the CRLF2 protein- a receptor component for TSLP- on the surface of B-ALL cells. The disease mechanisms of CRLF2 B-ALL are unclear; more importantly, the role of TSLP in the maintenance and progression of CRLF2 B-ALL is unknown. TSLP induces proliferation of normal human B-cell precursors and is produced by human bone marrow stromal cells, suggesting that it is present in the BM microenvironment where leukemia develops. **T**herefore we hypothesized that *TSLP contributes to CRLF2 B-ALL by increasing proliferation and/or survival of leukemia cells via regulation of genes downstream of CRLF2 pathway activation*. Using the novel hTSLP+/hTSLP- xenograft model, we demonstrated that TSLP up-regulates cell death and survival genes and biological pathways and induces apoptosis in CRLF2 B-ALL cells *in vivo* and *in vitro*. Further, TSLP transiently increases Bcl-2 pro-survival family member Mcl-1, suggesting that TSLP-induced cell death and survival mechanisms are mediated by Mcl-1. The studies described in this chapter provide evidence that TSLP plays a role in regulating the survival mechanisms of CRLF2 B-ALL and has future implications for the treatment of this disease.

Abbreviations

TSLP	Thymic Stromal Lymhopoieitin
TSLPRβ	Thymic Stromal Lymhopoieitin receptor beta (or CRLF2)
CRLF2	Cytokine Receptor-Like Factor 2 (or TSLPRβ)
IL-7Rα	Interleukin 7 Receptor alpha
CD34	Cluster of Differentiation 34 (stem cell marker)
CRLF2 B-ALL	CRLF2 B-cell Acute Lymphoblastic Leukemia
JAK	Janus Kinase
STAT	Signal Transducers and Activators of Transcription
BaF3	Murine Pro-B cell line
PI3K	Phosphoinositide-3-Kinase
AKT	Protein Kinase B
mTOR	Mammalian Target Of Rapamycin
ERK	Extracellular signal-Regulated Kinases
MAPK	Mitogen-Activated Protein Kinase
hTSLP	Human TSLP
Bcl-2	B-cell Lymphoma 2
Bcl-xl	Bcl-2 Like protein X
Mcl-1	Myeloid Cell Leukemia 1
BM	Bone Marrow
PB	Peripheral Blood
7-AAD	7-Amino-Actinomycin D
PDX	Patient Derived Xenograft

NSG	NOD/SCID Gamma (NOD.Cg-Prkdc^{scid}Il2rg^{tm1Wjl}/SzJ)
CD45	Cluster of Differentiation 45 (leukocyte marker)
CD19	Cluster of Differentiation 19 (B-cell marker)
CD10	Cluster of Differentiation 10 (B-cell marker)
DGA	Discriminatory Gene Analysis
GSEA	Gene Set Enrichment
IPA	Ingenuity Pathway Analysis
EIF2	Eukaryotic Initiation Factor 2
ROS	Reactive Oxygen Species
NADH	Nicotinamide Adenine Dinucleotide
ER	Endoplasmic Reticulum

Introduction

TSLP, initially detected in the conditioned medium of epithelial cells that are found in the thymic medulla is produced in the lung, bronchial tree, intestine and skin [1, 2]. TSLP performs physiological roles in inflammation, allergic reactions, helminthic infections and the development of various hematopoietic cells [3-5]. High levels of TSLP have been linked to asthma, allergy, atopic dermatitis and autoimmune diseases [6]. TSLP performs its functions by signaling through the TSLP receptor, which comprises of the IL-7Rα and TSLPRβ [7]. Using microarray, Lu, et al demonstrated that different cells express varying levels of TSLPRβ. For example, myeloid dendritic cells express high levels of TSLPRβ; $CD34^+$ human hematopoietic progenitor-derived mast cells express low levels of TSLPR; and B-cells show undetected levels of TSLPRβ [8]. Surprisingly, the low levels of TSLPRβ expressed on B-cells are sufficient for TSLP to bind and induce proliferation of B-cell precursors ([7]; chapter 2 and 3). However, more recently, several groups have shown that genetic defects in the *CRFL2* (another name for TSLPRβ) gene led to overexpression of the CRLF2 protein on the surface of leukemia cells [9-11]. These leukemia cells are a high-risk subset of B-cell Acute lymphoblastic leukemia referred to as CRLF2 B-ALL. CRLF2 B-ALL patients experience a 65% relapse rate and have an overall poor survival outcome [12].

Studies conducted by Children Oncology Groups (COGs) have been directed towards genomic profiling and risk stratification in order to identify high-risk patients such as CRLF2 B-ALL patients [13, 14]. Additional studies have been conducted to assess CRLF2 B-ALL patient response to current treatment regimens and to determine therapeutic outcome, but very little is known about the mechanisms that contribute to the

initiation, progression and maintenance of the disease [15, 16]. Recent molecular studies have shown that in some cases overexpression of CRLF2 is associated with activating mutations in JAK2, a kinase which acts downstream of TSLP-CRLF2 interactions [17]. The *CRLF2* gene defects and JAK2 activating mutations have been shown to cooperate in promoting constitutive dimerization, constitutive JAK-STAT activation and cytokine independent growth in the murine BaF3 cellular model system [10, 11].

These data have led others to the conclusion that over-expression of CRLF2 and activating JAK mutations are the major contributors to this disease and the current dogma is that CRLF2 B-ALL cells do not require TSLP-induced signals for survival and proliferation due to constitutive activation of the JAK-STAT pathway. Therefore studies to evaluate the efficacy of treatments for CRLF2 B-ALL are conducted in context of JAK-mutations and without TSLP-induced CRLF2 signals [18]. However, all JAK mutations are not activating and 30% of CRLF2 B-ALL patients have no mutations in JAKs [17]. Furthermore, our lab and others have shown that TSLP increases the phosphorylation of STAT5, S6 and ERK which provided evidence of activation of the JAK-STAT, PI3K/AKT/mTOR and ERK pathways and more importantly in cells with JAK mutations [19]**.** Thus, the contributions of TSLP (the ligand that stimulates CRLF2 signaling) to the maintenance/progression of CRLF2 B-ALL and the cellular and molecular mediators involved remain to be elucidated.

Here we use a novel hTSLP+/hTSLP- human-mouse xenograft *in vivo* system, *in vitro* studies and gene arrays to show that TSLP regulates cell death and survival mechanisms and induces apoptosis in CRLF2 B-ALL cells, in spite of the up-regulation of Bcl-2 family member Mcl-1.

Materials and Methods

Mice

Studies were performed using NOD.Cg-Prkdc^{scid} Il2rg^{tm1Wjl}/SzJ (NSG) mice (Jackson Laboratory). Mice were housed under pathogen-free conditions in the Loma Linda University Animal Care Facility and studies were conducted in accordance with Loma Linda University Institutional Animal Care and Use Committee (IACUC) approved protocols. Leukemia cell lines and primary cells (CRLF2 B-ALL and non-CRLF2 B-ALL primary cells) were expanded in NSG mice for 9-11 weeks. Animals were euthanized at end point by CO_2 asphyxiation. Animal tissues including bone marrow (BM), spleen and peripheral blood (PB) were harvested and processed. BM cells were collected by removing long bones (femora, humeri) from mice and flushing the bones with a PBS solution using a syringe.

In vivo Apoptosis Assay

hTSLP+/hTSLP- mice were produced by injecting NSG mice weekly with 5X10^6 HS27 stromal cells that were transduced with a lentiviral vector that expresses human TSLP (hTSLP+) or an empty vector (hTSLP-). Mice were then transplanted with 5-10X10^6 human CRLF2 B-ALL cell lines or primary cells. Prior to euthanasia, TSLP levels in animal sera were measured weekly by ELISA to monitor the levels of human TSLP in hTSLP+ mice and hTSLP– mice. CRLF2 B-ALL cells expanded in hTSLP+ or hTSLP- mice were harvested from tissues (BM, spleen and PB) and stained for flow cytometry analysis with the following markers: mouse CD45 to identify mouse leukocytes; human CD19 to identify human B-ALL cells; TSLPR (CRLF2) to identify

CRLF2+ B-ALL cells as a measure of bone marrow disease; and Annexin V and/or 7-AAD to detect cells that are in early or late stages of apoptosis.

Whole-genome Microarray

Primary CRLF2 B-ALL cells were harvested from the BM of hTSLP+ and hTSLP- mice and hCD19+ B-ALL cells were isolated by magnetic separation using the MACS cell separation kit (Miltenyi Biotec). After separation, cells were rapidly frozen and shipped to Miltenyi Biotec for sample preparation, whole genome microarray, and discriminatory gene analysis (Miltenyi Genomic Services, Germany).

In vitro Apoptosis Assay

CRLF2 B-ALL cell lines or primary cells were maintained in RPMI 1640 medium supplemented with penicillin/streptomycin, L-glutamine, 50 uM 2-ME and 20% fetal bovine serum (FBS). Cells were cultured with the above media in the presence or absence of TSLP for 3, 6 or 9 days, then harvested and stained with Annexin V and 7-AAD to identify cells in early stages (Annexin V+, 7-AAD–) or late stages (Annexin V+, 7-AAD+) of apoptosis for flow cytometry analysis. This experiment was repeated with IL-7. Cell cultures included neutralizing antibodies to TSLP or IL-7 and nonspecific isotype matched control antibodies.

In vitro Pro-survival Protein Assay

CRLF2 B-ALL cells were cultured in cell culture media with or without TSLP along with the appropriate controls (described above) for 3, 6 or 9 days. Cells were

harvested and assessed for the expression of Bcl-2 family members (anti-apoptotic proteins: Bcl-2, Bcl-xl and Mcl-1) using a caltag fixation and permeabilization intracellular flow cytometry protocol (Life Technologies).

Results

TSLP Induces Apoptosis in CRLF2 B-ALL Cells In vivo

The development of the novel hTSLP+/hTSLP- xenograft model described in chapter 2 provided an *in vivo* tool that can be used to study the role of TSLP in normal human B-cells (see chapter 3) and most importantly the role of TSLP in CRLF2 B-ALL. Using the hTSLP+/hTSLP- model, data described in chapters 2 and 3 showed that TSLP induces proliferation and survival of normal B-cells and induces activation of the mTOR pathway and its related genes in primary CRLF2 B-ALL cells. These data provided evidence that 1) the hTSLP+/hTSLP- model provides the human TSLP-CRLF2 interactions that are required to activate normal human B-cells and human CRLF2 B-ALL cells *in vivo* and 2) hTSLP induces cell proliferation and cell survival signals in normal B-cells. The results obtained from the studies that evaluated the effects of TSLP on normal B-cells supports our hypothesis that TSLP induces proliferation and survival in these cells, however, the effects of TSLP on human CRLF2 B-ALL cells remain to be elucidated. Therefore, using the novel hTSLP+/hTSLP- xenograft model, we evaluated the effects of TSLP on CRLF2 B-ALL cells by testing the overarching hypothesis that *TSLP contributes to CRLF2 B-ALL by increasing proliferation and/or survival of leukemia cells via regulation of genes downstream of CRLF2 pathway activation*.

To test this hypothesis, first we evaluated the effects of TSLP on CRLF2 B-ALL

cells *in vivo* by creating patient-derived xenografts (PDXs), administering varying levels of TSLP and assessing leukemia cell viability. PDXs were developed by transplanting NSG mice with primary CRLF2 B-ALL cells via tail vein injections and allowing the cells to expand *in vivo* for 9-11 weeks. Prior to or on the day of leukemia cell transplantation, NSG mice were injected with either low levels of TSLP (<10 pg/ml) or higher levels of TSLP (~20 pg/ml) and leukemic cell BM chimerism was determined using mouse and human cell markers. To accomplish this, BM cells were harvested from mice at euthanasia, cells were co-stained with mouse CD45, human CD19 and human CRLF2 to determine engraftment of human leukemia cells; and Annexin V to identify apoptotic cells.

When low levels of TSLP were administered, our data showed that ~88% of cells in the BM of +T mice were CRLF2 B-ALL cells while 83% of cells in the BM of –T mice were CRLF2 B-ALL cells (Figure 4.1, top panel). Engrafted cells were mCD45–hCD19+hCRLF2+. The percent of cells engrafted is a measure of BM disease, therefore based on this definition, the data suggests that there is no difference in BM disease in +T mouse compared to –T mouse.

To determine the effect of TSLP on the viability of engrafted cells, BM cells were also stained with Annexin V and 7-AAD. Cells were first gated using mCD45, hCD19 and hCRLF2 to determine the percent of hCD19+ cells (Figure 4.1, top panel) and the percent CRLF2 B-ALL cells (Figure 4.1, middle panel). The engrafted cells were gated to show Annexin V+ cells. The dot plot showed that the percent of living hCD19+ cells in the BM of +T mouse was half as much as the percent of hCD19+ cells in the BM of –T mouse (Figure 4.1, bottom panel). Our data showed no observable differences in BM

engraftment in +T and -T mice, however, there is a higher percent of apoptotic leukemic cells in the BM of the +T mouse compared to -T mouse.

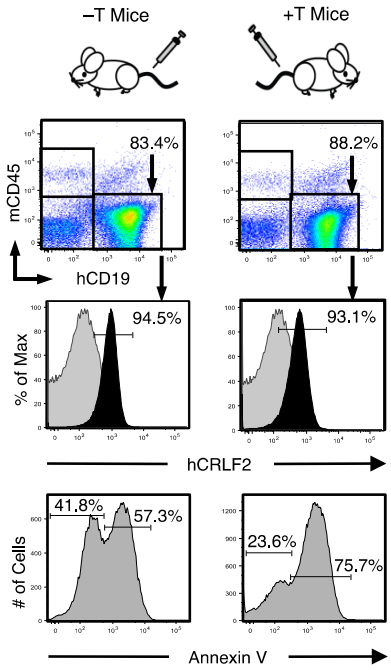

Figure 4.1: Primary CRLF2 B-ALL cells were injected into –T and +T mice and animals were euthanized 9 weeks post transplant, BM was harvested and cells were co-stained with mCD45, hCD19, hCRLF2 and Annexin V. hCD19+ cells were sub-gated to determine the percent of CRLF2+ and Annexin V+ cells.

When higher levels of TSLP was administered, our data showed that for primary CRLF2 B-ALL#1, 2.35 % of cells in the BM of +T mice were CRLF2 B-ALL cells compared 28.1 % of cells in the BM of –T mice- n=2 (Figure 4.2, top panel). For primary CRLF2 B-ALL#2, 0.2% of cells in the BM of +T mice were CRLF2 B-ALL cells, compared to 95% of cells in the BM of –T mice- n=2-10(Figure 4.2, bottom panel). Therefore at low levels of TSLP there was no observable difference in BM engraftment, while at higher levels of TSLP, there was a dramatic decrease in the percent of CRLF2 B-

ALL cells engrafted in the BM of +T mice. Data obtained from secondary and tertiary CRLF2 B-ALL PDX showed similar results, irrespective of the source of the cells for the 2o and 3o transplants, i.e. irrespective of whether BM or Spleen cells were used. The data suggests that at higher doses (~20 pg/ml – reported physiological levels), TSLP exerts an effect on CRLF2 B-ALL BM disease- that is, TSLP specifically reduces the tumor burden in mice.

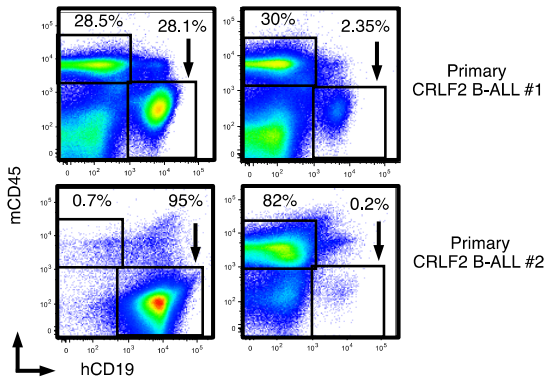

Figure 4.2: Primary CRLF2 B-ALL cells from two different patients (B-ALL#1 and B-ALL#2) were injected into –T and +T mice and animals were euthanized 9-11 weeks post transplant, BM was harvested and cells were co-stained with mCD45, hCD19 and hCRLF2. Gated hCD19+ cells is a measure of BM disease.

Results from staining with apoptotic markers and gating cells as described above in figure 4.1 showed that the CRLF2 B-ALL cells engrafted in +T mice and –T mice when during higher levels of TSLP, were Annexin V–. Virtually all cells engrafted in the BM of +T as well as –T mice were viable living cells.

In summary, our data showed that when low levels of TSLP is present in +T mice, there's a higher percentage of CRLF2 B-ALL cells in the BM, but most of these cells undergo apoptosis. However, when higher levels of TSLP are present in the +T mice,

there is low to no engraftment of CRLF2 B-ALL cells and these engrafted cells are viable. Taken together, these data suggest that increasing the levels of TSLP produces a differential effect on CRLF2 B-ALL cells *in vivo*. Further, this differential effect of TSLP is demonstrated by its induction of apoptosis in leukemia cells at lower levels and the absence of leukemia cells at higher levels. Moreover, these results were observed/maintained over subsequent transplants and were unique to the +T condition irrespective of the source of cells.

TSLP Activates Cell Death and Survival Pathways and Cellular Functions in CRLF2 B-ALL Cells In vivo

In order to gain a better understanding of how TSLP regulates the cellular functions we observed in CRLF2 B-ALL cells *in vivo*, we performed whole genome microarray studies to identify genes that are up-regulated by TSLP, the biological pathways that are implicated by these genes, and the molecular and cellular functions that ensue as a result of the up-regulation of these genes and pathways. To accomplish this, primary CRLF2 B-ALL cells were expanded in +T and -T mice for 9 weeks, BM was harvested, CD19+ leukemia cells were isolated by magnetic separation and the cells were shipped to Miltenyi Biotec (Miltenyi Genomic Services) for whole genome microarray and discriminatory gene analysis (DGA). GSEA and IPA were performed using whole genome microarray data files. Results from GSEA analysis showed that TSLP induced activation of the mTOR pathway and its related genes in primary CRLF2 B-ALL cells that were expanded in +T compared to –T mice (chapter 2 and Table 6). Studies have shown that the mTOR pathway functions to regulate cell growth and survival [20]. IPA

results provided additional evidence that the mTOR pathway was up-regulated by TSLP in these cells. In addition to the mTOR pathway, the IPA results also showed that a list of other canonical pathways were significantly up-regulated (compared to mTOR) by TSLP in CRLF2 B-ALL cells (Figure 4.3).

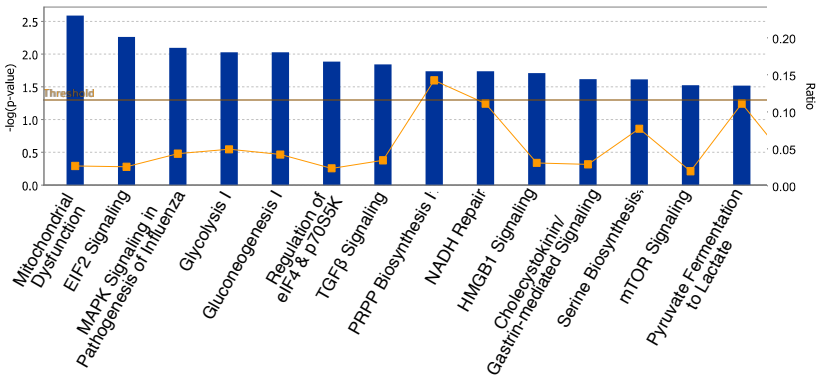

Figure 4.3: Ingenuity Pathway Analysis (IPA) was performed based on gene reporters that were significantly up-regulated (2.0 fold, $p \leq 0.05$). Graphed are the canonical pathways significantly enriched in samples taken from +T as compared to –T mice.

The data showed that in addition to the mTOR pathway, mitochondrial dysfunction (most significantly up-regulated) followed by EIF2 signaling and other cell metabolism pathways were also up-regulated by TSLP (Figure 4.3). Studies have shown that mitochondrial dysfunction is linked to the generation of reactive oxygen species (ROS) in cells; it affects processes such as lipid metabolism; and is implicated in the intrinsic (mitochondrial) apoptosis pathway [21-23]. EIF2 signaling has been shown to regulate protein translation in response to cellular stress that is induced by viral infection, heme deprivation, oxidative stress, ER stress, nutrient deprivation, heat shock, proteasome inhibition and UV irradiation [24]. Other studies have also shown that EIF2 can activate

both pro-apoptotic and pro-survival cellular pathways [25, 26]. Alternatively, mTOR signaling has been shown to induce cellular growth and proliferation [27]. Careful investigation of the top 10 pathways listed showed that mitochondrial dysfunction, EIF2 signaling, MAPK signaling in influenza are involved in cell death/cell stress mechanisms; while eIF4 and p70S6K signaling, glycolysis, gluconeogenesis, TGFβ , PRPP Biosynthesis, NADH repair and HMGB1 signaling are involved in cell survival mechanisms.

Additional IPA analyses revealed that the top associated network function that was up-regulated in the +T CRLF2 B-ALL sample but not in the –T sample was the network responsible for cellular assembly, cellular organization, cellular death and survival and cellular morphology. Most importantly, the top cellular and molecular function of the cell that was up-regulated by TSLP is cell death and survival, with a total of 34 genes involved in these processes (Table 1). Cell death and survival was followed by other cellular functions including free radical scavenging, lipid metabolism, molecular transport and small molecule biochemistry. In summary, the biological pathways up-regulated by TSLP reflect the involvement of cell death, cell stress and cell survival mechanisms. This data is further supported by the results that showed that the top cellular and molecular function of the cell that was regulated by TSLP was cell death and survival. Taken together, these data suggest that both cell death and cell survival functions as well as their downstream pathways are involved in TSLP-CRLF2 signaling in CRLF2 B-ALL cells that were expanded in the +T mouse.

Table 1: List of cellular and molecular functions that are up-regulated by TSLP in primary CRLF2 B-ALL cells expanded in +T mice compared to –T mice. The number of molecules refers to the number of genes that are up-regulated by TSLP and contribute to the respective cellular/molecular functions listed to the left.

Cellular and Molecular Functions of the Cell	#of Molecules	P-value
Cell Death and Survival	34	**7.97E-06 – 4.21E-02**
Free Radical Scavenging	12	**1.11E-04 – 3.19E-02**
Lipid Metabolism	8	**1.11E-04 – 3.62E-02**
Molecular Transport	16	**1.11E-04 – 3.62E-02**
Small Molecule Biochemistry	22	**1.11E-04 – 3.63E-02**

TSLP Induces Apoptosis in CRLF2 B-ALL Cells In vitro

The molecular data obtained from the IPA of CRLF2 B-ALL +T and –T PDXs suggested that TSLP may play a role in regulating cell death and cell survival mechanisms and further substantiated the apoptotic effects of TSLP on CRLF2 B-ALL cells that was observed *in vivo*. Therefore to further elucidate the mechanisms by which TSLP regulates cell death and survival, we evaluated the effects of TSLP on CRLF2 B-ALL cells *in vitro*. To accomplish this, we cultured human CRLF2 B-ALL cell lines with or without TSLP for 3, 6 or 9 days and assessed cell death by staining cells with apoptotic markers- Annexin V and 7-AAD. Cells were split every 3 days and fresh media containing cytokines was added. Cells that undergo early apoptosis were detected using Annexin V while cells that undergo late apoptosis were detected using 7-AAD. Total percent of apoptotic cells was represented as cells that were Annexin V+7-AAD+, while the percent of living cells was represented as cells that were Annexin V-7-AAD-. The

total number of living cells in culture under each condition and at each time point was determined by trypan blue cell counts.

Our results showed that there was no significant difference in the percent of apoptotic cells between cells that were treated with TSLP compared to untreated cells at day 3 (Figure 4.4, top-left panel). Similarly, there was no significant difference in the number of living cells in culture between cells that were treated with TSLP and those that were untreated (Figure 4.4, bottom-left panel). However, at day 6 there was an increase in the percent of apoptotic cells in the cultures that were treated with TSLP compared to untreated controls (Figure 4.4, top-middle panel). In support of the observed increase in the percent of apoptotic cells, we observed a decrease in the total number of living cells present in the cultures that were treated with TSLP compared to the untreated control (Figure 4.4, bottom-middle panel). Similarly, at day 9 we observed a pronounced increase in the percent of apoptotic cells in the cultures that were treated with TSLP compared to controls (Figure 4.4 top-right panel) and substantial decrease in the total number of living cells in these cultures (Figure 4.4 bottom-right panel). Further, the percent apoptosis in cells treated with TSLP at day 3 was very low (~20%) compared to day 6 (~50%) and day 9 (~80%) (Figure 4.4). Overall, the data showed that TSLP induces apoptosis in CRLF2 B-ALL cells *in vitro* which is increased at later time points, even though the concentrations of TSLP that was administered at each time point remained the same.

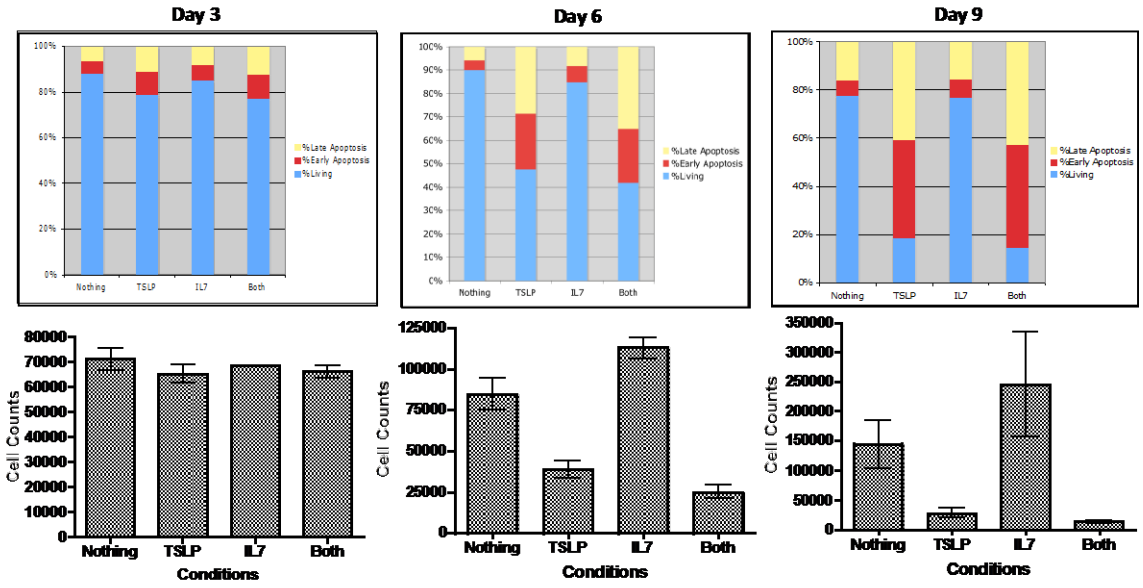

Figure 4.4 CRLF2 B-ALL cells were cultured in culture media with or without TSLP, IL-7 or both for 3, 6 and 9 days. Cells were split every 3 days for the duration of experiment. Cells were harvested and stained with Annexin V and 7-AAD and assessed by flow cytometry. Graphs show the percent of apoptotic cells that are in the early stage (Annexin V+-yellow) or late stage (7-AAD+- red) of apoptosis. Living cells are Annexin V-7-AAD- blue).

Since a component of the TSLP receptor (IL-7Rα) is shared by the cytokine IL-7, which is also produced by human BM stroma and is known to promote survival and proliferation of human B-cells [28]; we also evaluated apoptosis in cells grown with or without IL-7. Our results showed that at day 3, there was no difference in the percent of apoptotic cells in cultures treated with IL-7 compared to untreated cells. Similarly, there was no difference in the total number of living cells in the IL-7 cultures compared to the untreated cells. At days 6 and 9, we also observed no difference in the percent of apoptotic cells between the IL-7 cultures and controls, however, there was an increase in the total number of living cells in the IL-7 cultures compared to the untreated controls on days 6 and 9 (Figure 4.4). These data suggest that IL-7 increases cell survival by protecting cells from apoptosis and may also be inducing cells to proliferate.

In summary, our *in vitro* culture studies suggest that TSLP reduces cell survival by inducing apoptosis in cells while IL-7 increases cell survival by protecting cells from apoptosis.. Additionally, the *in vitro* data provides further evidence to support the *in vivo* data by demonstrating that TSLP induces apoptosis in CRLF2 B-ALL cells and strengthens the molecular data which emphasized that TSLP induces cell death and cell survival pathways.

TSLP Up-regulates Mcl-1 Expression as a Cell Survival Mechanism Prior to Inducing Apoptosis in CRLF2 B-ALL Cells In vitro

The IPA data showed that cell death and survival are the most significant cellular and molecular functions of the cell that are up-regulated by TSLP in primary CRLF2 B-ALL cells (Table 1). In addition, IPA also showed that while cell survival pathways such as mTOR and cell metabolism are up-regulated, cell death (mitochondrial dysfunction) and cellular stress pathways (EIF2 signaling) are also up-regulated by TSLP in these cells (Figure 4.3). Moreover, although pathways that produce opposing cellular functions (cell death versus survival) are activated by TSLP, the most significantly up-regulated pathways are the cell death and cellular stress pathways. This idea is strikingly demonstrated in the functional evidence provided by the *in vitro* data. The *in vitro* data showed that at day 3, cells are maintained in culture, but they ultimately undergo apoptosis at later time points. This data suggests that TSLP-induced signaling in CRLF2 B-ALL cells may involve regulation of the pro-survival versus pro-apoptotic switch. Therefore we wanted to elucidate the mechanisms involved in the TSLP-induced survival versus apoptosis.

Apoptosis (programmed cell death) is a mechanism used by cells to regulate cell numbers, to remove pathogens or to remove cellular debri and is often activated as a result of DNA damage, loss of cell-survival factors or due to cellular stress. This process may be intrinsic (initiated within the mitochondrion of the cell) or extrinsic (death receptor mediated). Since the IPA data provided evidence that mitochondrial dysfunction is up-regulated by TSLP in CRLF2 B-ALL cells, we focused our attention on mitochondrial mechanisms that regulate the pro-apoptotic versus anti-apoptotic signals within a cell. The intrinsic cell death pathway is regulated by the Bcl-2 family of proteins [29]. These proteins function to regulate the permeability of the mitochondrial membrane and to determine whether pro-apoptotic or anti-apoptotic signals will prevail in the cell [23]. Under cellular stress conditions, Bcl-2 pro-apoptotic family members are activated and direct the release of caspase activators in the mitochondria. Conversely, the Bcl-2 anti-apoptotic family members such as Bcl2, Bcl-xl and Mcl-1 are up-regulated to prevent the cell from undergoing apoptosis and function to increase cell survival. In order to understand the mechanisms involved in the survival of CRLF2 B-ALL cells at day 3, we evaluated the expression of the anti-apoptotic Bcl2 family members in human CRLF2 B-ALL cell lines *in vitro*.

To accomplish this, first we cultured primary CRLF2 B-ALL cells that were harvested from the BM of PDXs with or without TSLP for 3 days *in vitro*. At day 3, cells were harvested from culture, hCD19+ B-ALL cells were isolated by magnetic separation and cells were sent for whole genome microarray analysis. The DGA results showed that there was no change in the gene expression profile of Bcl-2 family members (pro-apoptotic and pro-survival) except for Mcl-1. The data showed that Mcl-1 was up-

regulated 1.6 fold in CRLF2 B-ALL cells that were treated with TSLP compared to untreated cells *in vitro*.

Next, we cultured CRLF2 B-ALL cell lines with or without TSLP *in vitro* for 3 days and assessed the expression of Bcl-2 pro-survival proteins. At day 3, cells were harvested from culture and the expression of Bcl-2 family pro-survival members Bcl-2, Bcl-xl and Mcl-1 was measured using intracellular flow cytometry. Our data showed no increases in Bcl-2 expression in cells stimulated with TSLP compared to untreated cells (Figure 4.5 left panel). However there was a minimal increase in the expression of Bcl-xl in TSLP treated cells (Figure 4.5 middle panel) and a substantial increase in the expression of Mcl-1 in TSLP treated cells compared to controls (Figure 4.5, right panel). Taken together the data shows that at day 3, TSLP has no effect on Bcl-2, but has an effect on Bcl-xl and Mcl-1. The increases observed for Mcl-1 suggests that at day 3, TSLP treated cells may be surviving primarily due to Mcl-1 expression. It is possible that by days 6 and 9, the cellular stress induced by TSLP overcomes the Mcl-1-induced pro-survival mechanisms and induces apoptosis in CRLF2 B-ALL cells *in vitro*.

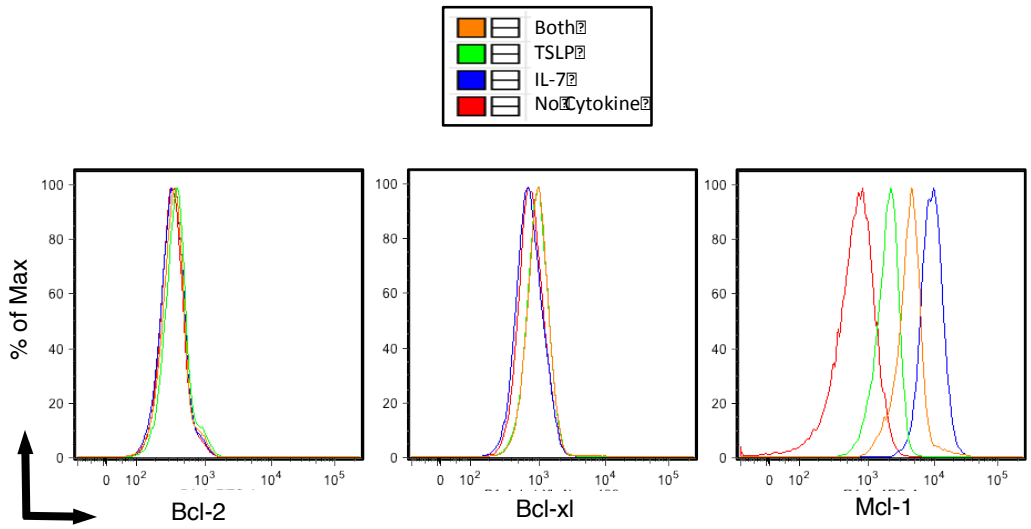

Figure 4.5: CRLF2 B-ALL cells were cultured in culture media with or without TSLP, IL-7 or both for 3. Cells were split every 3 days for the duration of experiment. Cells were harvested and stained with antibodies to Bcl-2, Bcl-xl, and Mcl-1 and assessed by intracellular flow cytometry. Histograms of all conditions are overlaid (No cytokine – red; TSLP- green; IL-7- blue; Both cytokines- orange).

We also evaluated the effects of IL-7 on the expression of Bcl-2 pro-survival family members in CRLF2 B-ALL cells *in vitro*. The results showed that at day 3, IL-7 had no effect on Bcl-2 or Bcl-xl protein expression, however IL-7 increased Mcl-1 expression in CRLF2 B-ALL cells. Interestingly enough, the increase in Mcl-1 expression due to IL-7 stimulation was greater than that observed in cells that were treated with TSLP. This data suggests that both cytokines have the ability to increase Mcl-1 expression in this cellular system.

In summary our data provides evidence that TSLP maintains cell survival at 72 hrs by up-regulating Mcl-1, while TSLP induces apoptosis at later time points, possibly due to the down-regulation of Mcl-1 over time *in vitro*. Future experiments that investigate the expression of Mcl-1 and other Bcl-2 pro-survival family members at later

time points (days 6 and 9) are required to confirm this hypothesis. In addition, the up-regulation of Mcl-1 protein expression by TSLP and IL-7 suggests that 1) Mcl-1 plays a crucial role in the cytokine-mediated survival of CRLF2 B-ALL cells and 2) provides evidence that Mcl-1 is a potential molecular target that can be targeted by therapeutic candidates in order to improve treatment outcomes for CRLF2 B-ALL.

Discussion

In normal B-cells, which express low levels of CRLF2, TSLP binds its receptor and activates the JAK/STAT pathway to induce proliferation in these cells *in vitro* [7]. Using the hTSLP+/hTSLP- xenograft model, our studies provide additional data showing that TSLP also induces survival in B-linage cells *in vivo* (chapter 3). In context of these studies, using the hTSLP+/hTSLP- xenograft model, we evaluated the effects of TSLP on CRLF2 B-ALL cells, which express higher levels of CRLF2. In this chapter, we demonstrate that at the genetic level, TSLP induces genes involved in cell death and survival pathways as well as genes involved in cell death and survival cellular and molecular functions in CRLF2 B-ALL cells. At the cellular level, our results show that TSLP induces apoptosis in CRLF2 B-ALL cells *in vivo* as well as *in vitro*. The findings from this chapter which show that TSLP induces apoptosis in CRLF2 B-ALL cells (CRLF2 high) is opposite to the findings from the previous chapter which show that TSLP induces proliferation and survival in normal B-cells (CRLF2 low). These data suggest that TSLP exerts different functional effects in normal B-cells, which express low levels of CRLF2 and B-cell leukemia cells, which express high levels of CRLF2.

A plausible explanation for the difference in functional effects that was observed in normal B-cells stimulated with TSLP compared to CRLF2 B-ALL cells stimulated with TSLP is the difference in activation of key mediators in TSLP-CRLF2 signaling pathways. Studies of TSLP-induced pathways show that in normal B-cells, TSLP induces weak activation of STAT5 (low level of pSTAT5), but is still able to induce proliferation in B-cells [7]. Initial studies that were conducted to understand the signaling mechanisms involved in CRLF2 B-ALL demonstrated that in the absence of TSLP, basal levels of pSTAT5 were observed [9]. Further investigation of the pathways activated downstream of CRLF2 in our studies show that TSLP increases the phosphorylation of STAT5 and ribosomal protein S6 in CRLF2 B-ALL cells *in vitro* (chapter 1). Data from other studies that evaluated the effects of TSLP on signaling pathways in CRLF2 B-ALL cells also observed increases in the phosphorylation of STAT5, S6, AKT and ERK, thus supporting our *in vitro* data [30]. Additionally, Tasian et al surmised that the observed increases in phosphorylation of proteins that are key regulators of the JAK/STAT and mTOR pathways suggests that there is increased activation of these pathways. Therefore they hypothesized that aberrant signaling occurs in CRLF2 B-ALL cells. However, studies conducted by Tasian et al did not address the long-term functions of TSLP (and this aberrant signaling) on the maintenance and progression of CRLF2 B-ALL. Our studies provide for the first time, evidence that shows that TSLP indeed induces aberrant signaling in CRLF2 B-ALL cells (signaling that is different from normal B-cells) and that this aberrant signaling results in the induction of apoptosis in CRLF2 B-ALL cells.

The mechanisms involved in the TSLP-induced apoptosis of cells are unclear. Results from our IPA show that TSLP induces mitochondrial dysfunction and EIF2

signaling in CRLF2 B-ALL cells, suggesting that the mechanisms may involve mitochondrial-mediated cell death and the cellular stress pathway. A credible argument that supports that TSLP may be inducing apoptosis via mitochondrion-mediated mechanisms, is the fact that we see an involvement of the Bcl-2 family members. The Bcl-2 family plays a pivotal role in regulating mitochondrial cell death and cell survival [23, 29] and our evaluation of the Bcl-2 anti-apoptotic proteins showed that Mcl-1 may be involved in maintaining the survival of CRLF2 B-ALL cells transiently prior to the induction of apoptosis. Another argument is that TSLP may employ EIF2 signaling pathways to induce cellular stress which overcomes cell survival mediated mechanisms such as the up-regulation of Mcl-1, and contribute to apoptosis in CRLF2 B-ALL cells. Studies have shown that environmental and/or endogenous stress signals can trigger the phosphorylation of eIF2α- a major component of the EIF2 pathway [24]. Prolonged activation of this pathway has been shown to induce apoptosis in cells [24]. Further, studies have confirmed that phosphorylation of eIF2α is coupled to the mitochondrial-mediated cell death machinery, which in turn down-regulates Mcl-1 expression, induces activation of Bax and bak resulting in apoptosis. To further support this argument, other studies have shown that Mcl-1 enhances the survival of hematopoietic cells and other cell types that are placed under apoptosis-inducing conditions and this enhancement is often short-term compared to that induced by Bcl2 [31]. Therefore studies that 1) evaluate the expression of Mcl-1 at later time points when apoptosis is observed in CRLF2 B-ALL cells and 2) evaluate the effects of TSLP on the expression of pro-apoptotic Bcl-2 family members and caspases which are part of the cell death machinery for the intrinsic pathway will provide evidence that validate the argument that TSLP induces apoptosis in

CRLF2 B-ALL cells by activating the EIF2 cellular stress and the mitochondrial pathways.

Overall, TSLP's ability to induce apoptosis in CRLF2 B-ALL cells provides a rationale for conducting future studies that can evaluate its therapeutic potential in the treatment of CRLF2 B-ALL. Further, the increased expression of Mcl-1 upon TSLP and IL-7 stimulation, provide evidence that Mcl-1 is involved in cytokine-mediated mechanisms and therefore provides a rationale for also evaluating the efficacy of mcl-1 inhibitors on CRLF2 B-ALL cells. If these studies are fruitful, then TSLP in combination with Mcl-1 inhibitors may prove to be beneficial for the treatment of CRLF2 B-ALL.

References

1. Friend, S.L., et al., *A thymic stromal cell line supports in vitro development of surface IgM+ B cells and produces a novel growth factor affecting B and T lineage cells*. Exp Hematol, 1994. **22**(3): p. 321-8.

2. Takai, T., *TSLP Expression: Cellular Sources, Triggers, and Regulatory Mechanisms*. Allergology International, 2012. **61**(1): p. 3-17.

3. Quentmeier, H., et al., *Cloning of human thymic stromal lymphopoietin (TSLP) and signaling mechanisms leading to proliferation*. Leukemia, 2001. **15**(8): p. 1286-92.

4. Siracusa, M.C., et al., *TSLP promotes interleukin-3-independent basophil haematopoiesis and type 2 inflammation*. Nature, 2011. **477**(7363): p. 229-U138.

5. Taylor, B.C., et al., *TSLP regulates intestinal immunity and inflammation in mouse models of helminth infection and colitis*. Journal of Experimental Medicine, 2009. **206**(3): p. 655-667.

6. Roan, F., et al., *The multiple facets of thymic stromal lymphopoietin (TSLP) during allergic inflammation and beyond*. Journal of Leukocyte Biology, 2012. **91**(6): p. 877-886.

7. Scheeren, F.A., et al., *Thymic stromal lymphopoietin induces early human B-cell proliferation and differentiation*. Eur J Immunol, 2010.

8. Lu, N., et al., *TSLP and IL-7 use two different mechanisms to regulate human CD4+ T cell homeostasis*. J Exp Med, 2009. **206**(10): p. 2111-9.

9. Russell, L.J., et al., *Deregulated expression of cytokine receptor gene, CRLF2, is involved in lymphoid transformation in B-cell precursor acute lymphoblastic leukemia*. Blood, 2009. **114**(13): p. 2688-98.

10. Yoda, A., et al., *Functional screening identifies CRLF2 in precursor B-cell acute lymphoblastic leukemia*. Proc Natl Acad Sci U S A, 2010. **107**(1): p. 252-7.

11. Mullighan, C.G., et al., *Rearrangement of CRLF2 in B-progenitor- and Down syndrome-associated acute lymphoblastic leukemia*. Nat Genet, 2009. **41**(11): p. 1243-6.

12. Chen, I.M., et al., *Outcome modeling with CRLF2, IKZF1, JAK, and minimal residual disease in pediatric acute lymphoblastic leukemia: a Children's Oncology Group study*. Blood, 2012. **119**(15): p. 3512-22.

13. Harvey, R.C., et al., *Identification of novel cluster groups in pediatric high-risk B-precursor acute lymphoblastic leukemia with gene expression profiling:*

correlation with genome-wide DNA copy number alterations, clinical characteristics, and outcome. Blood, 2010.

14. Mullighan, C.G., et al., *Genome-wide analysis of genetic alterations in acute lymphoblastic leukaemia*. Nature, 2007. **446**(7137): p. 758-64.

15. Cario, G., et al., *Presence of the P2RY8-CRLF2 rearrangement is associated with a poor prognosis in non-high-risk precursor B-cell acute lymphoblastic leukemia in children treated according to the ALL-BFM 2000 protocol*. Blood, 2010.

16. Chen, I.M., et al., *Outcome modeling with CRLF2, IKZF1, JAK and minimal residual disease in pediatric acute lymphoblastic leukemia: a Children's Oncology Group Study*. Blood, 2012.

17. Harvey, R.C., et al., *Rearrangement of CRLF2 is associated with mutation of JAK kinases, alteration of IKZF1, Hispanic/Latino ethnicity, and a poor outcome in pediatric B-progenitor acute lymphoblastic leukemia*. Blood, 2010. **115**(26): p. 5312-21.

18. Maude, S.L.T., S.K.; Vincent, T.; Hall, J.W.; Sheen, C. et al, *Targeting JAK1/2 and mTOR in murine xenograft models of Ph-like acute lymphoblastic leukemia (ALL)*. Blood, 2012.

19. Tasian, S.K., et al., *Aberrant STAT5 and PI3K/mTOR pathway signaling occurs in human CRLF2-rearranged B-precursor acute lymphoblastic leukemia*. Blood, 2012.

20. Brown, V.I., et al., *Thymic stromal-derived lymphopoietin induces proliferation of pre-B leukemia and antagonizes mTOR inhibitors, suggesting a role for interleukin-7Ralpha signaling*. Cancer Res, 2007. **67**(20): p. 9963-70.

21. Murphy, M.P., *Mitochondrial dysfunction indirectly elevates ROS production by the endoplasmic reticulum*. Cell Metab, 2013. **18**(2): p. 145-6.

22. Vamecq, J., et al., *Mitochondrial dysfunction and lipid homeostasis*. Curr Drug Metab, 2012. **13**(10): p. 1388-400.

23. Mayer, B. and R. Oberbauer, *Mitochondrial regulation of apoptosis*. News Physiol Sci, 2003. **18**: p. 89-94.

24. Fritsch, R.M., et al., *Translational repression of MCL-1 couples stress-induced eIF2 alpha phosphorylation to mitochondrial apoptosis initiation*. J Biol Chem, 2007. **282**(31): p. 22551-62.

25. Rajesh, K., et al., *Phosphorylation of the translation initiation factor eIF2alpha at serine 51 determines the cell fate decisions of Akt in response to oxidative stress*. Cell Death Dis, 2015. **6**: p. e1591.

26. Fulda, S., et al., *Cellular stress responses: cell survival and cell death*. Int J Cell Biol, 2010. **2010**: p. 214074.

27. Laplante, M. and D.M. Sabatini, *mTOR signaling in growth control and disease*. Cell, 2012. **149**(2): p. 274-93.

28. Parrish, Y.K., et al., *IL-7 Dependence in human B lymphopoiesis increases during progression of ontogeny from cord blood to bone marrow*. J Immunol, 2009. **182**(7): p. 4255-66.

29. Willis, S., et al., *The Bcl-2-regulated apoptotic pathway*. J Cell Sci, 2003. **116**(Pt 20): p. 4053-6.

30. Tasian, S.K., et al., *Aberrant STAT5 and PI3K/mTOR pathway signaling occurs in human CRLF2-rearranged B-precursor acute lymphoblastic leukemia*. Blood, 2012. **120**(4): p. 833-42.

31. Liu, H., et al., *Stabilization and enhancement of the antiapoptotic activity of mcl-1 by TCTP*. Mol Cell Biol, 2005. **25**(8): p. 3117-26.

CHAPTER FIVE

IDENTIFICATION OF SMALL MOLECULE DRUGS THAT SHOW EFFICACY AGAINST CRLF2 B-ALL AND OTHER HIGH-RISK B-ALL

Abstract

Patients diagnosed with high-risk B-ALL including CRLF2 B-ALL experience high rates of relapse and poor patient survival outcomes. Current chemotherapy regimens have been successful at achieving >95% remission rates, but they have been unsuccessful at treating patients that relapse and subsequently experience a poor prognosis. The success of Imatinib- a small molecule kinase inhibitor that targets the aberrant tyrosine kinase that is encoded by the BCR-ABL oncogene- which was used in combination with other chemotherapy agents to treat Ph+ hematological malignancies provided a paradigm for the use of targeted therapy in high-risk cancers. Therefore, using a similar approach, we identified two categories of small molecule drugs that are known to inhibit genetic lesions and cellular processes involved in high-risk B-ALL cells and reduce cellular survival. Here we show that the Mcl-1 inhibitor MIM1 showed efficacy by reducing the survival of CRLF2 B-ALL cells *in vitro*. We also show that the NM drug series showed efficacy by reducing the survival of chemo-resistant high-risk B-ALL cells *in vitro* and increasing the survival of NSG mice *in vivo*. The drug candidates that were identified and evaluated in these studies can be used for further preclinical testing on high-risk B-ALL subsets in order to determine their therapeutic value. They offer the potential to be used in combination with standard chemotherapy that is currently used to treat high-risk B-ALL.

Abbreviations

ALL	Acute Lymphoblastic Leukemia
B-ALL	B-cell Acute Lymphoblastic Leukemia
MRD	Minimal Residual Disease
BCR-ABL	Breakpoint Cluster Region joined to *ABL1* gene
CRLF2	Cytokine Receptor Like Factor 2
MIM1	Mcl-1 Inhibitor Molecule 1
Mcl-1	Myeloid Cell Leukemia 1
7-AAD	7-Amino-Actinomycin D
TSLP	Thymic Stromal Lymphopoietin
MTT	3-(4,5-dimethylthiazol-2-yl)-2,5-diphenyltetrazolium bromide
NSG	NOD/SCID Gamma (NOD.Cg-Prkdc^{scid}Il2rg^{tm1Wjl}/SzJ)
DMSO	Dimethyl Sulfoxide
TKI	Tyrosine Kinase Inhibitor
ABT-737	Bcl-2, Bcl-xl and Bcl-w inhibitor
IL-7	Interleukin 7
IC_{50}	Half maximal Inhibitory Concentration

Introduction

ALL is heterogeneous, thus treatment is administered based on phenotype, genotype and risk factors [1]. Current therapies for high-risk ALL patients include intense combination chemotherapy and/or allogenic bone marrow transplant [2]. Treatment for children with ALL is typically divided into two phases: 1) **remission-induction phase:** this occurs at the time of diagnosis and the goal is to eradicate 99% of initial leukemic cells and restore normal hematopoiesis; 2) **post-induction therapy phase**: this occurs after complete remission and involves either intensification therapy and/or continuation therapy to remove the residual disease [1, 3]. Remission-induction chemotherapy consists of a combination of 3 drugs: vincristine, glucocorticoid (prednisone or dexamethasone), and L-asparaginase or anthracycline in conjunction with intrathecal therapy. In most cases, the result of such a combination is a complete remission rate of greater than 95-98% in patients. Children with higher risk are often treated with a combination of four or more drugs during induction therapy [1]. A commonly used treatment regimen for high-risk childhood ALL include high-dose methotrexate with mercaptopurine, high-dose asparaginase given for an extended period, and re-induction treatment [4]. Tyrosine kinase inhibitors such as Imatinib are currently used concurrently with chemotherapy to treat high-risk BCR-ABL+ ALL patients and JAK recommended for clinical trials [5].

Despite the improvements, intense combination chemotherapy currently used to treat high-risk B-ALL patients fails in ~25% of patients [6]. Patients experience relapse and a poor prognosis with relapse being the leading cause of cancer-related death in children [6, 7]. The current chemotherapy provides little scope for significant

intensification because there are many short-term and long-term side effects in patients due to toxicity and it has not been successful in reducing minimal residual disease (MRD) and the incidence of relapse [5]. Most high-risk cases occur due to the presence of genetic lesions in patient genotype that are unique to subsets of patients and are not targeted by general chemotherapy. As a result, these genetic lesions contribute to MRD, relapse and poor patient survival subsequent to remission. Therefore our goal was to identify potential therapeutic candidates that can target molecular lesions that were identified in chapter 4 and in previous studies and determine the efficacy of these drugs in decreasing the survival of high-risk leukemia cells.

Here we evaluated the efficacy of the Mcl-1 inhibitor MIM1 and two new classes of Novomedix small molecule drugs and demonstrated that these drugs have the ability to reduce the survival CRLF2 B-ALL cells and high-risk B-ALL cells respectively.

Materials and Methods

In vitro Mcl-1 Inhibitor MTT Assay

CRLF2 B-ALL cell line was maintained in RPMI 1640 phenol red free medium supplemented with penicillin/streptomycin, L-glutamine, 50 uM 2-ME and 20% fetal bovine serum (FBS). Cells were then cultured in the above media with varying concentrations of Mcl-1 inhibitor MIM1 at 37oC and 5.0 % CO2 using a 96 well plate (in triplicate). At 72 hrs, cells were removed and the MTT assay was performed using the Vybrant MTT cell proliferation assay kit (Life Technologies). The plate containing the cells was read using a microplate absorbance reader. Absorbance is read at 570nm.

In vitro NM Drug Apoptosis Assay

Nalm6 cells were maintained in RPMI 1640 medium supplemented with penicillin/streptomycin, L-glutamine, 50 uM 2-ME and 10% fetal bovine serum (FBS). Cells were then cultured with the above media and NM drugs (735, 785 or 869) or DMSO control for 48 hrs. Cells were harvested at 48 hrs and stained with Annexin V and 7-AAD to identify cells in early apoptotic (Annexin V+, 7-AAD–) or late apoptotic (Annexin V+, 7-AAD+) stages using flow cytometry. The IC_{50} of the drug candidates were obtained from the drug company and drugs were administered at their respective IC_{50}

In vivo NM Drug Efficacy Assay

NSG mice were transplanted with Nalm6 cells. Eight (8) days after transplantation, drugs were administered to mice daily according to the following drug conditions: 922, 1123, 911, vincristine, vehicle and untreated. Mice were evaluated daily by observation and time of death was recorded in order to plot a survival curve.

Results

Mcl-1 Inhibitor MIM1 Reduces Cell Viability in CRLF2 B-ALL Cells In vitro

TSLP-induced up-regulation of the Mcl-1 gene and protein in CRLF2 B-ALL cells described in chapter 4 and TSLP-induced up-regulation of Mcl-1 protein in IL-7R+ progenitors in normal B-cells described in chapter 3 supports the idea that Mcl-1 may impact B-cells by contributing to cell survival. Further, the increases in Mcl-1 protein expression observed in CRLF2 B-ALL cells upon TSLP stimulation and the increases in

Mcl-1 expression as well as cell survival observed at later time points (days 6 and 9) upon IL-7 stimulation, provide further evidence that Mcl-1 plays an important role in the survival of B-ALL cells (chapter 4). Together, these data suggest that the regulation of in CRLF2 B-ALL cells by TSLP and IL-7 induced signaling may be involved in adjusting the apoptosis versus cell survival switch in these cells. Therefore, we hypothesized that small molecule drugs, which target Mcl-l expression can reduce the survival of CRLF2 B-ALL cells *in vitro*. To test this hypothesis, we utilized a commercially available Mcl-1 inhibitor MIM1 to perform dose response experiments and evaluate its *in vitro* efficacy on CRLF2 B-ALL cells using an enzyme-based cell viability, proliferation and function test (a metabolic activity test). The MTT assay measures mitochondrial dehydrogenase activity in living cells. In most cell types, the total mitochondrial activity is related to the number of viable cells, therefore the MTT assay is often used as a drug screening assay and as a measure of *in vitro* cytotoxicity of drugs on cell lines or primary cells [8]. CRLF2 B-ALL cells were cultured in culture media with varying concentrations of MIM1 for 72 hrs. Cells were harvested and the MTT assay was performed. The results from this dose response experiment showed that MIM1 reduced cell viability of CRLF2 B-ALL cells with an IC_{50} of 20 uM (Figure 5.1). At 30 uM, cell viability was reduced by 75%; between 50 uM and 100 uM, there were little to no viable cells present in culture (Figure 5.1). These data suggest that MIM1 can induce reduction of CRLF2 B-ALL cell viability by 50% at concentrations at a concentration as low as 20 uM and that MIM1's cytotoxic effects are increased at concentrations $\geq$ 30 uM.

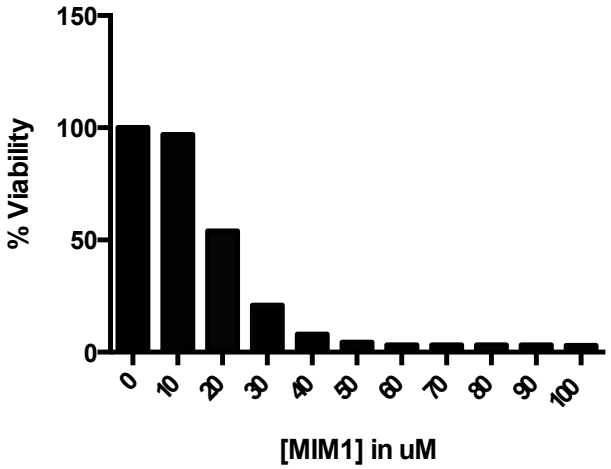

Figure 5.1: CRLF2 B-ALL cells (MUTZ5) were cultured with different concentrations of MIM1 and harvested at 72 hours. Cells were washed, labeled with MTT. Samples were read at an absorbance of 570nm.

NM Small Molecule Drugs Induce Apoptosis in Nalm6 B-ALL Cells In vitro

In order to identify other promising therapeutic candidates, our lab embarked on a collaborative study with Novomedix Drug Company. Novomedix has developed two new classes of small molecule drugs that can inhibit biological pathways, which often lead to the development of diseases. Novomedix screened a library of 200 compounds that are modulators of pathways involved in immune dysfunction and cancer. They identified: 1) a tetrazole- 735 and its analog 869 and 2) a pyridine- 785 and its analog 790. 735 and 790 were subsequently submitted to the National Cancer Institute (NCI) for screening on a panel of 60 human tumor cell lines. Both parent drugs were approved for testing, indicating that their chemical structures were novel compared to existing anti-cancer compounds which were tested by NCI. Novomedix subsequently found that the drugs were safe based on *in vitro* toxicology studies conducted in primary lung fibroblast cells and hepatocytes and *in vivo* toxicology studies conducted in CD-1 mice. Additional

studies were performed to compare the efficacy of traditional chemotherapy drugs currently used (e.g vincristine, dexamethasone) to NM drug series and the results demonstrated that the NM drugs showed better efficacy on lymphoma cells and other diseased cell types. Further mechanistic studies revealed that the NM drug series target cell cycle proteins, cyclin D1 and D3.

Studies have shown that acute lymphoblastic leukemia patients that suffer relapse often exhibit increased expression of cell cycle genes and proteins such as the cyclins leading to protection from apoptosis, increased proliferation and increased cell survival [9]. Therefore we hypothesized that NM drug series can target the cell cycle machinery (genes) and reduce the survival of high-risk B-ALL cells. To test this hypothesis, we performed drug efficacy studies on chemo-resistant B-ALL cells Nalm6, by assessing cellular apoptosis using recommended IC_{50} concentrations. The IC_{50} of each drug was determined by Novomedix using other cell types and they were as follows: 735 = 300nM; 785 = 430nM; 869 = 65nM. Nalm6 cells were cultured with NM compounds or DMSO control. Cells were then harvested at 48 hrs and the Annexin V/7-AAD assay was performed using flow cytometry. Percent apoptosis was determined by combining the percent of cells in the early stages of apoptosis (Annexin V+) and the percent of cells in the late stages of apoptosis (7-AAD+).

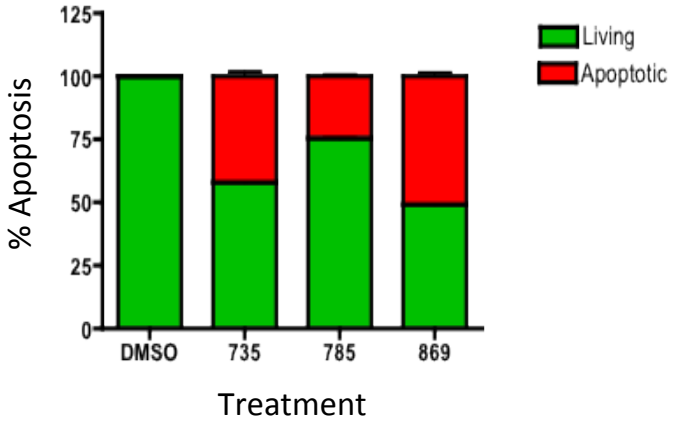

Figure 5.2: Nalm6 B-ALL cells were cultured with the Novomedix (NM) compounds 735, 785 and 869 or DMSO vehicle control. Cells were harvested at 48 hours and stained for flow cytometry to detect Annexin V and 7-AAD. Percentages of cells that are living (green) or apoptotic cells (Annexin V+7-AAD+ - red) are shown above.

Our data showed that all three drugs induced cellular apoptosis when compared to cells treated with DMSO, however 735 and 869 were the most potent (Figure 5.2). 785 induced 25% apoptosis at 430 nM; 735 induced ~43% apoptosis at 300 nM and 869 induced 50% apoptosis at 65nM. The recommended IC_{50} for 785 was based on assessments completed on other cell types by the company and as such was not the ideal IC_{50} concentration for Nalm6 cells. Therefore further testing is required to determine the optimum IC_{50} for 785 in this system. Our results suggest that a higher dose of 785 would be required to show substantial efficacy against Nalm6 cells. Conversely, 869 shows the most promise since it required a lower dose to achieve 50% cell death (IC_{50} nM). These data suggest that Novomedix drugs 735 and 869 are promising drug candidates that can be used to perform further testing to demonstrate their ability to reduce proliferation and induce apoptosis in other subsets of high-risk B-ALL cells including CRLF2 B-ALL.

NM Small Molecule Drugs Increase the Survival of NSG Mice Transplanted with Chemo-resistant B-ALL Cells In vivo

After we had determined the efficacy of NM drugs on high-risk B-ALL cells *in vitro,* we investigated the efficacy of NM drugs *in vivo* by evaluating their effects on the survival of NSG mice transplanted with high-risk B-ALL cells (Nalm6). Some of the drug analogs for the NM735 and NM785 drug series were potent and successful at inducing apoptosis of Nalm6 cells *in vitro*, however they proved to be toxic to animals during *in vivo* safety testing. Therefore we selected analogs of NM735 and NM785 that were successful during *in vivo* safety testing. Hence for *in vivo* drug efficacy studies, we used NM1123, NM922 and NM911. Typically, NSG mice transplanted with Nalm6 cells experience a poor survival outcome due to the aggressiveness of the disease, that is, animals die between 18-21 days. Based on our *in vitro* results, we hypothesized that NM drugs will increase the survival of NSG mice transplanted with Nalm6. To test this hypothesis, NSG mice were transplanted with $1x10^7$ Nalm6 cells per mouse intravenously and 8 days after transplantation, drugs were administered daily via intraperitoneal injections for 21 days or until the animals died. NM drugs were administered at 25 mg/kg per mouse and vincristine was administered at 0.15 mg/kg per mouse. Experimental groups were as follows: untreated, vehicle (DMSO only- negative control), vincristine (positive control), NM1123, NM922 and NM911. For all groups, n=5 mice except for the untreated group (n=2 mice), and NM1123 (n=6). Drug response was assessed by 1) recording visual observations of animals daily and at time/day of death and 2) recording the number of days treated animals lived compared to control animals.

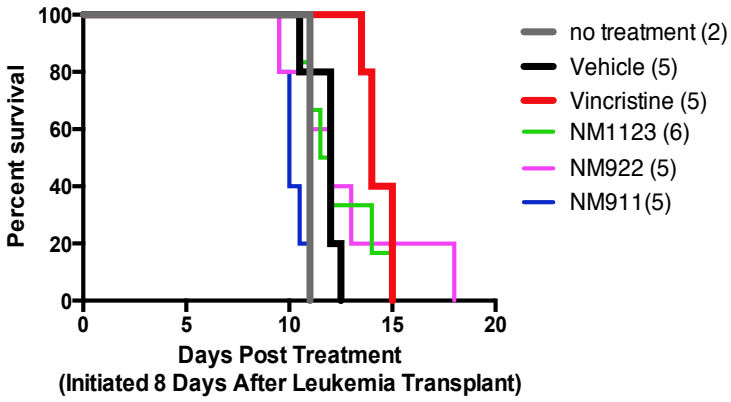

Figure 5.3: A survival curve showing percent survival of animals placed in 6 treatment groups. NSG mice were transplanted with $1x10^7$ Nalm6 cells and were treated with four different candidate drugs: vincristine- positive control (red), NM1123 (green), NM922 (pink) and NM911 (blue). The negative controls groups were the no treatment group (grey) and vehicle-DMSO group (black).

Our results showed that on day 18 (11 days post drug treatment) all untreated animals died (Figure 5.3). By day19 (12 days post drug treatment), all vehicle (DMSO treated) animals died. This time of survival (18-19 days) is typically observed for NSG mice transplanted with Nalm6 cells only. All animals treated with NM911 died by day 18 (11 days post drug treatment). NM911 treated mice died earlier and on the day of untreated mice. Visual observations of these mice revealed that they experienced anal bleeding. These observations along with the time of death suggests that in addition to the leukemia, NM911 treated animals may have died due to toxic effects of the drug. All NM 1123 treated animals died by day 22 (15 days post treatment) and the same was observed for the vincristine controls. All NM 922 treated animals died by day 25 (18 days post treatment). The survival curve summarizes the results and visually compares the data obtained from each drug. In summary the data showed that vincristine and NM1123 increased the survival of Nalm6 NSG mice by 4 days (when compared to the untreated

group), while NM922 increased the survival of these mice by 7 days. These *in vivo* studies demonstrate that NM922 showed greater efficacy on Nalm6 cells compared to vincristine and other NM drugs. NM922 is therefore a promising drug candidate that can be used for further *in vitro and in vivo* preclinical testing to evaluate its effects on the survival of several high-risk B-ALL subsets including CRLF2 B-ALL.

Discussion

With current therapies, ~25% of pediatric B-ALL patients still relapse and they experience poor survival outcomes [5, 10]. Within this patient population, genomic profiling studies have identified several high-risk B-ALL subtypes that are resistant to chemotherapy, including those consisting of alterations in the BCR-ABL, *IKZF1* or *CRLF2* genes [5]. The translocation leading to the BCR-ABL+ B-ALL subtype was the first of these genetic alterations to be identified and tyrosine kinase inhibitors (TKIs) that specifically target the aberrant kinase activity produced by the BCR-ABL genetic defect have been developed into drugs [11]. One such drug, Imatinib, when used in combination with standard therapy, has increased the survival of children with BCR ABL+ B-ALL from ~35% to 80% [10, 12]. These studies provided a paradigm for identifying candidate drugs that target specific genetic lesions or aberrant signaling pathways associated with high-risk B-ALL, and using them in combination with standard therapy to improve survival outcomes in children. We used a similar approach by identifying small molecule drugs that are known to target molecular lesions/cellular pathways and evaluating the efficacy of these drugs on high-risk B-ALL survival.

Our results in chapter 4 showed that TSLP induced apoptosis in CRLF2 B-ALL cells rendering it as a potential therapeutic to be considered for further preclinical drug efficacy testing against CRLF2 B-ALL. In addition to inducing apoptosis, TSLP also up-regulated Mcl-1 expression in CRLF2 B-ALL cells *in vitro* (chapter 4). An increase in Mcl-1 expression was also observed when CRLF2 B-ALL cells were stimulated with IL-7 (chapter 4). Mcl-1 has been shown to regulate the survival of many cells and is often up-regulated in cancer cells [13]. Therefore we assessed the efficacy of the Mcl-1 inhibitor MIM1 on CRLF2 high-risk B-ALL and our results showed that MIM1 showed efficacy by significantly reducing the survival of these cells. The mechanisms by which MIM1 reduces the survival of CRLF2 B-ALL cells remain to be elucidated. Future studies that assess the mechanisms involved in MIM1's ability to inhibit the expression of Mcl-1 in CRLF2 B-ALL cells *in vitro* and the ability of MIM1 to reduce bone marrow disease *in vivo* are required. Additionally, it will be important to assess the effects of other Mcl-1 inhibitors such as Maritoclax and other Bcl-2 family inhibitors such as ABT-737 in context of MIM1 in order to fully validate the therapeutic value of Mcl-1 inhibitors on the CRLF2 B-ALL high-risk subset of leukemia.

In most high-risk B-ALL, cells increase in numbers by undergoing proliferation and cyclins have been shown to contribute to this process [14-16]. Thus we assessed the efficacy of a new class of small molecule drugs (NM lead series) on chemo-resistant high-risk B-ALL. Our results showed that NM735 and NM869 showed efficacy by reducing the survival of Nalm6 cells *in vitro*, while NM 922 and NM1123 (analogs of 735 and 869) showed *in vivo* efficacy by increasing the survival of Nalm6 NSG mice compared to untreated controls. NM drugs (NM1123 and NM922) showed efficacy that

was similar or better than vincristine- a chemotherapy drug that is currently used as part of the treatment regimen for patients with high-risk leukemia. Vincristine is considered to be among the most potent drugs, however, it is toxic to patients at high concentrations [17]. The vincristine effects that we observed in mice was based on daily administration of the drug, while in current practice, it is administered to patients once per week. Thus the effects we see are at high doses, which would be toxic for patients and would undermine the true effects of NM922. Future experiments conducted to evaluate NM drugs in context of less frequent dosing (weekly as opposed to daily) of vincristine are required in order to optimize the *in vivo* effects observed for NM922 in high-risk B-ALL cells. Additionally, NM drug series should be tested on other subsets of high-risk B-ALL including CRLF2 B-ALL cells to fully evaluate its therapeutic value.

Improved remission rates in recent years are primarily due to the administration of higher doses of standard chemotherapy [7]. However, these higher doses have resulted in increased toxicity and side effects for patients and to compound this, they have been ineffective in reducing the relapse-rate of CRLF2 B-ALL and other high-risk B-ALL [7, 18, 19]. Targeted therapy is therefore advantageous in that it can decrease toxicity by targeting distinct cell lineages, cell cycle proteins or dysfunctional tumor suppressors which all contribute to relapse but are often not targeted using current treatment regimens. Our studies provide evidence of the efficacy of two categories of drugs, which target molecular lesions and oncogenic cellular processes that can be used for further preclinical testing on CRLF2 B-ALL and other high-risk B-ALL. They offer the potential to be used in combination with reduced doses of standard therapy while increasing overall efficacy of treatment in high-risk B-ALL.

References

1. Pui, C.H. and W.E. Evans, *Treatment of acute lymphoblastic leukemia*. N Engl J Med, 2006. **354**(2): p. 166-78.

2. Hunger, S.P., et al., *Improving Outcomes for High-Risk ALL: Translating New Discoveries Into Clinical Care*. Pediatric Blood & Cancer, 2011. **56**(6): p. 984-993.

3. Pieters, R., et al., *A treatment protocol for infants younger than 1 year with acute lymphoblastic leukaemia (Interfant-99): an observational study and a multicentre randomised trial*. Lancet, 2007. **370**(9583): p. 240-250.

4. Silverman, L.B., et al., *Improved outcome for children with acute lymphoblastic leukemia: results of Dana-Farber Consortium Protocol 91-01*. Blood, 2001. **97**(5): p. 1211-1218.

5. Mullighan, C.G., *New Strategies in Acute Lymphoblastic Leukemia: Translating Advances in Genomics into Clinical Practice*. Clinical Cancer Research, 2011. **17**(3): p. 396-400.

6. Harvey, R.C., et al., *Identification of novel cluster groups in pediatric high-risk B-precursor acute lymphoblastic leukemia with gene expression profiling: correlation with genome-wide DNA copy number alterations, clinical characteristics, and outcome*. Blood, 2010. **116**(23): p. 4874-4884.

7. Nguyen, K., et al., *Factors influencing survival after relapse from acute lymphoblastic leukemia: a Children's Oncology Group study*. Leukemia, 2008. **22**(12): p. 2142-50.

8. van Meerloo, J., G.J. Kaspers, and J. Cloos, *Cell sensitivity assays: the MTT assay*. Methods Mol Biol, 2011. **731**: p. 237-45.

9. Kirschner-Schwabe, R., et al., *Expression of late cell cycle genes and an increased proliferative capacity characterize very early relapse of childhood acute lymphoblastic leukemia*. Clinical Cancer Research, 2006. **12**(15): p. 4553-4561.

10. Hunger, S.P., et al., *Improving outcomes for high-risk ALL: translating new discoveries into clinical care*. Pediatr Blood Cancer, 2011. **56**(6): p. 984-93.

11. Druker, B.J., et al., *Activity of a specific inhibitor of the BCR-ABL tyrosine kinase in the blast crisis of chronic myeloid leukemia and acute lymphoblastic leukemia with the philadelphia chromosome*. New England Journal of Medicine, 2001. **344**(14): p. 1038-1042.

12. Fielding, A.K., *Current treatment of Philadelphia chromosome-positive acute lymphoblastic leukemia*. Hematology Am Soc Hematol Educ Program, 2011. **2011**: p. 231-7.

13. Thomas, L.W., C. Lam, and S.W. Edwards, *Mcl-1; the molecular regulation of protein function*. Febs Letters, 2010. **584**(14): p. 2981-2989.

14. Sicinska, E., et al., *Requirement for cyclin D3 in lymphocyte development and T cell leukemias*. Cancer Cell, 2003. **4**(6): p. 451-461.

15. Filipits, M., et al., *Cyclin D3 is a predictive and prognostic factor in diffuse large B-cell lymphoma*. Clinical Cancer Research, 2002. **8**(3): p. 729-733.

16. Rojas, P., et al., *Cyclin D2 and cyclin D3 play opposite roles in mouse skin carcinogenesis*. Oncogene, 2007. **26**(12): p. 1723-30.

17. van den Bent, M.J., *Prevention of chemotherapy-induced neuropathy: leukemia inhibitory factor*. Clin Cancer Res, 2005. **11**(5): p. 1691-3.

18. Pui, C.H., *Central nervous system disease in acute lymphoblastic leukemia: prophylaxis and treatment*. Hematology Am Soc Hematol Educ Program, 2006: p. 142-6.

19. Kamdem, L.K., et al., *Genetic predictors of glucocorticoid-induced hypertension in children with acute lymphoblastic leukemia*. Pharmacogenet Genomics, 2008. **18**(6): p. 507-14.

CHAPTER SIX

DISCUSSION

Summary of Chapter Findings and Relevance to the Leukemia Field

The objective of my dissertation studies was to elucidate the TSLP-CRLF2-mediated cellular and molecular mechanisms that contribute to high-risk CRLF2 B-ALL and to evaluate promising drug candidates to target CRLF2 B-ALL and other high-risk B-ALL. Our working hypothesis was that *TSLP contributes to CRLF2 B-ALL by increasing proliferation and/or survival of leukemia cells via regulation of genes downstream of CRLF2 pathway activation*. To accomplish our objective, we developed three aims. The first aim was to optimize the novel hTSLP+/hTSLP- xenograft model for use in defining the role of TSLP in CRLF2 B-ALL; the second aim was to identify TSLP-induced cellular and molecular mechanisms that contribute to CRLF2 B-ALL**;** and the third aim was to assess candidate drugs' efficacy against high-risk B-ALL.

The molecular mechanisms that contribute to the development and maintenance of high-risk B-ALL that are linked to the recently discovered CRLF2 genetic defect remain unclear and despite the success of current therapeutic strategies with some high-risk B-ALL, CRLF2 B-ALL patients still experience at a 65% relapse rate [1]. Research groups that currently study CRLF2 B-ALL are focused primarily on genomic profiling studies, the identification of molecular lesions within CRLF2 pathways such as JAK2 mutations and aberrant signaling of the JAK-STAT and mTOR pathways [1-7]. This current direction of the field is based upon studies conducted using a BaF3 model system- an IL-3-dependent murine cell line transduced with mutant JAK and/or mutant CRLF2

[5, 6]. In these studies, researchers demonstrated that cells that overexpress CRLF2 (due to the presence of CRLF2 genetic defects) and consist of mutations in JAK2 showed constitutive activation of JAK/STAT signaling and cytokine independent growth, which was enough to transform cells [5, 6, 8]. These results were not observed in BaF3 cells that harbored CRLF2 overexpression alone or in cells with JAK2 mutations alone [5]. Further co-immunoprecipitation studies demonstrated that human CRLF2 and phosphorylated mutant JAK2 interact physically [5]. Therefore the current hypothesis in the field is that CRLF2 and JAK2 cooperate to lead to leukemogenesis [9, 10] and the contributions of TSLP-the endogenous ligand for CRLF2- to the disease mechanisms of CRLF2 B-ALL remain to be elucidated.

Our approach to understanding CRLF2 B-ALL disease mechanisms was to determine the effects of TSLP on the disease. To do this, as proposed in aim 1, first we developed and optimized a novel hTSLP+/hTSLP- model system described in chapter 2. The rationale for developing this model was based on the fact that mouse TSLP does not activate human CRLF2 BALL cells *in vitro*. To confirm that the human TSLP produced in our model acts on human cells; using the human TSLP *in vivo* model system, we demonstrated that human TSLP signals produced in the model activates human CRLF2 on normal B-cells and increases the number of CD19+ B-cells in the bone marrow (chapter 2). It is established in the field that TSLP induces proliferation of normal murine B-cells and it was more recently shown that TSLP induces proliferation of human fetal B-cells *in vitro* [11, 12]. Therefore, the ability of the human TSLP produced in our model to expand normal B-cells confirmed the previously published findings and provided the first *in vivo* data, all of which served as a validation of the model. Next we confirmed that

TSLP produced in the model also activates CRLF2 B-ALL cells *in vivo*. Our results showed that the TSLP produced in the model up-regulated one of the main TSLP-CRLF2 pathways, the mTOR pathway, in CRLF2 B-ALL cells *in vivo* [13]. Other groups have shown that TSLP activates the mTOR pathway in pre-B ALL cells and in CRLF2 B-ALL cells *in vitro* [7, 14, 15]. Thus, the ability of the human TSLP produced in our model to induce the mTOR pathway in CRLF2 B-ALL cells *in vivo* provided additional validation for the hTSLP model system. Moreover, this is the first study to produce a hTSLP+/hTSLP- human-mouse xenograft system and it is the first demonstration of the use of this system to induce B-lymphopoiesis in normal B-cells (chapters 2, 3) and activate TSLP-regulated pathways in CRLF2 B-ALL cells *in vivo* (chapter 2).

In order to further delineate the mechanisms of TSLP-induced signaling in CRLF2 B-ALL cells as proposed in aim 2, our approach was to first understand the TSLP-induced mechanisms in normal B-cells and then use this as a framework for evaluating and understanding the contributions of TSLP to the disease mechanisms involved in CRLF2 B-ALL cells. Using the hTSLP+/hTSLP- model system, we demonstrated that TSLP up-regulates Mcl-1 and induces proliferation of CD19– CD34+IL7Rα+ progenitors, resulting in a 3-4-fold expansion of the CD34+ pro-B cells; and that this expansion is maintained during the subsequent stages of B-cell development (chapter 3). Additionally, the data showed that the observed increases in B-cell numbers were due not only to proliferation, but also due to protection from apoptosis (chapter 3). Though the roles of TSLP and IL-7 have been well studied in murine B-cell development, the roles of both cytokines in human B-cell development remained controversial. Our studies are significant in that the hTSLP+/hTSLP- model system

provides both cytokines (human TSLP which is species-specific and murine IL-7 which is cross-reactive) allowing the opportunity to study the effects of TSLP in context of IL-7 for the first time *in vivo*. Our studies were also significant in that they introduced for the first time a survival role for TSLP in human B-cells, which is distinctly different from the roles of IL-7 (chapter 3). Moreover, TSLP's effect on normal B-cells provides evidence that supports our hypothesis stated in the first paragraph of this discussion.

After confirming that the human TSLP in our model can activate normal human B-cells, which express low levels of CRLF2; we used the hTSLP+/hTSLP- *in vivo* model system to evaluate the effects of TSLP on CRLF2 B-ALL cells, which express high levels of CRLF2. Our results showed that at low levels of TSLP, there was no difference in the percent of CRLF2 B-ALL cells that were engrafted in the bone marrow of PDXs (chapter 4). However, assessment of the percent of viable CD19+ cells showed that of the cells that were engrafted, there was an increase in the percent of apoptotic cells in the +T mice compared to the –T mice. When higher levels of TSLP were added, there was little to no leukemia cells engrafted in the BM (chapter 4). Microarray results comparing gene expression patterns from CRLF2 B-ALL cells expanded in +T mice compared to –T mice, showed that TSLP up-regulates genes that are involved in cell death and survival functions of the cell (chapter 4). Additional genetic data showed that TSLP also up-regulates genes that are involved in cell death and survival signaling pathways; the cell death pathways being more significant (chapter 4). The genetic data provided evidence to support the *in vivo* data showing that TSLP regulates both cell death and survival mechanisms, but primarily induces apoptosis in CRLF2 B-ALL cells *in vivo*. Therefore we performed *in vitro* experiments to further confirm TSLP's effects on these cells. This

was accomplished by assessing the survival of cells stimulated with TSLP *in vitro*. Our results showed that TSLP increased Mcl-1 expression and maintained cell survival at early time points, but later induced apoptosis in CRLF2 B-ALL cells (chapter 4). These studies are the first to evaluate the long-term functional effects of TSLP on CRLF2 B-ALL cells *in vitro* and more importantly *in vivo* thereby introducing a novel role for TSLP as a possible therapeutic candidate. Interestingly, the data showing that TSLP induces apoptosis in CRLF2 B-ALL does not support our hypothesis stated in paragraph 1 of this discussion. Therefore future studies that further elucidate the mechanisms by which TSLP exerts its effects are required to fully understand its role in the disease and its therapeutic value. We also identified Mcl-1 as a potential molecular target that can be considered for inhibitor studies against CRLF2 B-ALL.

Patients diagnosed with CRLF2 B-ALL still experience higher rates of relapse and currently no targeted treatment exists [1]. Studies have recommended the use of JAK inhibitors in clinical trials for the treatment of Ph-like ALL, including CRLF2 B-ALL, however preclinical and clinical testing are still underway and not all CRLF2 leukemias harbor JAK mutations [16, 17]. Therefore there is a need for the testing of drug candidates that the offer potential to induce cytotoxic effects on CRLF2 B-ALL cells. We addressed this need in aim 3, which was accomplished by conducting drug efficacy studies against CRLF2 B-ALL and other high-risk B-ALL cells (chapter 5). Results showing that TSLP induces apoptosis in CRLF2 B-ALL cells require further testing, but provide evidence that TSLP can be considered as a lucrative potential therapy for CRLF2 B-ALL (chapter 4). Based on the results which showed that TSLP also increased the expression of Mcl-1, a Bcl-2 family member which functions to increase cell survival, we

evaluated the efficacy of the Mcl-1 inhibitor MIM1 on CRLF2 B-ALL cells *in vitro* (chapter 5). Our results showed that MIM1 reduced the viability of CRLF2 B-ALL cells and showed cytotoxic effects as MIM1's concentration was increased; proposing MIM1 as another drug candidate that can be used for further efficacy studies against CRLF2 B-ALL (chapter 5). *In vitro* and *in vivo* drug efficacy studies were also performed on another subset of high-risk B-ALL that is chemo-resistant using a new class of drugs (NM drug series), which inhibit cyclin-D-mediated proliferation in cells. The results showed that NM735 and NM869 showed efficacy against chemo-resistant B-ALL cells *in vitro* and NM922 showed efficacy against these same cells *in vivo* (chapter 5). The NM series are potential candidates that can be used for further efficacy studies against chemo-resistant B-ALL and other high-risk B-ALL such as CRLF2 B-ALL. Taken together, we have identified 3 potential candidates that can be used for further preclinical efficacy studies against CRLF2 B-ALL.

Conclusions and Future Implications

Overall, our studies were significant because 1) we were able to develop and optimize a novel xenograft model that provides human TSLP *in vivo*; 2) we used the human TSLP model to further investigate the TSLP-induced mechanisms involved in CRLF2 B-ALL (against a backdrop of normal B-lymphopoeisis); 3) we identified drug candidates that can be furthered evaluated as potential therapies for the treatment of CRLF2 B-ALL. Our studies provide new data that will contribute to a new understanding in the field of CRLF2 B-ALL disease mechanisms in context of TSLP. There are several points to consider as we assimilate this new data. First, it is difficult to study the role of

TSLP in CRLF2 B-ALL *in vivo* because current xenograft models that are used to study pediatric acute lymphoblastic leukemia lack human TSLP. PDXs are successful because most mouse cytokines are cross-reactive, having the ability to act on human leukemia cells and provide the growth signals that are necessary for these cells to expand *in vivo* [18]. However, TSLP is species specific [18]. The hTSLP+/hTSLP- model described in these studies provides the human TSLP that is required to design experiments that address the TSLP-mediated disease mechanisms of CRLF2 B-ALL and conduct preclinical testing of potential therapeutic candidates. Second, the TSLP-mediated signaling and cellular functions in CRLF2 B-ALL are different from TSLP's functions in normal cells. In normal B-cells, TSLP activates the JAK/STAT pathway and induces proliferation [12]. In CRLF2 B-ALL cells, basal levels of pJAK2, pSTAT5 and pS6 are present in the absence of TSLP, which is hypothesized as contributing to the constitutive activation of the JAK/STAT pathway (aberrant signaling) and leading to enhanced leukemia cell growth [6, 19]. Further, CRLF2 B-ALL cells stimulated with TSLP show increases in pSTAT5, and pS6 compared to untreated cells that express basal levels of pSTAT5, suggesting further increases in the activation of JAK/STAT and PI3K/AKT/mTOR pathway [7]. However, our functional studies (*in vitro* and *in vivo*) described in the previous chapters, show that though there is increased pSTAT5 and pS6 in the presence of TSLP with which we would expect to see increased proliferation compared to normal B-cells or untreated CRLF2 B-ALL cells, instead we observed the induction of apoptosis (chapters 2 and 4). Our studies show that stimulating CRLF2 B-ALL cells with TSLP reduces the survival of these cells by inducing apoptosis, suggesting that the TSLP-mediated signaling is not only different from what occurs in

normal B-cells, but is also different from what occurs in the leukemia cells in the absence of TSLP (Figure 6). This finding is paradigm shifting and has major future implications for understanding the disease mechanism of CRLF2 B-ALL and the designing of treatment strategies for the treatment of the disease.

Therefore the major questions that remain to be addressed are: 1) what mechanisms are involved in the TSLP-induced apoptosis of CRLF2 B-ALL?; 2) to what end does TSLP induce apoptosis in CRLF2 B-ALL cells?; 3) is TSLP inducing apoptosis to eradicate cancer cells thereby rendering it as a potential therapeutic candidate for the treatment of CRLF2 B-ALL?; 4) what is the therapeutic value of TSLP in relation to the treatment of CRLF2 B-ALL? 5) or is it a mechanism used by TSLP to regulate the cellular apoptosis versus cell survival switch in order to produce resilient clones of cells that can resist chemotherapy treatment and later contribute to MRD and relapse? Future studies that are designed to answer these questions will provide a basis for fully elucidating the involvement of TSLP in the initiation, maintenance and/or progression of CRLF2 B-ALL.

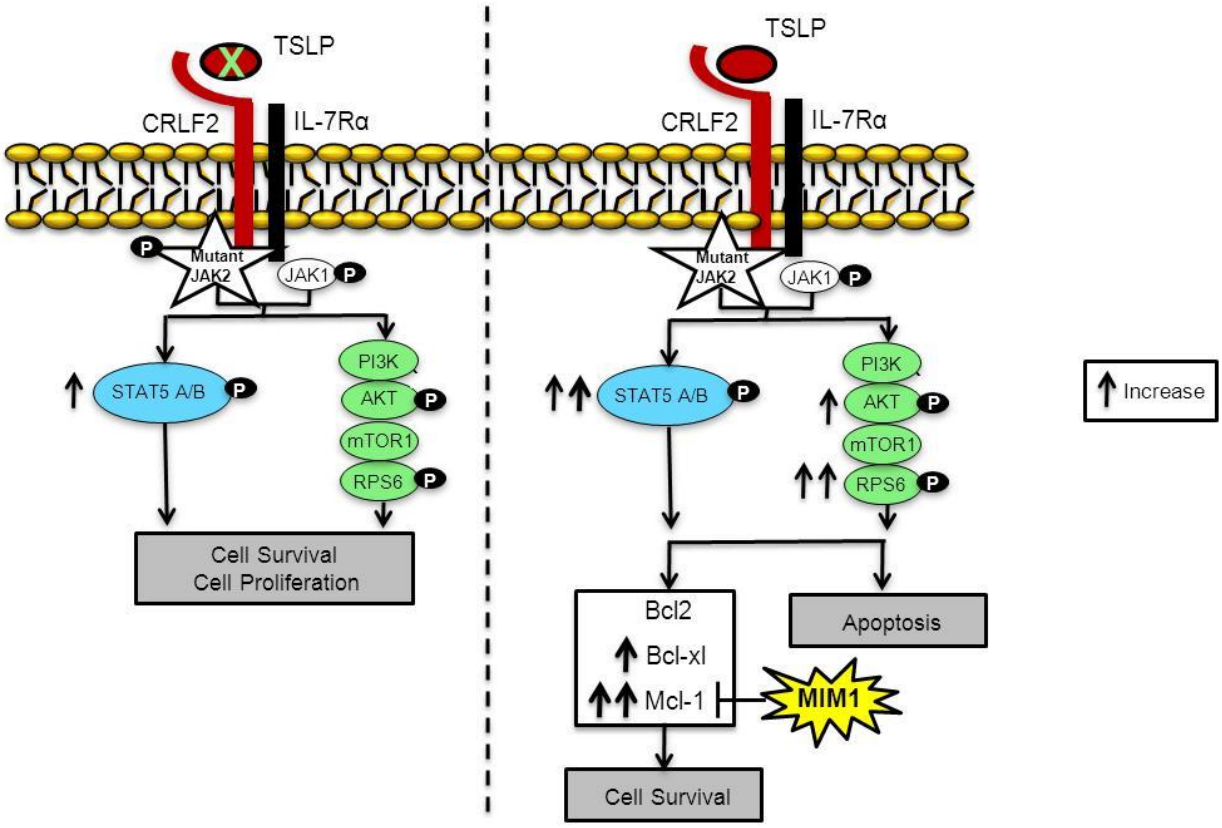

Figure 6: TSLP-induced Mechanisms in CRLF2 B-ALL. This cartoon serves as a visual illustration to show the differences in CRLF2 B-ALL mechanisms in the absence and presence of TSLP.

References

1. Chen, I.M., et al., *Outcome modeling with CRLF2, IKZF1, JAK, and minimal residual disease in pediatric acute lymphoblastic leukemia: a Children's Oncology Group study*. Blood, 2012. **119**(15): p. 3512-22.

2. Harvey, R.C., et al., *Identification of novel cluster groups in pediatric high-risk B-precursor acute lymphoblastic leukemia with gene expression profiling: correlation with genome-wide DNA copy number alterations, clinical characteristics, and outcome*. Blood, 2010. **116**(23): p. 4874-4884.

3. Mullighan, C.G., et al., *Genome-wide analysis of genetic alterations in acute lymphoblastic leukaemia*. Nature, 2007. **446**(7137): p. 758-64.

4. Cario, G., et al., *Presence of the P2RY8-CRLF2 rearrangement is associated with a poor prognosis in non-high-risk precursor B-cell acute lymphoblastic leukemia in children treated according to the ALL-BFM 2000 protocol*. Blood, 2010. **115**(26): p. 5393-5397.

5. Mullighan, C.G., et al., *Rearrangement of CRLF2 in B-progenitor- and Down syndrome-associated acute lymphoblastic leukemia*. Nat Genet, 2009. **41**(11): p. 1243-6.

6. Yoda, A., et al., *Functional screening identifies CRLF2 in precursor B-cell acute lymphoblastic leukemia*. Proc Natl Acad Sci U S A, 2010. **107**(1): p. 252-7.

7. Tasian, S.K., et al., *Aberrant STAT5 and PI3K/mTOR pathway signaling occurs in human CRLF2-rearranged B-precursor acute lymphoblastic leukemia*. Blood, 2012. **120**(4): p. 833-42.

8. Hertzberg, L., et al., *Down syndrome acute lymphoblastic leukemia, a highly heterogeneous disease in which aberrant expression of CRLF2 is associated with mutated JAK2: a report from the International BFM Study Group*. Blood, 2010. **115**(5): p. 1006-17.

9. Roll, J.D. and G.W. Reuther, *CRLF2 and JAK2 in B-progenitor acute lymphoblastic leukemia: a novel association in oncogenesis*. Cancer Res, 2010. **70**(19): p. 7347-52.

10. Lu, X., L.J. Huang, and H.F. Lodish, *Dimerization by a cytokine receptor is necessary for constitutive activation of JAK2V617F*. J Biol Chem, 2008. **283**(9): p. 5258-66.

11. Ray, R.J., et al., *Characterization of thymic stromal-derived lymphopoietin (TSLP) in murine B cell development in vitro*. Eur J Immunol, 1996. **26**(1): p. 10-6.

12. Scheeren, F.A., et al., *Thymic stromal lymphopoietin induces early human B-cell proliferation and differentiation*. Eur J Immunol, 2010.

13. Zhong, J., et al., *TSLP signaling pathway map: a platform for analysis of TSLP-mediated signaling*. Database (Oxford), 2014. **2014**: p. bau007.

14. Brown, V.I., et al., *Thymic stromal-derived lymphopoietin induces proliferation of pre-B leukemia and antagonizes mTOR inhibitors, suggesting a role for interleukin-7Ralpha signaling*. Cancer Res, 2007. **67**(20): p. 9963-70.

15. Tasian, S.K., et al., *Thymic Stromal Lymphopoietin Stimulation of Pediatric Acute Lymphoblastic Leukemias with CRLF2 Alterations Induces JAK/STAT and PI3K Phosphosignaling*. Blood, 2010. **116**(21): p. 182-183.

16. Roberts, K.G., et al., *Targetable kinase-activating lesions in Ph-like acute lymphoblastic leukemia*. N Engl J Med, 2014. **371**(11): p. 1005-15.

17. Harvey, R.C., et al., *Rearrangement of CRLF2 is associated with mutation of JAK kinases, alteration of IKZF1, Hispanic/Latino ethnicity, and a poor outcome in pediatric B-progenitor acute lymphoblastic leukemia*. Blood, 2010. **115**(26): p. 5312-21.

18. Chen, Q., M. Khoury, and J. Chen, *Expression of human cytokines dramatically improves reconstitution of specific human-blood lineage cells in humanized mice*. Proc Natl Acad Sci U S A, 2009. **106**(51): p. 21783-8.

19. Russell, L.J., et al., *Deregulated expression of cytokine receptor gene, CRLF2, is involved in lymphoid transformation in B-cell precursor acute lymphoblastic leukemia*. Blood, 2009. **114**(13): p. 2688-98.

APPENDIX A (CHAPTER 2)

SUPPLEMENTAL MATERIALS

Supplemental Methods

Cell Culture Media

MUTZ5 and MHH-CALL4 were maintained in RPMI 1640 medium (Irvine Scientific, Santa Ana, CA) supplemented with penicillin/streptomycin, L-glutamine, 50 uM 2-ME and 20% FBS (Omega Scientific, Tarzana, CA). This media was also used for *in vitro* cultures with and without TSLP (both for phospho-flow assays and for gene expression profiling in response to TSLP). HS27 stroma were maintained in RPMI 1640 medium (Irvine Scientific) supplemented with penicillin/streptomycin, L-glutamine, 50 uM 2-ME and 10% FBS (Omega Scientific).

Flow Cytometry

Cells were prepared for surface antigen detection and assessed by flow cytometry using protocols described in companion paper. Dead cells were identified using fixable viability dye as described in companion paper. Specific antibody clones and conjugates are shown below.

Table 2. List of Antibodies, Clones and Manufacturer Information 1 (chapter 2).

Antibody	Clone	Manufacturer
Ig κ light chain FITC	G20-193	BD Pharmingen (San Jose, CA)
Ig λ light chain FITC	JDC-12	
Anti-phospho STAT5 (pY694) PE	47/Stat5 (pY694)	BD Biosciences (San Jose, CA
Anti-Phospho AKT (pS473) Alexa Fluor 488	M89-61	
Anti-Phospho S6 (pS235/S236) Alexa Fluor 488	N7-548	
CD34 PerCP	581	BioLegend (San Diego, CA)
CD19 APC	HIB19	
TSLPR APC	1B4	
CD19 APC	HIB19	eBioscience (San Diego, CA)
CD19 PE.Cy7	SJ25C1	
CD45 PE.Cy7	HI30	
Anti-Mouse CD45 FITC	30F11	Miltenyi Biotec (Auburn, CA)
CD19 APC	LT19	
CD127 PE (IL-7Ra)	MB15-18C9	

Phospho-flow Cytometry Staining

Human CRLF2 B-ALL cell lines were harvested from continuous culture and primary CRLF2 B-ALL cells were obtained as BM from patient-derived xenografts. Cells were rested in culture without cytokines for 2 hrs, and then cultured with mTSLP, hTSLP or no cytokine for 30 mins (S6 and AKT) or 1 hour (STAT5). Cells were then harvested and stained with antibody to phosphorylated STAT5 (pSTAT5), AKT (pAKT) or S6 (pS6) as previously described for STAT5 (1). Primary CRLF2 B-ALL patient-derived samples were also stained with CD19 APC prior to fixation and permeabilization for detection of phospho proteins and CD19+ cells were gated for phospho-flow cytometry plots.

ELISA Assays of TSLP

Concentrations of hTSLP in the supernatant of transduced HS27 stromal culture and in sera collected from NSG mice injected with transduced stroma were measured using the Human TSLP ELISA MAX Kit (BioLegend, San Diego, CA). Stromal cell supernatants were harvested from confluent flasks when stromal cells were passaged (typically two times per week) and sera was obtained from mice at weekly time points at the time of weekly stromal cell injection. Data was collected using the uQuant microplate spectrophotometer (BioTek Instruments Inc., Winooski, VT) and analyzed using the KC Junior, version 1.6 (BioTek Instruments, Inc., Winooski, VT)

Lentiviral Vector and TSLP-expressing Human Stromal Cells

TSLP vector was generated using standard molecular cloning techniques with complementary DNA encoding human TSLP (purchased from Thermo Scientific Open Biosystems). In this vector, the EF-1α promoter was used to drive TSLP expression. A control vector with GFP was also generated. The lentiviral vector packaging and titering were performed as previously described (2). In brief, VSV-G–pseudotyped lentiviral vectors were prepared by calcium phosphate–mediated 3-plasmid transfection of 293T cells. Briefly, 27 μg transfer vector construct, 17.5 μg second-generation gag-pol packaging construct pCMV.R8.74, and 9.5 μg VSV-G expression construct pMD2.G were used for transfection of $12x10^6$ 293T cells overnight in 25 ml DMEM with 10% fetal bovine serum. The cells were treated with 10 mM sodium butyrate during the first of three 12-hour vector supernatant collections. The supernatant was filtered through 0.22-μm-pore-size filters and concentrated 100-fold by ultracentrifugation before freezing and

storing at –80° C. All vector stocks were titered by transducing HT1080 cells with analysis for GFP expression by flow cytometry or real-time PCR.

Processing of Samples from Xenograft Mice

Flow cytometry analysis of peripheral blood (PB) was used to establish chimerism with human cells prior to euthanasia. PB was collected using tail-tip excision (tail nick) and placed into a microtainer serum separator tube (BD Gold, 200/cs). Samples were centrifuged at 1500 rpm for 15 mins. Serum was removed for ELISA analysis. Blood cells were subjected to red blood cell lysis (3) and remaining white blood cells were stained for human surface markers. NSG mice were euthanized 5-7 weeks after CB CD34+ transplantation or 9 weeks after CRLF2 B-ALL transplantation. On the day of euthanasia fresh Bone Marrow (BM), spleen and PB were harvested. Single cell suspensions were obtained from the BM by using 26g syringe and PBS to flush the femora and humeri and by filtering cells with a 70 micron cell strainer (BD Biosciences, San Jose, CA). Cells obtained from all tissues were stained immediately for flow cytometry analysis or were frozen for future use.

Microarray Analysis of Gene Expression in CRLF2 B-ALL Cells

Mice engineered to be +T and –T by stromal cell injection were transplanted with primary CRLF2 B-ALL cells from a Hispanic pediatric patient. Following transplant, mice received weekly intraperitoneal injection of $5X10^6$ +T or –T stroma from Transduction 1 (see Results section). Nine weeks post transplant, BM was harvested and frozen for later use. For microarray to evaluate *in vivo* TSLP-induced changes in gene expression, xenograft BM was thawed and human B-ALL cells were isolated by magnetic separation using the Human CD19 microbead kit (Miltenyi Biotec, Inc., San

Diego, CA) according to manufacturer's protocol and rapidly frozen on dry ice (Samples E1-E3 and F1-F3 described below). For microarray to evaluate *in vitro* TSLP-induced changes in gene expression (Fig. 4), xenograft BM was thawed and cultured *in vitro* for 3 days with TSLP at 15ng/ml or without TSLP and with neutralizing anti-TSLP antibody (R&D Systems, Minneapolis, MN) or control antibody (Jackson ImmunoResearch). Following culture, cells were harvested and thawed and human B-ALL cells were isolated by magnetic separation using the Human CD19 Microbead Kit according to manufacturer's protocol and rapidly frozen on dry ice (samples A1-A3, B1-B3, C1-C3 and D1-D3 as described below). Frozen cells were shipped to Miltenyi Biotec (Miltenyi Genomic Services) for RNA isolation, sample preparation, whole genome microarray, and discriminatory gene analysis (DGA) as follows:

Total RNA Isolation. Human total RNA was isolated using the NucleoSpin® RNA kit (Macherey-Nagel, Bethlehem, PA). RNA quality and integrity were determined using the Agilent RNA 6000 Nano Kit on the Agilent 2100 Bioanalyzer (Agilent Technologies, Santa Clara, CA). RNA was quantified by measuring A260nm on the ND-1000 Spectrophotometer (NanoDrop Technologies, Wilmington, DE).

RNA Amplification and Labelling. Sample labelling was performed as detailed in the "One-Color Microarray-Based Gene Expression Analysis protocol (version 6.6, part number G4140-90040). Briefly, 50 ng RNA for the samples from groups A, B, E and F, 10 ng RNA for the samples of group C and D, and the complete available amount of RNA for the samples C3 and D1 was used for the amplification and labelling step using the Agilent Low Input Quick Amp Labelling Kit (Agilent Technologies). Yields of

cRNA and the dye-incorporation rate were measured with the ND-1000 Spectrophotometer (NanoDrop Technologies).

Table 3. Microarray Sample Key.

Sample	Source of Cells	In vitro Culture, Condition
A1, A2, A3	CRLF2 B-ALL cells from +T mice	Yes, +TSLP
B1, B2, B3	CRLF2 B-ALL cells from +T mice	Yes, –TSLP
C1, C2, C3	CRLF2 B-ALL cells from –T mice	Yes, +TSLP
D1, D2, D3	CRLF2 B-ALL cells from –T mice	Yes, –TSLP
E1, E2, E3	CRLF2 B-ALL cells from +T mice	No, ----------
F1, F2, F3	CRLF2 B-ALL cells from –T mice	No, ----------

Hybridization of Agilent Whole Human Genome Oligo Microarrays. The hybridization procedure was performed according to the "One-Color Microarray-Based Gene Expression Analysis protocol (version 6.6, part number G4140-90040) using the Agilent Gene Expression Hybridization Kit (Agilent Technologies). Briefly, 0.6 μg Cy3-labeled fragmented cRNA in hybridization buffer was hybridized overnight (17 hours, 65 °C) to Agilent Whole Human Genome Oligo Microarrays 8x60K v2 (AMADID 039494) using Agilent's recommended hybridization chamber and oven. Following hybridization, the microarrays were washed once with the Agilent Gene Expression Wash Buffer 1 for 1 min at room temperature followed by a second wash with preheated Agilent Gene Expression Wash Buffer 2 (37 °C) for 1 min.

Scanning and Data Analysis: Fluorescence signals of the hybridized Agilent Microarrays were detected using Agilent's Microarray Scanner System G2505C (Agilent

Technologies). The Agilent Feature Extraction Software (FES) 10.7.3.1 was used to read out and process the microarray image files.

Discriminatory Gene Expression Analysis. After probe summarization, quantile normalization and log2 transformation, differentially expressed genes were identified by a combination of effect size and statistical significance. For the analysis of the individual comparisons, only reporters with an at least two-fold median up- or downregulation in +T samples compared to –T samples and an adjusted p-value (Student's t-test, two-tailed, equal variance, Benjamini-Hochberg correction for multiple testing) $p \leq 0.05$ were considered relevant. In an additional filtering step, only Agilent reporters with signal intensity values significantly above local background ($p < 0.01$ as calculated by the Rosetta Resolver® gene expression data analysis system) in at least two samples of the group with higher median expression were selected (4). All microarray data reported in this publication were deposited in the NCBI's Gene Expression Omnibus at National Center for Biotechnology Information and are accessible via the GEO series accession number GSE65274.

Real Time Quantitative RT-PCR

Expression of select genes observed in microarray results was validated using quantitative reverse transcriptase - polymerase chain reaction (qRT-PCR) using primers shown below. Total RNA (2.0μg) was reverse transcribed using poly d(T)20 primers and SuperScript II reverse transcriptase (Life Technologies, Grand Island, NY). The resulting cDNAs were used for qRT-PCR analysis of their mRNA levels on a StepOne Plus 7500 Real-time PCR system (Applied Bioscience Inc., Foster City, CA) using specific primers for each gene (see supplemental table 2 for primer sequences) following the

manufacturer's instructions. The fluorescence threshold value was calculated and normalized to the values of 18s rRNA. The fold change in mRNA expression of genes between the TSLP-treated W31 cell group versus untreated group was achieved by the ratio of fluorescence threshold value in the treated groups versus that of the untreated group. The fold change for each gene was paired with that of microarray analysis. Linear regression analysis of the fold change versus that of microarray was performed with Origin 6.0. The graph shows the best-fit line, the formula for the best-fit line (Y = a + bX), its correlation coefficient (r), and the probability (P) that the r value is a false positive.

Table 4. Primer List for Genes Validated by qRT-PCR

Gene	Forward Primer	Reverse Primer
BIVM	5'-GGCCAGAGGCAATGCAAAG	5'-TGAGGTCTAATACTTTCCGCTGT
PTH2	5'-CTGGTTCTCCACAGGTGATG	5'-CATGTACGAGTTCAGCCACT
FOSL2	5'-AACACCCTGTTTCCTCTCCG	5'-ATCTACCCGGAATTTCTGCGG
RAMP1	5'-GCAGGACCATCAGGAGCTACA	5'-GCCTACACAATGCCCTCAGTG
SLC4A8	5'-TGGGTCCAGTAGGGAAAGGT	5'-ACCGTCACCTGGTCTAGGAA
NR4A2	5'-GTAACTCGGCTGAAGCCATGC	5'-GTCGTAGCCTGTGCTGTAGTT
KCNH8	5'- GCAAGATCAATTTGCATCCACTAT	5'- AAGGCAGGGCAGCGATTA
THSD7A	5'- CCATCTCGAGTCTTTGTTCACATT	5'- CATTTGGGAATTGTGCTTCTCA
RAB26	5'-CCAGGCCCTTCTGACTTTGT	5'-CTGCTTGTTGGGACTGTTGC
RGS1	5'-CTCCCTGGGTGAACAGCTTG	5'-GCTTCTTCAACTCTGCGCCT
NELL1	5'-GATATGAAGCCACCCGTGTT	5'-CTGAAGGTCAGGGTCCATCC
MDF1	5'-GAAGTTGCAGACACACCCATCTC	5'-GTCCAGGACGATGTTGCACAG
KREMEN2	5'-TGAGGACCCAGAGGCCC	5'-CAGACAGCTCCCCCAATCG
CPNE8	5'-CGCCTCCTCCCAATATGGAC	5'-ATTTCTGCAGGACACGGACA

Gene Set Enrichment Analysis

Microarray data was evaluated at the level of gene sets to define and quantitate trends in gene expression similar to published data. Ranked gene lists were created and

submitted to the online public repository provided by the BROAD Institute for Gene Set Enrichment Analysis (GSEA) (5, 6) to evaluate Oncogenic Signatures that are enriched in CRLF2 B-ALL cells expanded in +T as compared to –T mice (www.broadinstitute.org/gsea).

Ingenuity Pathway Analysis

The complete list of differentially expressed genes obtained from microarray datasets were uploaded and analyzed using the Ingenuity Pathway Analysis tool (IPA; Ingenuity Systems, Redwood City, CA) to identify significant biological pathways that are up-regulated in CRLF2 B-ALL cells expanded in +T compared to –T mice. The pathways were identified using the "Canonical Pathway" feature of IPA. The activity of a pathway was deemed significant if its p-value is less than or equal to 0.05 and is calculated using the right-tailed Fisher Exact Test.

Supplemental Figures

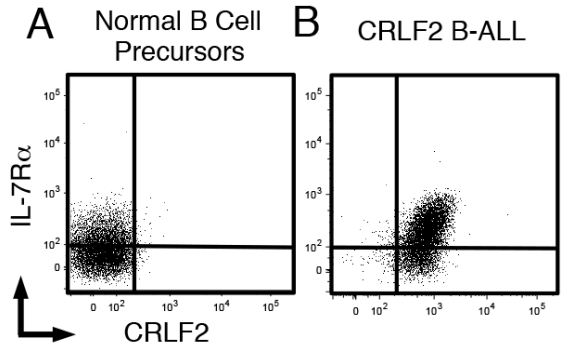

Figure 1: Expression of CRLF2 and IL-7Rα on normal human B cell precursors and CRLF2 B-ALL harvested from xenograft mice. (A) Bone marrow was harvested from xenograft mice transplanted with human CD34+ cord blood cells or and stained for flow cytometry. Plotted is CRLF2 and IL-7Ra expression on B cell precursors (hCD19+ and Ig kappa & lambda–) B) Bone marrow was harvested from a patient-derived xenograft generated using the primary CRLF2 B-ALL sample shown in Fig. 1B, right panel. Plotted is the CRLF2 and IL-7Ra on human CRLF2 B-ALL (hCD19+) cells.

Supplemental Tables

Table 5.

qRT-PCR validation of genes that are differentially regulated in CRLF2 B-ALL cells expanded in +T as compared to –T xenograft mice. The table shows the list of genes that were selected from the microarray dataset for validation by qRT-PCR analysis and their respective fold changes as determined by microarray and by qRT-PCR. The first 7 genes are up-regulated, while the last 7 genes are down-regulated.

Gene	Microarray (fold change)	qRT-PCR (fold change)
BIVM	4.440	6.907
PTH2	3.477	2.784
FOSL2	2.793	1.843
RAMP1	2.725	2.227
SLC4A8	2.628	6.417
NR4A2	2.138	3.548
KCNH8	2.154	2.355
THSD7A	–3.628	–6.648
RAB26	–2.727	–2.726
RGS1	–2.749	–2.498
NELL1	–3.586	–3.143
MDF1	–2.168	–7.621
KREMEN2	–2.336	–2.003
CPNE8	–3.008	–4.695

Table 6: Genes regulated downstream of mTOR signaling. GSEA data summary table shows genes that are part of the mTOR gene set which were enriched in CRLF2 B-ALL cells expanded in +T mice as compared to –T mice. Genes are listed in order of increasing enrichment score (ES).

Gene Symbol	Rank in Gene List	Rank Metric Score	Running ES	Core Enrichment
ECHDC2	148	0.690	0.0435	Yes
FBLN5	176	0.662	0.0935	Yes
BIN2	275	0.560	0.1304	Yes
CD1A	291	0.548	0.1723	Yes
CD1B	463	0.451	0.1955	Yes
EFHC1	721	0.361	0.2054	Yes
POLH	800	0.343	0.2268	Yes
SPRY1	946	0.304	0.2402	Yes
GPA33	973	0.296	0.2616	Yes
ZNF14	1165	0.252	0.2677	Yes
H1F0	1219	0.242	0.2829	Yes
ZBTB20	1232	0.238	0.3008	Yes
ANXA5	1238	0.236	0.3189	Yes
PCNXL2	1293	0.224	0.3326	Yes
CBX7	1405	0.205	0.3407	Yes
BAALC	1442	0.198	0.3537	Yes
NFE2	1606	0.172	0.3555	Yes
RAG1	1610	0.171	0.3687	Yes
PBXIP1	1705	0.159	0.3745	Yes
HBP1	1721	0.157	0.3857	Yes
TNRC6B	1854	0.139	0.3872	Yes
SLC2A11	1901	0.134	0.3945	Yes
GIMAP6	1966	0.129	0.4000	Yes
MME	1976	0.128	0.4094	Yes
HHAT	1984	0.127	0.4189	Yes
GALNT7	2003	0.125	0.4273	Yes
TPM2	2041	0.121	0.4342	Yes
TXNIP	2069	0.119	0.4415	Yes
GCC2	2090	0.117	0.4493	Yes
REL	2151	0.112	0.4538	Yes
SUV420H1	2285	0.100	0.4521	Yes
ZNF673	2306	0.099	0.4584	Yes
SENP7	2310	0.098	0.4659	Yes
SLC35D1	2381	0.094	0.4683	Yes
PNRC1	2432	0.091	0.4719	Yes
TRIOBP	2437	0.091	0.4787	Yes
SYNE2	2453	0.090	0.4847	Yes
YPEL5	2507	0.087	0.4878	Yes
CBFA2T3	2519	0.087	0.4938	Yes
ZNF682	2527	0.087	0.5001	Yes
DNTT	2535	0.086	0.5064	Yes
CD1E	2539	0.086	0.5129	Yes
RAG2	2577	0.084	0.5168	Yes
CHIC2	2670	0.079	0.5164	Yes
RCOR3	2674	0.079	0.5224	Yes
KIAA0355	2741	0.076	0.5236	Yes
TPP1	2818	0.073	0.5239	Yes
DMXL1	2834	0.072	0.5284	Yes
WDR45	2848	0.071	0.5331	Yes
ZXDC	2875	0.070	0.5367	Yes
CCNG2	2913	0.068	0.5394	Yes
MARCH8	2986	0.066	0.5394	Yes
BCOR	3024	0.064	0.5418	Yes
ZNF180	3026	0.064	0.5468	Yes
HIST1H2AC	3058	0.063	0.5495	Yes
SLC23A2	3078	0.063	0.5531	Yes

Supplemental References

1. Parrish YK, Baez I, Milford TA, Benitez A, Galloway N, Rogerio JW, et al. IL-7 Dependence in human B lymphopoiesis increases during progression of ontogeny from cord blood to bone marrow. Journal of immunology. 2009 Apr 1;182(7):4255-66.

2. Meng X, Neises A, Su RJ, Payne KJ, Ritter L, Gridley DS, et al. Efficient reprogramming of human cord blood CD34+ cells into induced pluripotent stem cells with OCT4 and SOX2 alone. Mol Ther. 2012 Feb;20(2):408-16.

3. Kang EM, Areman EM, David-Ocampo V, Fitzhugh C, Link ME, Read EJ, et al. Mobilization, collection, and processing of peripheral blood stem cells in individuals with sickle cell trait. Blood. 2002 Feb 1;99(3):850-5.

4. Weng L, Dai H, Zhan Y, He Y, Stepaniants SB, Bassett DE. Rosetta error model for gene expression analysis. Bioinformatics. 2006 May 1;22(9):1111-21.

5. Mootha VK, Lindgren CM, Eriksson KF, Subramanian A, Sihag S, Lehar J, et al. PGC-1alpha-responsive genes involved in oxidative phosphorylation are coordinately downregulated in human diabetes. Nat Genet. 2003 Jul;34(3):267-73.

6. Subramanian A, Tamayo P, Mootha VK, Mukherjee S, Ebert BL, Gillette MA, et al. Gene set enrichment analysis: a knowledge-based approach for interpreting genome-wide expression profiles. Proc Natl Acad Sci U S A. 2005 Oct 25;102(43):15545-50.

APPENDIX B (CHAPTER 3)

SUPPLEMENTAL MATERIALS

Supplemental Methods

Human Samples

Umbilical cord blood (CB) and bone marrow (BM) were obtained in accordance with protocols approved by the Loma Linda University Institutional Review Board (IRB) and with the Helsinki Declaration of 1975, as revised in 2008. Umbilical cord blood (CB) was obtained from placentas after caesarean section delivery of full-term neonates at Loma Linda University Medical Center. Mononuclear cells were isolated using Ficoll-Paque Plus (GE Healthcare Bio-Sciences, AB) or by red blood cell (RBC) lysis (1). CD34+ cells were isolated by magnetic separation with CD34+ microbeads (Miltenyi Biotec, Auburn, CA) and stored in liquid nitrogen for subsequent use. Pediatric bone marrow (BM) samples were obtained as waste samples remaining after clinical procedures under an LLU Institutional Review Board (IRB) approved protocol. Adult BM and stromal cells were purchased from Lonza Inc. (Walkersville, MD). Stromal cells were isolated from pediatric and adult BM as previously described (2) and maintained in IMDM medium supplemented with 15% horse serum, 15% FBS, hydrocortisone, 2-mercaptoethanol, penicillin-streptomycin and L-glutamine.

In vitro Co-cultures

Human only *in vitro* co-cultures were initiated as previously described (3). Briefly, CB CD34+ cells were seeded onto pre-plated primary human BM stromal cells, at 10,000 to 20,000 cells per well in 96-well plates. For some experiments, numbers were scaled up to give equivalent cell densities in 6-well and 12-well plates. Cultures were

maintained in RPMI 1640 medium (Irvine Scientific, Santa Ana, CA) supplemented with penicillin/streptomycin, L-glutamine, 50 uM 2-mercaptoethanol and 5 % human AB serum lot tested to support human B cell production (Omega Scientific, Tarzana, CA). All cultures, including control, were supplemented with IL-3 (1 ng/ml; first week only) and Flt-3 Ligand (1 ng/ml, continuously). For selective cytokine stimulation TSLP (10 ng/ml) and/or IL-7 (5 ng/ml) or no cytokines (control cultures) were added. All cytokines were from R&D Systems Inc. (Minneapolis, MN). If TSLP or IL-7 was not added, cultures were further supplemented with an anti-human neutralizing antibody to counter activity of any endogenously produced TSLP or IL-7. Cultures without a specific neutralizing antibody (anti-IL-7 and/or anti-TSLP) were supplemented with an isotype-matched control for the neutralizing antibody. Anti-human neutralizing or control antibody for IL-7 was used at 10 ng/ml (BD Pharmingen, Franklin Lakes, NJ).). Anti-human neutralizing or control antibody for TSLP was used at 1 ug/ml (R&D Systems and Jackson ImmunoResearch, West Grove, PA). Media, cytokines, and antibodies were replenished weekly. Cultures were maintained for three weeks, and then harvested. For BrdU incorporation, selective cytokine cultures were labeled with 10 μM BrdU (Sigma-Aldrich, St. Louis, MO) for the final 24 hours of culture.

Flow Cytometry

For detection of surface antigens, cells were stained using standard flow cytometry protocols, followed by fixation and permeabilization as described below to detect intracellular antigens. To discriminate living from dying cells, in some experiments, cells were stained with fixable viability dyes (eBioscience, San Diego, CA),

per manufacturer's instructions. Apoptosis was quantified by flow cytometry using Annexin-V FITC (Biolegend, San Diego, CA) and 7-AAD (eBioscience, San Diego, CA) according to manufacturer's instructions.

To assess intracellular IgM, Ki-67, Bcl-2, Bcl-xL, and Mcl-1, the Fix & Perm® cell fixation and permeabilization kit (Life Technologies, Grand Island, NY)) was used according to manufacturer's instructions. All antibodies were monoclonal, anti-human antibodies, unless otherwise stated. Intranuclear detection of BrdU was performed using BrdU Flow Kit option no. 2 (BD Pharmingen) according to manufacturer's instructions. Briefly, cells were harvested, surface stained, washed then fixed with BD cytofix/cytoperm buffer (BD Biosciences) for 15-30 minutes at room temperature. Cell suspensions were washed, then stored overnight in freezing medium (90% FBS and 10% DMSO) at –80ºC. The following day, thawed cells were washed, re-fixed in BD cytofix/cytoperm buffer and washed with BD perm/wash buffer. Cells were treated with DNase (300 ug/ml, Sigma-Aldrich) for 1 hour at 37ºC, washed then stained with anti-BrdU FITC or isotype-matched control for 20 minutes at room temperature. Cells were washed then resuspended in 1% PFA for acquisition.

To assess intracellular PAX-5, cells were first surface stained for viability and surface markers, then fixed and permeabilized with FoxP3 fix/perm buffer (eBioscience) for 30-60 minutes at 4ºC in the dark. Cells were washed, resuspended in permeabilization buffer and stained with PAX-5 PE or isotype-matched controls for 30 minutes at room temperature. Cells were washed then resuspended in 1% PFA for acquisition. In some experiments, cells were simultaneously stained for PAX-5 and BrdU. In these

experiments cells were first stained for PAX-5 according to manufacturer's directions, followed by BrdU staining according to manufacturer's instructions.

Table 7: List of Antibodies, Clones and Manufacturer Information 2 (chapter 3)

Antibody	Clone	Manufacturer
BrdU FITC	B44	BD Biosciences (San Jose, CA)
Bcl-2 FITC	Bcl-2/100	
Ig κ light chain FITC	G20-193	
Ig λ light chain FITC	JDC-12	
IgM PE Cy-5	G20-127	
CD19 APC	HIB19	
CD34 PerCP	8G12	
CD34 APC	8G12	
CD34 APC.Cy7	581	Biolegend (San Diego, CA)
IgD PE	IA6-2	
Bcl-xL Alexa-fluor 488	54H6	Cell Signaling Technology (Beverly, MA)
CD19 APC	HIB19	eBioScience (San Diego, CA)
CD19 PE.Cy7	SJ25C1	
CD45 PE.Cy7	HI30	
CD127 PE	eBioRDR5	
Ig κ light chain eFluor 450	TB28-2	
Ig λ light chain eFluor 450	1-155-2	
PAX-5 PE	1H9	
Goat anti-rabbit IgG Alexa Fluor 647		Life Technologies (Molecular Probes) (Grand Island, NY)
Anti-Mouse CD45 FITC	30F11	Miltenyi Biotec (Auburn, CA)
CD19 APC	LT19	
CD34 APC	AC136	
CD127 PE	MB15-18C9	
Polyclonal Mcl-1	S-19	Santa Cruz Biotechnology

Polymerase Chain Reaction

Total RNA was extracted from 8 to 9 x 10^5 human stromal cells with RNA-STAT 60 reagent (Tel-Test Inc., Friendswood, TX). cDNA was synthesized using Omniscript Reverse Transcriptase (Qiagen, Valencia, CA). The expression of TSLP, IL-7 and β-2 microglobulin as a control, were assessed by touch down PCR. The primers used were: TSLP forward 5'-TCG TAA ACT TTG CCG CCT AT-3' and reverse 5'-TGG TGC TGT GAA ATA TGA CCA-3' (324 bp); IL-7 forward 5'- CTC CCC TGA TCC TTG TTC TG and reverse 5'- TCA TTA TTC AGG CAA TTG CTA CC-3' (151 bp); β-2 microglobulin forward 5'-CTC GCG CTA CTC TCT CTT TC-3' and reverse 5'-CAT GTC TCG ATC CCA CTT AAC-3' primers.

Touch-down PCR conditions for TSLP were as follows: 95°C for 5 min (1 cycle); 95°C for 1 min, 61°C for 30 sec. 72°C for 1 min (2 cycles); 95°C for 1 min, 59°C for 30 sec. 72°C for 1 min (2 cycles); 95°C for 1 min, 57°C for 30 sec. 72°C for 1 min (2 cycles); 95°C for 1 min, 55°C for 30 sec. 72°C for 1 min (2 cycles); 95°C for 1 min, 53°C for 30 sec. 72°C for 1 min (2 cycles); 95°C for 1 min, 51°C for 30 sec. 72°C for 1 min (30 cycles); 72°C for 10 min (1 cycle); and final hold step of 4°C.

Touchdown PCR conditions for IL-7 were as follows: 95°C for 5 min (1 cycle); 95°C for 1 min, 63°C for 45 sec. 72°C for 1 min (2 cycles); 95°C for 1 min, 61°C for 45 sec. 72°C for 1 min (2 cycles); 95°C for 1 min, 59°C for 45 sec, 72°C for 1 min (2 cycles); 95°C for 1 min, 57°C for 30 sec. 72°C for 1 min (2 cycles); 95°C for 1 min, 55°C for 45 sec. 72°C for 1 min (2 cycles); 95°C for 1 min, 53°C for 45 sec. 72°C for 1 min (30 cycles); 72°C for 10 min (1 cycle); and final hold step of 4°C.

Amplified PCR products were visualized with a 2.2% FlashGel (Lonza, Walkerswood, MD). PCR products were purified with QIAquick PCR purification kit (Qiagen, Valencia, CA) and sequenced at the Genomics Core (University of California, Riverside, CA).

Animal Studies

Studies were performed using NOD.Cg-Prkdcscid Il2rgtm1Wjl/SzJ (NSG) mice (Jackson Laboratory). Mice were housed under specific pathogen-free conditions in the Loma Linda University animal facility and studied in accordance with an Institutional Animal Care and Use Committee (IACUC) approved protocols. Mice were transplanted by tail vein injection with freshly thawed, CB CD34+ cells after sub-lethal irradiation at 225 rads. Mice were engineered by intraperitoneal injection with HS-27 stromal cells (ATCC, Manassas, VA) that had been transduced to express human TSLP (+T mice) or transduced with empty vector (–T mice) as previously described (4). Transduction of stroma and injection of stromal cell is described in the companion paper. NSG mice were euthanized by CO_2 asphyxiation, five to seven weeks after CB CD34+ transplantation and bone marrow and spleen were harvested. Samples were lysed of red blood cells and then frozen or stained immediately for flow cytometry analysis.

Supplemental References

1. Kang EM, Areman EM, David-Ocampo V, Fitzhugh C, Link ME, Read EJ, et al. Mobilization, collection, and processing of peripheral blood stem cells in individuals with sickle cell trait. Blood. 2002 Feb 1;99(3):850-5.

2. Nolta JA, Thiemann FT, Arakawa-Hoyt J, Dao MA, Barsky LW, Moore KA, et al. The AFT024 stromal cell line supports long-term ex vivo maintenance of engrafting multipotent human hematopoietic progenitors. Leukemia. 2002 Mar;16(3):352-61.

3. Parrish YK, Baez I, Milford TA, Benitez A, Galloway N, Rogerio JW, et al. IL-7 Dependence in human B lymphopoiesis increases during progression of ontogeny from cord blood to bone marrow. J Immunol. 2009 Apr 1;182(7):4255-66.

4. Meng X, Neises A, Su RJ, Payne KJ, Ritter L, Gridley DS, et al. Efficient reprogramming of human cord blood CD34+ cells into induced pluripotent stem cells with OCT4 and SOX2 alone. Mol Ther. 2012 Feb;20(2):408-16.